STUDY OF UNSTEADY STATE BEHAVIOR OF GAS STORAGE RESERVOIR ON ELECTRONIC DIFFERENTIAL ANALYZER

by

Hyungduk D. Yoo

A dissertation submitted in partial fulfillment
of the requirements for the degree of
Doctor of Philosophy in the
University of Michigan

1959

Doctoral Committee:

Assistant Professor M. Rasin Tek, Chairman
Associate Professor Donald T. Greenwood
Professor Donald L. Katz
Professor Victor L. Streeter
Professor Robert R. White

ACKNOWLEDGEMENTS

The author wishes to express his appreciation to the following individuals and organization for the contributions to the research which was the basis of this dissertation:

The Michigan Gas Association for the financial assistance through their fellowship program at the University of Michigan.

Assistant Professor M. Rasin Tek, chairman of the doctoral committee, for his sincere interest and useful advice, and for his donation of time.

Associate Professor Donald T. Greenwood for his valuable assistance, advice, constructive criticism, and for his aid in securing the use of electronic differential analyzer.

Professor Donald L. Katz for his invaluable guidance in formulating the problem, for his aid in securing the gas field data, and for his direct supervision of the MGA fellowship program.

Professor Robert R. White for his personal guidance during the initiation of the research, and for his encouragement and personal help which kept me going to see this work through.

Professor Victor L. Streeter for his interest, and for his donation of time to discuss the problem.

Miss M. Elaine Willans and Mrs. Celeste Hussey for the help in preparing the text material in the final form. The UMRI Technical Illustration Office personnel for doing the drawings. The UMRI Reproduction Department personnel for making the final reproduction of this dissertation.

TABLE OF CONTENTS

	Page
ACKNOWLEDGEMENTS	ii
LIST OF TABLES	vii
LIST OF FIGURES	viii
NOMENCLATURE	xiii
ABSTRACT	xvii
I. INTRODUCTION	1
a. General	1
b. Literature Review	1
c. Purpose of the Research	3
II. THEORETICAL DEVELOPMENT	4
a. Mathematical Model	4
b. Partial Differential Equation Governing the Liquid Flow Through a Porous Medium.	6
c. Boundary Conditions and Simulation Equations	7
d. Analog Simulation	11
III. BASIC STUDIES USING THE DEVELOPED METHOD	20
a. Equipment	21
b. Pressure Case for an Aquifer of Limited Extent	21
c. Pressure Case of Infinite Aquifer	29
d. Rate Case of Infinite Aquifer	32
e. Volume Case of Infinite Aquifer	34
IV. APPLICATIONS FOR AQUIFER BEHAVIOR STUDY	35
a. Isolated Field	35
i) Effect of Permeability on Water-Return Ability for a Limited Aquifer	35
ii) Effect of Aquifer Size on Water-Return Ability	37

Page

iii) Effect of Phase Shift in Pressure Cycle on Water-Return Ability 39

iv) Effect of Twilight Zone Resistance 41

v) Effect of Areal Shape of Reservoir 42

b. Effect of a Fault on Unit Step Responses 47

i) Constant Terminal Rate Case with a Fault 47

ii) Constant Terminal Pressure Case with a Fault 49

iii) Three Identical Reservoirs on a Delta 53

iv) Use of the Constructed Unit Step Response Curves 56

c. Interference Among Two or More Fields Situated on a Common Aquifer 56

i) Interference Theory 57

ii) The Effect of Flux at Field A on Fields C and D 57

iii) The Effects of Fluxes at Fields C and D on Field A Performance 60

iv) The Effects of Fluxes at Fields C, D, and E on Field A Performance 62

d. Moving Boundary Problem 69

i) Partial Differential Equation 69

ii) Approximate Solution and Performance 70

iii) Use of the Instantaneous Solution 74

(A) Instantaneous Point and Line Source Solutions to Diffusivity Equation 77

(B) Uniform Cylindrical Surface Source Moving Radially (Radial Flow) 78

Page

(C) Ring Source Moving Radially 81
(D) Nonuniform Cylindrical Surface Source Moving Radially (Flow in all Directions) 82
(E) Radially Growing Disk Source on an Infinite Aquifer of Infinite Thickness 85
(F) Solutions for Finite Thickness of Aquifer Sand 86

iv) Unit Step Responses of Growing Disk Source Model for Finite Aquifer Thickness 87

(A) Unit Volume Step Response 87
(B) Unit Pressure Step Response 89

V. ANALYSIS OF RESERVOIR VARIABLES 93

VI. THEORETICAL CORRELATION OF AQUIFER GAS STORAGE PERFORMANCE 99

a. Cylindrical Flux Area with Linear Cumulative Flux Function 99

b. Cylindrical Flux Area with Quadratic Cumulative Flux Function 100

c. Disk Flux Area with a Cumulative Flux Function 103

VII. OTHER USES OF ELECTRONIC DIFFERENTIAL ANALYZER FOR RESERVOIR ENGINEERING PROBLEMS 110

a. Computation of Convolution Integrals 110

b. Gas Content as Input Signal 110

c. Effect of Gas Flow Resistance on Water Flux 111

d. Time-Varying Twilight Zone Resistance 113

e. Effect of Thick Twilight Zone 114

f. Oil Field Pressure Decline from Production Data 114

Page

VIII. APPLICATIONS TO OTHER CHEMICAL ENGINEERING TRANSIENT PROBLEMS 116

a. Reactor 116

b. Wetted Wall Column 117

c. Jacketed Heating Vessel 117

d. Flow Through Complex Piping System 118

IX. SUMMARY AND CONCLUSIONS 119

APPENDIX I. An Example of Detail Derivation for an Aquifer Simulation Circuit from Transfer Function Expression. 125

APPENDIX II. Electronic Differential Analyzer Circuits Referred in the Thesis. 130

APPENDIX III. The Electronic Differential Analyzer Suitable for Reservoir Engineering Study. 150

REFERENCES 152

LIST OF TABLES

Table		Page
I	Comparison of Analog Results with Theoretical Cumulative Flux Function for Sinusoidal Pressure Variation ($t_D = 7.52\ \theta$)	28
II	Comparison of Analog Results with Theoretical Cumulative Flux Function for Constant Pressure Case, ($r_D = \infty$, $K = 0.1$, $a = 1$)	30
III	Comparison of Analog Results with Theoretical Pressure Change Function for Constant Rate Case, ($r_D = \infty$, $K = 5$, $a = 4$)	31
IV	Comparison of Analog Results with Theoretical Pressure Change Function for Constant Rate Case, ($r_D = \infty$, $K = 0.1$, $a = 1$)	32
V	Comparison of Analog Results with Theoretical Pressure Change Function at $r_D = 15$ for Constant Rate Case (Infinite Aquifer) Using Volume Variation as Input Signal	34
VI	Comparison of Constant Rate Case Solution to a Non-circular Geometry (Figure 17) and Equal-area Circular Geometry	48
VII	Influence of Field A on Fields C and D ($a = 4$ and $b = 10^{-4}$)	60
VIII	Volume Variations of Fields C and D	62
IX	Pressure Variations to Find Cumulative Flux at Field A	63
X	Volume Variation of Field E	67
XI	Unit Volume Step Response to get Pressure Change Function for Growing Disk of Finite Aquifer Thickness,	89

LIST OF FIGURES

Figure		Page
1	Radial Flow Model	5
2	Graphical Integration for the Cumulative Flux Function with Arbitrary Pressure Variation	5
3	Overall Blockdiagram of the Analog Simulation Arrangement	12
4	General Analog Simulation Circuit	15
5	Input-Output Relationships for the Different Reservoir-Terminal Conditions	19
6	Electronic Differential Analyzers Arranged for Pressure Case with a Fault in the Aquifer	21
7	LM 10 Circuit Diagram for $r_D = 10$ to get Cumulative Flux Function	24
8	Comparison of the Analog Result with Theoretical Value to a Constant Pressure Case, $r_D = 10$	25
9	Specified Pressure Variation in Field A and the Generated Function	26
10	Comparison of Analog Results with Digital Results for Field A ($r_D = 10$)	27
11	Constant Rate Case Solution as a Function of Location and Time ($r_D = \infty$)	33
12	Effect of Permeability on Water-Return Ability for Limited Aquifer ($r_D = 10$)	36
13	Effect of Aquifer Size on Water-Return Ability	38
14	Effect of Phase Shift in Pressure Cycle on Water-Return Ability	40
15	Radial Flow Model with Twilight Zone Resistance	42

Figure		Page
16	Errors Introduced by Added Resistance due to Water-Gas Zone	44
17	A Noncircular Reservoir Model	45
18	Radial Flow Model with a Fault at $(\frac{d}{r_g})$	45
19	Constant Rate Case Solution with a Fault at r_D	46
20	Overall Operations Required for Pressure Case with a Fault in the Aquifer	50
21	Arrangement of Equipment for Pressure Case with a Fault in the Aquifer	50
22	Constant Pressure Case Solution with Fault at r_D	52
23	Constant Rate Case Solution for Three Identical Reservoirs on a Delta	54
24	Constant Pressure Case Solution for Three Identical Reservoirs on a Delta	55
25	Reservoir Pore Volume Variation for Field A Considering the Interference of Fields C and D	58
26	Reservoir Pore Volume Variation for Field A Considering the Interference of Fields C, D, and E	61
27	Horizontal Radial Plug Flow Moving Boundary Model	71
28	Moving Boundary Dimensionless Time Versus Actual Time	71
29	Pressure Gradient at the Reservoir as a Function of Dimensionless Time	73
30	Approximate Gas Bubble Growth with Time for Constant Pressure of Infinite Aquifer	75
31	Approximate Gas Bubble Growth with Time for Constant Pressure Case of Infinite Aquifer (For Fixed or Growing Radius)	76

Figure		Page
32	Line Source from Point Sources	79
33	Uniform Cylindrical Surface Sources from Line Sources	79
34	Ring Source from Point Sources	83
35	Shape of the Gas Cap Rock	83
36	Nonuniform Cylindrical Surface Source from Ring Sources	84
37	Disk Source from Concentric Ring Sources	84
38	Constant Pressure Case Solution to Growing Disk Model of Finite Aquifer Thickness	92
39	Illustration of Unit Pressure Step Response Curves	95
40	Reservoir Pore Volume Versus Time Integral of Pressure for Field B	101
41	Gas Reservoir Pore Volume Variation for Field B	104
42	Aquifer Gas Storage Performance Curve for Field B	106
43	Comparison Between Field B Data and Predicted Pore Volume	108
44	Comparison Between Observed and Predicted Pressure for Field B	109
45	Cross Sectional View of a Gas Storage Reservoir	112
46	LM 10 Circuit Diagram for $r_D = 10$ to get Cumulative Flux Function with Annual Sinusoidal Pressure Variation	131
47	LM 10 Circuit Diagram for $r_D = \infty$ to get Cumulative Flux Function	132

Figure		Page
48	LM 10 Circuit Diagram to get Cumulative Flux Function for Infinite Aquifer	133
49	LM 10 Circuit Diagram for $r_D = \infty$ to get Pressure Change Function ($r_D = 1$)	134
50	LM 10 Circuit Diagram to Get Pressure Change Function at $r_D = 15$	135
51	LM 10 Circuit Diagram to get Cumulative Flux Function ($r_D = \infty$)	136
52	LM 10 Circuit Diagram to get Cumulative Flux Function with a Fault in the Aquifer at $\frac{2d}{r_g} = 2.46$	137
53	LM 10 Circuit Diagram of Unit A to get Flux Function	138
54	LM 10 Circuit Diagram of Unit B for $r_D = 2$ to get Pressure Change Function	139
55	LM 10 Circuit Diagram to get Cumulative Flux Function ($r_D = \infty$)	140
56	LM 10 Circuit Diagram of Unit B for $r_D = 4$ to get Pressure Change Function	141
57	LM 10 Circuit Diagram of Unit B for $r_D = 8$ to get Pressure Change Function	142
58	LM 10 Circuit Diagram to get Pressure Change Function Using Volume as Input for Growing Disk Model of Finite Aquifer Thickness	143
59	Gas Reservoir Pore Volume Variation from Gas Content as Input Signal	144
60	Circuit Diagram for the Effect of Linear Gas Flow Resistance on Water Flux	145

Figure		Page
61	General Circuit to get Cumulative Flux with Time-Varying Twilight Zone Resistance	146
62	Simulation of Gas Storage Aquifer with Thick Low Permeability Twilight Zone	147
63	Undersaturated Oil Field Pressure Decline from Oil Production Data	148
64	Interference Between Undersaturated Oil Fields	149

NOMENCLATURE

A	Operational amplifer gain, dimensionless
a	Constant relating $t_D = a.\theta$, or $(\frac{k}{c\phi\mu r_g^2})$ (1/month)
a_n	Roots of characteristic equation(4)
b	A group of reservoir constants, $(\frac{\mu}{2\pi kh})$ psi $\frac{\text{month}}{\text{cu ft}}$
c	Sum of aquifer water and formation compressibility vol/vol/atm.
c'	Sum of aquifer water and formation compressibility vol/vol/psi.
C_e	Electrical Capacitor, microfarad (mfd)
D	Differential operator, d/dt_D
d/r_g	Dimensionless distance to a fault
e(s)	Laplace Transform of E
e_s	Summing junction voltage, volts
E	Rate function
erf(x)	Error function defined. $\frac{2}{\sqrt{\pi}}\int_o^x e^{-\lambda^2} d\lambda$
$f_1(s)$	Laplace Transform of Cumulative flux function for constant pressure case
$f_1'(s)$	Laplace transform of pressure change function of constant rate case
g	Laplace transform of G
G	Pressure function
h	Aquifer water sand thickness, ft
I_o	Bessel function of the 1st kind of an imaginary argument and zero order

J_o, J_1	Bessel functions of the first kind, of zero and 1st order, respectively
k	permeability, darcy
K	Computer time constant
K_o, K_1	Bessel function of second kind of zero and first order respectively
$(\frac{k}{\mu})_1$	Mobility in the outer aquifer
$(\frac{k}{\mu})_2$	Mobility in the twilight zone
L	Laplace Transform
Δl	Thickness of twilight zone
LM 10	Sterling model electronic differential analyzer
n	Gas content, lb moles
P	Pressure
P_o	Amplitude of sinusoidal pressure, psi
P'	Pressure across the twilight zone
P_g	Pressure at the gas field
P_f	Closed reservoir pressure
P_s	Flowing sand face pressure
P'_{tD}	Dimensionless pressure change function for constant terminal rate case, tabulated in the literature. (4)(12)(13)(14)
P_{tD}	Pressure change function with arbitrary terminal rate, cu ft/month
P_{tDAa}	Pressure change function at A by A's production
P_{tDAb}	Pressure change function at A by B's production

P'_{tD}	Growing disk model unit volume step response for pressure change, dimensionless
$(\frac{\partial P'}{\partial z})_{z=0}$	Vertical pressure gradient at z = 0 for unit step pressure, atm/ft
q	Strength of source
Q	Gas flow rate
Q'_{tD}	Dimensionless cumulative flux function for constant pressure case, tabulated in the literature (4)(12)(13)
Q_{tD}	Cumulative flux function with arbitrary pressure, psi
Q''_{tD}	Growing disk model unit pressure step response for cumulative flux, dimensionless
r	Radius of aquifer, cm
r'	Radius of aquifer, ft
r_g	Gas field radius
r_D	r/r_g, dimensionless radius
R	Gas constant, 10.73 psi cu ft/lb-mole °R
R_f	Feedback resistor, megohm
s	Laplace transform variable
S_F	Gas cap rock shape factor, $\frac{\phi\pi}{2S_f}$
S_f	r_g^2/y, where y is the height of the gas bubble
S_1	Time integral of pressure, psi-wk
S_2	Double time integral of pressure, psi-wk^2
$sf_1(s)_{Aa}$	Transfer function corresponding to the cumulative flux contribution at A due to the pressure change at A by A's production
t_D	Dimensionless time (see also nomenclature "a")

T	Temperature, °R
v	Velocity vector, cm/sec
V_g	Reservoir pore volume, million (MM) cu ft
V_o	Initial reservoir pore volume, MM cu ft
W	Cumulative water flux, cu ft
x, y, z	Cartesian coordinates, ft
x', y', z'	Location of source or sink, ft
z	Gas compressibility factor, or cartesian coordinate
λ	Dummy variable of integration
μ	Viscosity of water, cp
ρ	Density of water, lb/cu ft
θ	Time, month
θ'	Time, second
θ_A	Angle, dimensionless
ω	Frequency, dimensionless, or 1/dimensionless time
τ	A time variable
ϕ	Fractional void space or porosity

STUDY OF UNSTEADY STATE BEHAVIOR OF GAS STORAGE RESERVOIR ON ELECTRONIC DIFFERENTIAL ANALYZER

by Hyungduk D. Yoo

ABSTRACT

The purposes of this study are to develop a gas storage aquifer simulation method on an electronic differential analyzer to handle any arbitrary terminal reservoir conditions and to improve the understanding of the unsteady state behavior of an aquifer using the developed method as a tool, whenever needed. From the simulation, the reservoir volume change or the reservoir pressure change is to be obtained. The importance of such study arises from the standpoint of safeguarding the gas storage operation and for the interpretation of the reservoir engineering data. This study has common interest to both underground gas storage and oil production research.

In the first part, the analog simulation method on an electronic differential analyzer is presented. The simulation is essentially equivalent to the continuous computation of a convolution integral. From the mathematical constant terminal case solution based on a theoretical model study, a proper transfer function is set up on an electronic differential analyzer to obtain the desired solution by feeding in the specified reservoir terminal conditions as an input signal. The specification of the reservoir terminal conditions may be the reservoir pressure, the pore volume or the water flux. The results of the developed method are compared, for the basic cases, with the theoretical solution.

In the second part, the developed method is used as a tool for the theoretical aquifer behavior study. The study is categorized into the isolated fields, the effect of a fault on the unit step responses, the

interference among two or more fields on a common aquifer and the moving boundary problems.

In the third part, the analysis of reservoir variables and a theoretical correlation method for aquifer gas storage field are presented. The correlation method is based on the analysis of the unit impulse response characteristic of the reservoir system. Other possible uses of an electronic differential analyzer for reservoir engineering problems are given. The applications to other chemical engineering transient problems of linear characteristics are also discussed.

The following general conclusions can be drawn from the study:

1) The developed analog simulation method of an aquifer on an electronic differential analyzer is an excellent method to study the transient behavior of an underground gas storage reservoir. It operates continuously, quickly, and economically.. The accuracy is well within the range usually required for typical gas storage operations.

2) The results obtained, based on the theoretical model study for various cases encountered in the gas storage operations, are given in figures and tables to improve the understanding of aquifer behavior.

3) Because of the difficulties involved in the mathematical formulation of the actual problems, and the large number of reservoir variables, there is no reason why one should stick to the model concept based on a series of assumptions. The model study can only be a guide to select a reasonable unit step response curve of a reservoir system.

4) The developed analog simulation method can be applied to any other physical linear system to analyze its transient behavior. In most reservoir problems, the pseudo-linearity assumption of the system response seems valid.

I. INTRODUCTION

a. General: The pressure volume variations occuring in natural gas reservoirs converted to storage operations are of interest from the standpoint of both the long range economics of gas storage operations and the short range interpretation of reservoir engineering data.

A large number of gas producing sands, eventually converted to gas storage use, occur with fluid communication with a large body of water-bearing formation called aquifer surrounding or underlaying the gas reservoir. As the pressure in the gas bubble adjacent to the aquifer changes by a cyclic variation due to seasonal injection and withdrawal of the natural gas, the motion of aquifer gas interface causes the net volume available for gas storage to fluctuate, grow or shrink, and for this reason a gas storage reservoir may be considered as a flexible tank. Consequently, the pressure-volume behavior of the gas reservoir subjected to water drive is, in general, governed by the average pressure within the gas reservoir, compressibility of the gas and expansibility of the aquifer fluid and the physical properties of both the gas-bearing sand and the surrounding aquifer formation. The knowledge of the aquifer behavior or the water movement in and out of the gas storage reservoir from the reservoir pressure-production data is necessary to design an underground gas storage reservoir or to safeguard its future performance. Certain design aspects of the development of gas storage fields are treated by Katz, Vary, and Elenbaas.[1] The study of the Prediction of Gas Storage Reservoir Behavior on digital computer is made by K.H. Coats.[2]

b. Literature Review: Since the early 1930's the solution to radial diffusivity equation for a limited aquifer for constant terminal conditions has been known.[3] The solution for the constant terminal conditions for an infinite aquifer was published in 1949.[4]

The problem of handling the unsteady flow of water through a porous medium with time-varying boundary conditions has been studied by many investigators through the use of graphical[5], digital computing

techniques[6] or on an R-C type electrical analog machine called a reservoir analyzer.[7][8][9][10][11] The digital computer performs a series of arithmetic calculations to superimpose the solutions of constant terminal conditions, while the R-C type analyzer permits the simulation of the continuous medium by means of "lumped-cell" electrical resistance and capacitance elements based on finite difference approximations. The graphical method is based on the convolution integral solution of the partial differential equation.

No information has been reported in the literature on the simulation of the aquifer behavior on a general purpose electronic differential analyzer, other than the reports and papers written up by the author.

As for the general literature survey of the gas storage reservoir engineering and its basic mathematics and, also, the digital computer techniques, reference is made to Coats' thesis (April, 1959).[2] There are several literature sources which contain the engineering solutions to the radial diffusivity equation with constant terminal conditions. Van Everdingen and Hurst[4], Chatas[12], Katz[13], and Mortada[14] are the typical sources of this information for ready engineering uses. The basic mathematical studies for analytical solutions to the radial diffusivity equation for a variety of boundary conditions, applicable to reservoir engineering problems, are compiled in several books: Muskat[3], Carslaw and Jaeger[15], and Churchill.[16]

With respect to the moving boundary problems, some recent studies have been reported for heat conduction problems by Otis[17], Bailey and Larkin[18], and Ramey.[19]

The impulse function concept is fully discussed by Gardner and Barnes[20], and Josephs.[21] For the basic analog computer techniques, reference must be made to the standard textbooks by Johnson[22], and Korn and Korn.[23]

The unsteady state gas flow through a porous medium has been studied by many investigators. One of the first researchers is Bruce.[24]

Very recently, Hutchinson[25] presented an empirical technique for water drive analysis. The date of conception of a similar idea, which is impregnated in this thesis, was long before the Hutchinson's paper.

c. Purpose of the Research The general purpose of the research was to develop a method of simulating a gas storage aquifer of fixed radius on an electronic differential analyzer to study the unsteady state behavior of the underground gas storage reservoir. The object of such simulation is to obtain the flux of water or the change in pressure at the reservoir continuously and economically. In order to accomplish the general purpose, several sub-problems were studied, and the specific objectives were the following

1) A method of simulating a gas storage aquifer of fixed radius on an electronic differential anlyzer to handle the arbitrary terminal conditions regardless of the aquifer size for the terminal pressure case and the terminal rate or volume case.

2) Application of the developed simulation method for aquifer behavior study which includes the treatment of isolated gas storage field, fault case, interference of more than two fields on a common aquifer, and moving boundary problems.

3) Analysis of reservoir variables and theoretical correlation method for aquifer gas storage field performance.

II THEORETICAL DEVELOPMENT

One can approach the gas storage reservoir problems by (a) considering purely mathematical models and relationships to obtain the system response or by (b) correlation of the past reservoir performance history without setting up a definite working model, but on the basis of logical analysis of the system response characteristics of the reservoir in consideration. The correlation approach is discussed fully in the last part of this thesis, while the model study approach is presented here.

a. Mathematical Model: As a theoretical approach to study how the aquifer behaves, one can set up a mathematical model, derive an equation governing the flow of brine through a porous medium, and solve the partial differential equation with the given boundary conditions. In doing this a series of assumptions must be made.

It is generally understood that a uniform cylindrical surface source model is acceptable for a fixed radius gas storage reservoir-aquifer system. The gas storage reservoir (R) is considered sitting on an aquifer as shown in Figure 1. The basic assumptions necessary to adopt this study model are:

1) The model in consideration is circular with radial geometry, and the flow of aquifer fluid is strictly radial. The aquifer radius can be of limited or infinite extent.

2) The permeability, porosity, viscosity of the brine (aquifer fluid), and the compressibility of the brine and the formation are constant.

3) The blanket sand is not thick enough to give appreciable vertical pressure distribution.

4) The gas-water interface is fully segregated and the displacement of the gas by water, or water by gas, is considered to be piston-like.

5) The effect of twilight zone resistance and the areal reservoir geometry effects are small.

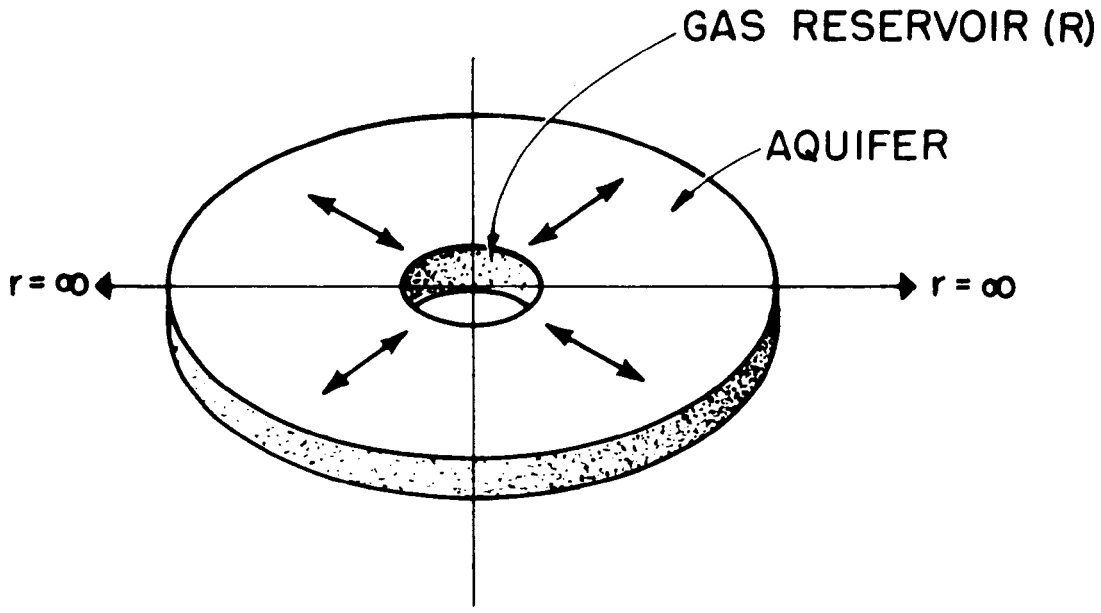


Fig. 1 - Radial flow model.

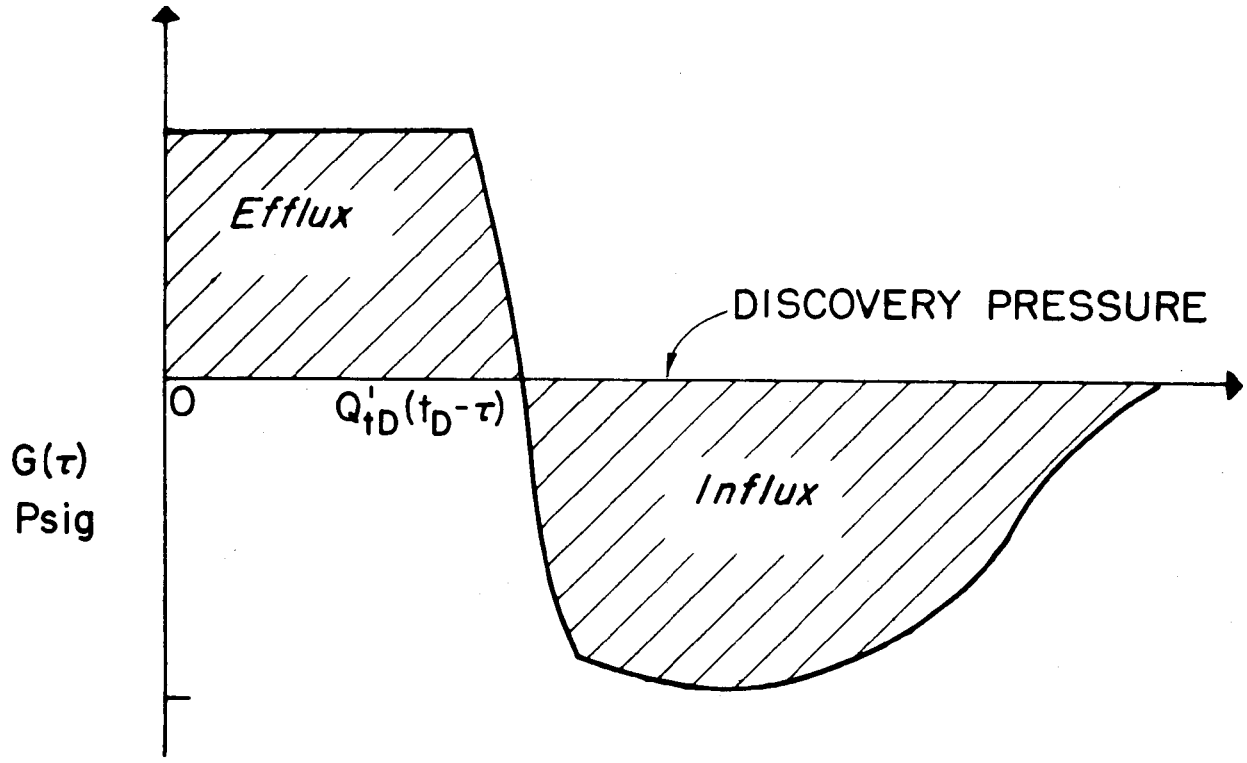


Fig. 2 - Graphical integration for the cumulative flux function with arbitrary pressure variation.

b. Partial Differential Equation Governing the Liquid Flow Through a Porous Medium:

For the mathematical model adopted for the study, a partial differential equation called radial diffusivity equation (4) can be derived by combining the equation of continuity (1), Darcy's flow equation (2), and the equation of state of brine (3).

$$\text{div}\,(\rho\, v) = -\phi \frac{\partial \rho}{\partial \theta'} \tag{1}$$

$$v = -\frac{k}{\mu} \text{grad}\,(P) \tag{2}$$

$$\rho \cong \rho_o \left[1 - c\,(P_o - P) \right] \tag{3}$$

$$\frac{\partial^2 P}{\partial r^2} + \frac{1}{r} \frac{\partial P}{\partial r} = \frac{c\phi\mu}{k} \frac{\partial P}{\partial \theta'} \tag{4}$$

In these equations the following symbols are used:

c	Compressibility of brine plus formation, vol/vol/atm
k	Permeability, darcy
P	Pressure, atm
r	Radial distance, cm
v	Velocity, cm/sec
ϕ	Porosity of the porous medium, dimensionless
ρ	Density of brine, gr/cu cm
θ'	Time, sec
μ	Viscosity, cp

Equation (1) is nothing more than a material balance equation about an infinitesimal volume element, and this equation holds true as long as the porosity is uniform throughout the porous medium. The Darcy's equation is known to hold as long as the flow velocity does not become excessive and turbulence does not set in. Equation (3) is an expression of the equation of state for brine when c is very small.

Equation (4) can be rewritten in the following simpler form.

$$\frac{\partial^2 P}{\partial r_D^2} + \frac{1}{r_D}\frac{\partial P}{\partial r_D} = \frac{\partial P}{\partial t_D} \qquad (5)$$

where,

$$r_D = \frac{r}{r_g}, \quad \text{dimensionless radius}$$

$$t_D = \frac{k\theta}{c\phi\mu r_g^2}, \quad \text{dimensionless time.}$$

Equation (5) is the working partial differential equation derived based on the assumptions listed in the previous page. For the full description of the fundamentals of gas storage reservoir performance, the reader is referred to Coats' thesis.[2]

c. Boundary Conditions and Simulation Equations: The two basic cases encountered in most reservoir engineering studies are constant terminal pressure and constant terminal rate cases. If the pressure is specified at the reservoir boundary, the problem may be referred to as terminal pressure case. On the other hand, if the rate is specified, one would have the terminal rate case. In gas storage a variable pressure case often applies; for this case the pressure at the aquifer boundary is specified as a function of time.

For the pressure case the mathematical statements of the boundary conditions are:

$$P(1, t_D) = G(t_D)$$

$$P(\infty, t_D) = 0$$

$$P(r_D, 0) = 0$$

With these boundary conditions, the Laplace transform of the solution to equation (5) is given as the following:(4)

$$Q_{tD}(s) = \frac{1}{s}\{g(s)\}\left\{\frac{\sqrt{s}\cdot K_1(\sqrt{s})}{K_0(\sqrt{s})}\right\}$$

$$= g(s)\left\{\frac{s\cdot K_1(\sqrt{s})}{s^{3/2}\cdot K_0(\sqrt{s})}\right\} = g(s)\{s\cdot f_1(s)\} \qquad (6)$$

where $Q_{tD}(s)$ is the Laplace Transform of the cumulative water flux function; and g(s) is the Laplace Transform of the pressure function $G(t_D)$. It can be shown that the above equation may be presented in the following form

$$Q_{tD} = \int_0^{t_D} \left(\frac{\partial P}{\partial r_D}\right)_{r_D=1} dt_D = \int_0^{t_D} \frac{dG}{d\tau}\cdot Q'_{tD}(t_D-\tau)\,d\tau \qquad (7)$$

where Q'_{tD} is the constant pressure case cumulative flux function. The graphical interpretation of this convolution integral at a time t_D is given in Figure 2.

Equation (6) can be rewritten to take the form:

$$\frac{Q_{tD}(s)}{g(s)} = s\cdot f_1(s) \qquad (8)$$

Equation (8) becomes a useful equation on an electronic differential analyzer and is called a simulation equation for terminal pressure case. Once the $Q_{tD}(t_D)$ function is found, the cumulative water flux or the reservoir volume change from the initial reservoir pore volume can be calculated by the following equation.

$$W = (2\pi r_g' h)\frac{k}{\mu}\int_0^{\theta}\left(\frac{\partial P}{\partial r}\right)_{r_g} d\theta = 2\pi r_g'^2 h C' \phi Q_{tD} \qquad (9)$$

Instead of specifying the reservoir pressure, one can specify the rate or flux at the reservoir boundary. With the following boundary conditions.

$$\frac{\partial P}{\partial r_D}(1, t_D) = -E(t_D)$$

$$P(\infty, t_D) = 0$$

$$P(r_D, 0) = 0$$

the Laplace Transform of the pressure change function at the distance of r_D can be shown to be:[4]

$$\bar{P}_D(r_D, s) = \{e(s)\}\left\{\frac{s \cdot K_0(r_D\sqrt{s})}{s^{3/2} \cdot K_1(\sqrt{s})}\right\}$$

$$= e(s)\left\{s \cdot f_1'(r_D, s)\right\} \qquad (10)$$

The corresponding equations of the terminal rate case to equations (7) and (8) of the terminal pressure case are:

$$P_{xD}(r_D, t_D) = \int_0^{t_D} \frac{dE}{d\tau} \cdot P'_{xD}(t_D - \tau)\, d\tau \qquad (11)$$

where P'_{tD} is the constant rate case pressure change function, and

$$\frac{P_{xD}(r_D, s)}{e(s)} = s \cdot f_1'(r_D, s) \qquad (12)$$

The actual pressure change is then

$$P(r, \theta') = \left(\frac{\mu}{2\pi kh}\right) \cdot P_{xD}(r_D, t_D) \qquad (13)$$

As shown in equations (9) and (13), the problem of finding the pressure change or the reservoir pore volume change narrows down to finding Q_{tD} and P_{tD}.

A careful examination of the equations reveals that $f_1(s)$ and $f'_1(r_D, s)$ are the Laplace Transforms of the constant terminal pressure case cumulative flux function and the constant terminal rate case pressure change function, respectively. Equations (8) and (12) will be used as the working equations of the analog simulation. This analog simulation is equivalent to the computation of the superposition or convolution integral expressed in equation (7) or (11).

At this point the concept of the impulse function must be explained in relation to the constant terminal conditions, since the impulse functions are basic tools for linear system analysis. The unit impulse can be defined as a pulse of infinite amplitude and zero duration. The unit impulse is characterized by the fact that the area under the pulse is

unity when the pulse is plotted against time. When the terminal reservoir condition is subjected to a unit step function - e.g. constant unit terminal pressure, the system response becomes the unit step response because $g(s)$ is $1/s$ and $sg(s)$ is unity to give $Q_{cD}(s) = f_1(s)$ in equation (8). It is noted that the unit impulse can be considered as the derivative of a step function. In this thesis, frequently unit impulse responses are mentioned because we are interested in $sf_1(s)$ or $sf_1'(s)$, and they are referred to the derivatives of the constant terminal case solutions.

d. Analog Simulation. The essential feature of analog simulation on an electronic differential analyzer is to obtain the desired reservoir performance as an output by feeding in the known information as an input signal. The known information may be the arbitrary reservoir pressure variation, the reservoir pore volume variation, or the water flux. A pictorial representation of the overall analog simulation arrangement is shown in Figure 3.

The discussion below is devoted to the representation of a transfer function on an electronic differential analyzer. Considering equation (8) which has been derived for the terminal pressure case,

$$\frac{Q_{tD}(s)}{g(s)} = s \cdot f_1(s) \qquad (8)$$

it is found that $f_1(s)$ is the Laplace Transform of the constant terminal pressure case cumulative flux function or the pressure case unit step response. Therefore, $sf_1(s)$ can be approximated from the solution of the constant terminal pressure case as the system is a physical problem. Since the initial value of the cumulative flux function is zero, from the well-known property of the Laplace Transform rule[1b] of a derivative, $sf_1(s)$ can be expressed better in the following form:

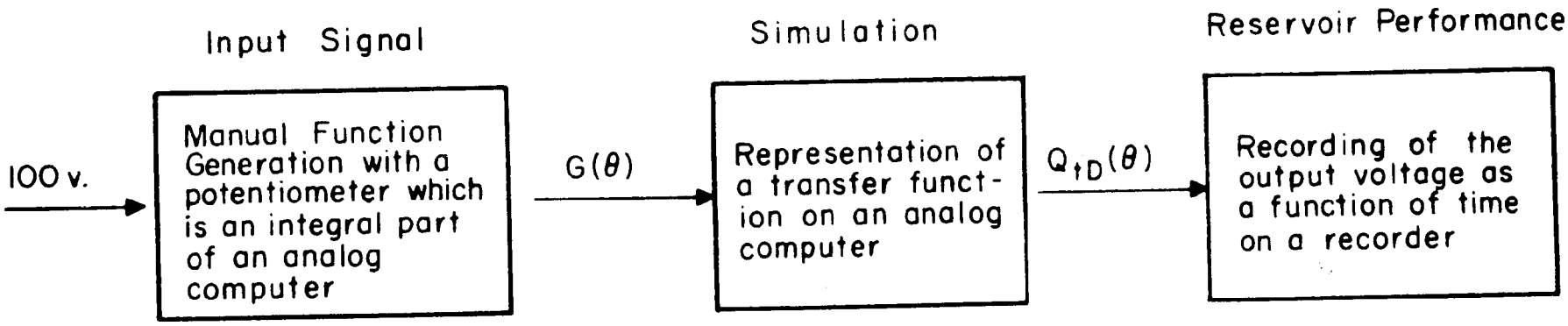


Fig. 3 - Overall block diagram of the analog simulation arrangement.

$$\mathcal{L}\left\{\frac{dQ'_{xD}}{dt_D}\right\} = s f_1(s) - 0$$

This relationship can be used to approxima e $sf_1(s)$ from $\left(\frac{dQ'_{xD}}{dt_D}\right)$ or directly from Q'_{tD}.

Suppose that $sf_1(s)$ is approximated as a sum of a_o, a_1/s, $\frac{a_2}{1+\frac{s}{b_2}}$, and $\frac{a_3}{1+\frac{s}{b_3}}$, or

$$\frac{Q_{xD}(s)}{g(s)} = s.f_1(s) = a_o + \frac{a_1}{s} + \frac{a_2}{1+\frac{s}{b_2}} + \frac{a_3}{1+\frac{s}{b_3}} \quad (14)$$

then, one can write:

$$Q_{xD}(s) = a_o g(s) + \frac{a_1 g(s)}{s} + \frac{a_2 g(s)}{1+\frac{s}{b_2}} + \frac{a_3 g(s)}{1+\frac{s}{b_3}}$$

Therefore, the inversion of $Q_{tD}(s)$ is the sum of the inversion of the individual terms:

$$Q_{xD}(t_D) = \left[Q_{xD}(t_D)\right]_o + \left[Q_{xD}(t_D)\right]_1 + \left[Q_{xD}(t_D)\right]_2 + \left[Q_{xD}(t_D)\right]_3$$

where,

$$\mathcal{L}\left\{\left[Q_{xD}(t_D)\right]_o\right\} = a_o g(s) \quad (15)$$

$$\mathcal{L}\left\{\left[Q_{xD}(t_D)\right]_1\right\} = \frac{a_1 g(s)}{s} \quad (16)$$

$$L\left\{\left[Q_{xD}(t_D)\right]_2\right\} = \frac{a_2\, g(s)}{1 + \frac{s}{b_2}} \tag{17}$$

$$L\left\{\left[Q_{xD}(t_D)\right]_3\right\} = \frac{a_3\, g(s)}{1 + \frac{s}{b_3}} \tag{18}$$

These individual terms are to be considered for their theoretical possibilities for analog simulation.

Equation (15) can be written directly in the time domain:

$$\frac{\left[Q_{xD}(t_D)\right]_0}{G(t_D)} = a_0$$

The analog simulation for this relationship is represented by amplifier No. 1 in Figure 4 to give the following input-output relationship: (Those who are not familiar with analog computers are referred to Appendix I and also to references (22) and (23).

$$+ \frac{\left[Q_{xD}(t_D)\right]_0}{G(t_D)} = a_0$$

Equation (16) needs to be written in the time domain.

Since. $Q_{tD}(0) = 0$,

$$s \cdot L\left\{\left[Q_{xD}(t_D)\right]_1\right\} = L\left\{\frac{dQ_{xD}}{dt_D}\right\}_1 = a_1\, g(s)$$

or

$$\left\{\frac{dQ_{xD}}{dt_D}\right\}_1 = a_1\, G(t_D)$$

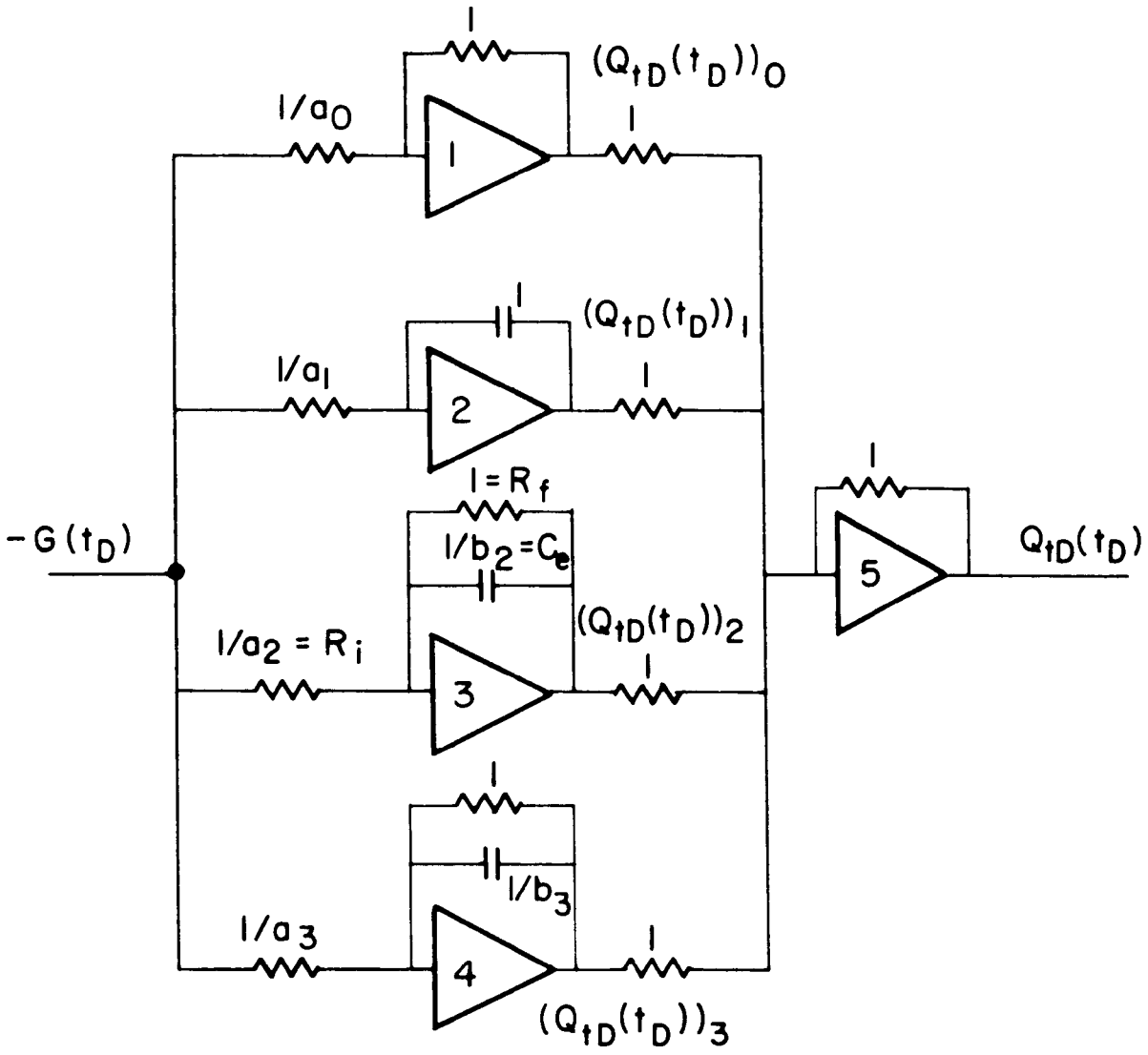


Fig. 4 - General analog simulation circuit.

or

$$\frac{[Q_{tD}(t_D)]_1}{G(t_D)} = \frac{a_1}{D}$$

where D is the differential operator $\frac{d}{dt_D}$.

The analog simulation for this relationship is given by the amplifier No. 2 in Figure 4:

$$[Q_{tD}(t_D)]_1 = +a_1 \int_0^{t_D} G(t_D)\, dt_D$$

or

$$\frac{[Q_{tD}(t_D)]_1}{+G(t_D)} = \frac{a_1}{D}$$

Equation (17) can be rewritten as:

$$\frac{s}{b_2}[Q_{tD}(s)]_2 + [Q_{tD}(s)]_2 = a_2 g(s)$$

Since $Q_{tD}(0) = 0$,

$$\frac{1}{b_2}\left[\frac{dQ_{tD}}{dt_D}\right]_2 + [Q_{tD}(t_D)]_2 = a_2 G(t_D)$$

or

$$\frac{[Q_{tD}(t_D)]_2}{G(t_D)} = \frac{a_2}{\left(1 + \frac{D}{b_2}\right)}$$

The analog simulation for this relationship is taken care of by the amplifier No. 3 in Figure 4:

$$\frac{[Q_{tD}(t_D)]_2}{-G(t_D)} = \frac{a_2}{1 + \frac{D}{b_2}} = \frac{\left(\frac{R_f}{R_i}\right)}{1 + R_f C_e D}$$

Equation (18) is much the same as equation (17). Thus, summing up the individual simulation with the amplifier No. 5, the terminal pressure case can be simulated on an electronic differential analyzer as shown in Figure 4.

The consequence of this simulation is that the equation (8) has analogous meaning on an electronic differential analyzer that can be regarded in terms of system transfer function since the transfer function is the expression that establishes the relationship of the input and output variables of a system as an operator equation. When constant pressure is fed in, the output becomes the constant pressure case solution. Once the constant pressure response check is made for a linear system, in general, the arbitrary pressure response can be obtained with the same circuit by simply feeding in the proper pressure variation.[20][21]

The terminal rate case can be handled by the identical technique on the basis of equation (12) instead of equation (8). The same general circuit shown in Figure 4 applies to the terminal rate case by feeding in the rate variation to obtain the pressure change function as an output.

Unfortunately, the rate data are not available, but in most any case the volume variation data are available. From the definition of rate,

$$e(s) = L\left\{\frac{d(V_g - V_o)}{dt_D}\right\} = s\cdot(V_g - V_o)(s) - 0$$

Substituting this equation into equation (12), one can obtain

$$\frac{P_{tD}(\gamma_D, s)}{(V_g - V_o)(s)} = s^2 f_1'(\gamma_D, s) \qquad (19)$$

Equation (19) is the analog simulation equation for the volume case. If one can approximate $s^2 f_1(r_D, s)$ and set up the transfer function as shown in Figure 4, $P_{tD}(r_D, t_D)$ can be obtained by feeding in the volume variation rather than the rates.

The three different cases of the reservoir terminal conditions are summarized and depicted in Figure 5.

When a constant terminal case solution is available, one can find the proper transfer function which can be set up on an electronic differential analyzer, the desired solution can be obtained as an output, which can be recorded as a function of time.

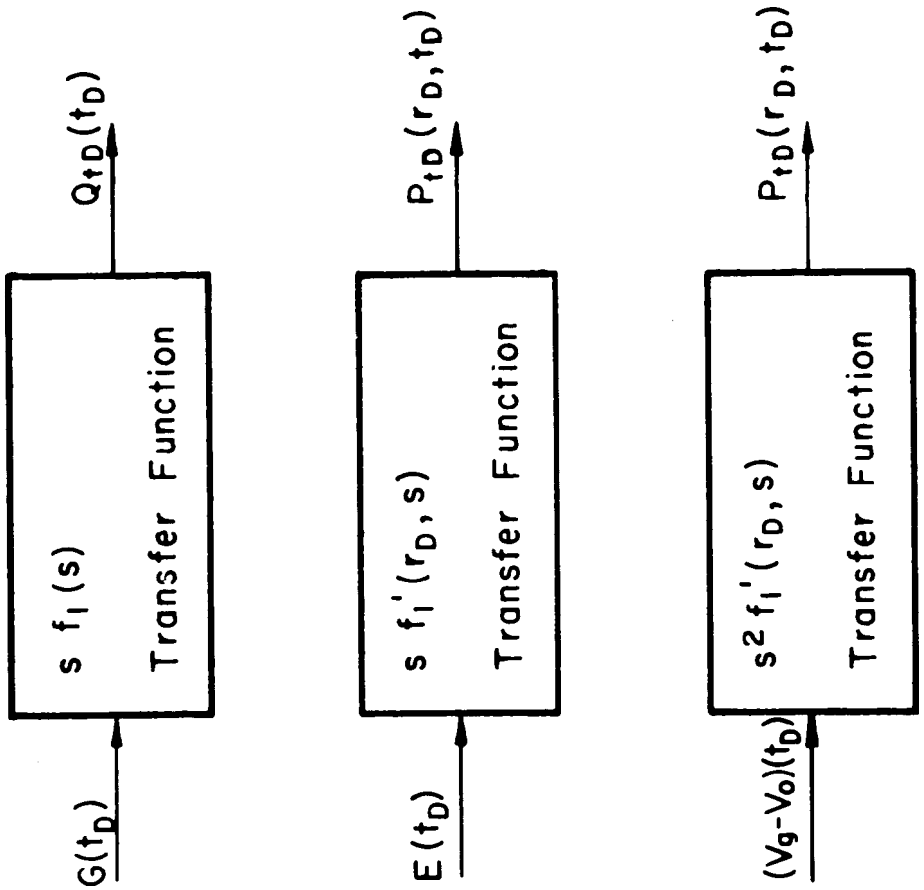


Fig. 5 — Input-output relationships for the different reservoir-terminal conditions.

III BASIC STUDIES USING THE DEVELOPED METHOD

In the previous chapter, a method of analog simulation of gas storage aquifer is developed. It is intended to use this method and compare the analog results with theoretical values as proofs of the method. Before the actual examples of the method, a brief description of the equipment is given.

a. Equipment: For the present work the Sterling model LM 10 electronic differential analyzer is used. The LM 10 electronic differential analyzer is a small computer equipped with 10 High Gain DC amplifiers and 10 ten-turn precision helipots. The function $G(t_D)$ is generated manually with a 10-turn precision helipot. The potentiometer setting is changed as a function of time to give the desired voltage by means of a vernier dial. The output is recorded by using a two-channel Brush Recorder. Figure 6 shows a photograph of the actual equipment set-up (which is used for pressure case with a fault on an infinite aquifer).

b. Pressure Case for an Aquifer of Limited Extent: As a first illustration and proof of the method, an aquifer of $r_D = 10$ is chosen. The $r_D = 10$ is a ratio of the size of the aquifer to that of the gas bubble. For this aquifer size three different checks or comparisons are made against theoretical or digitally computed values. These checks are: 1) the unit step response check with that of Van Everdingen and Hurst[4] table; 2) the application to the actual field A to check with the digital computer solution; and 3) the comparison of the response for sinusoidal pressure variation case with that of a mathematical solution.

The first step toward analog simulation is to obtain the transfer function based on the previous knowledge of unit impulse response. Fortunately, the unit step response for $r_D = 10$ is already expressed in an equation form, rather than in a tabular form. The unit step response solution for the pressure case has been reported for a limited aquifer as follows[4]:



Fig. 6 - Electronic differential analyzers arranged for pressure case with a fault in the aquifer

$$Q'_{tD} = \frac{r_D^2 - 1}{2} - 2\sum_{a_1, a_2 \cdots}^{\infty} \frac{\left(e^{-a_n^2 t_D} \right) \left(J_1^2(a_n r_D) \right)}{\left[J_0^2(a_n) - J_1^2(a_n r_D) \right] a_n^2}$$

Since the series converges very rapidly for $r_D = 10$, the first term alone gives a good approximation, and the flux function for the constant terminal pressure case for the aquifer size of $r_D = 10$ can be written as:

$$Q'_{tD} = 49.5 - 47.3\, e^{-0.0122 t_D} = 49.5 - 47.3 e^{-0.0122 a\theta} \qquad (20)$$

where "a" is a constant relating the actual time in months to the dimensionless time t_D or

$$t_D = \frac{k\theta'}{c\phi\mu r_g^2} = a\theta$$

and "a" has a unit of 1/month. It is necessary to change the dimensionless time to the actual time because the machine is running in the actual time, but in a condensed scale. For example, one month of actual reservoir time is one second of machine running time if the machine time constant K is one. In equation (20), it is important to note that Q'_{tD} is dimensionless while Q_{tD} in equation (9) has a dimension of pressure in psi. Upon taking Laplace Transform with respect to 0 and multiplying by s, equation (20) gives:

$$s f_1(s) = \left(49.5 - \frac{47.3 s}{s + 0.0122a} \right)$$

By rearranging, this equation can be written as follows:

$$s f_1(s) = 2.2 \left(1 + \frac{21.5}{1 + \frac{s}{0.0122a}} \right) \qquad (21)$$

Equation (21) has the same form as that of equation (14), for which the theoretical possibility of analog simulation has been shown in the previous chapter. Based on equation (21), an LM 10 circuit diagram for $r_D = 10$ to get cumulative flux function is obtained as shown in Figure 7. The details of obtaining the potentiometer settings and component sizes are given in the Appendix. The general feature of the circuit is the same as that of the circuit given in Figure 4.

By feeding in a constant voltage at potentiometer No. 8, which is equivalent to having a constant reservoir pressure, the response is obtained. The response is the cumulative flux function at constant pressure case, and the analog result is compared with theoretical values[4] in Figure 8. The comparison in Figure 8 shows a good agreement, and the unit step response check is essentially a calibration operation. It is possible to calibrate the response by readjusting the potentiometer settings.

Since the circuit has been established by the unit step response check, the same circuit can be used for any pressure variations by simply generating the specified pressure variation with potentiometer No. 8. Figure 9 shows the generated pressure input and the function to be generated for the actual Field A. For this pressure variation, the response is obtained and compared with the results of digital computation[7] in Figure 10. The reservoir volume is plotted against time.

In order to secure further proof of the developed method, the case of sinusoidal input pressure was studied.

Equation (7) applies to a limited aquifer when the Q'_{tD} is taken as the constant terminal pressure case solution of a limited aquifer. When

$$G(t_D) = P_o \sin \omega t_D,$$

$$Q_{tD} = \omega \int_0^{t_D} P_o \cos \omega (t_D - \tau) \cdot Q'_{tD}(\tau)\, d\tau$$

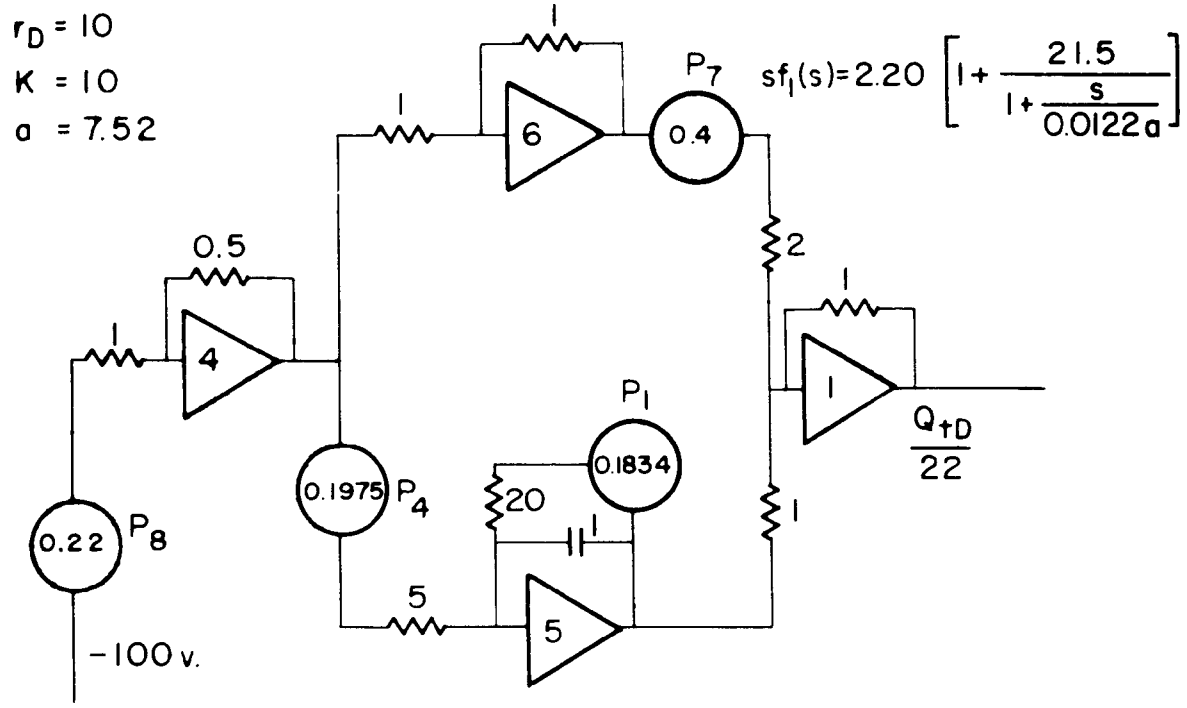


Fig. 7- LM10 circuit diagram for $r_D = 10$ to get cumulative flux function.

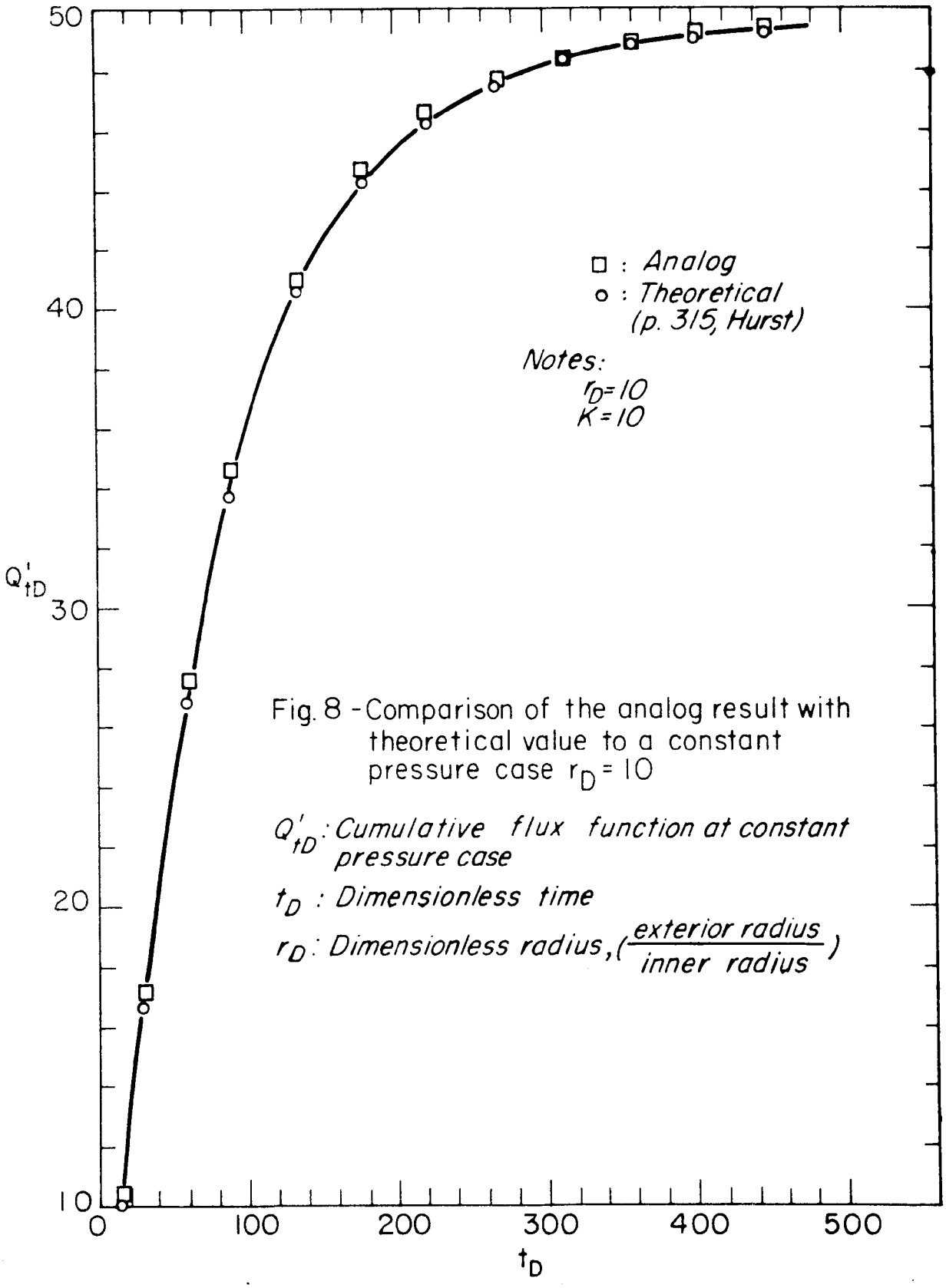


Fig. 8 - Comparison of the analog result with theoretical value to a constant pressure case $r_D = 10$

Q'_{tD} : Cumulative flux function at constant pressure case

t_D : Dimensionless time

r_D : Dimensionless radius, $\left(\frac{\text{exterior radius}}{\text{inner radius}}\right)$

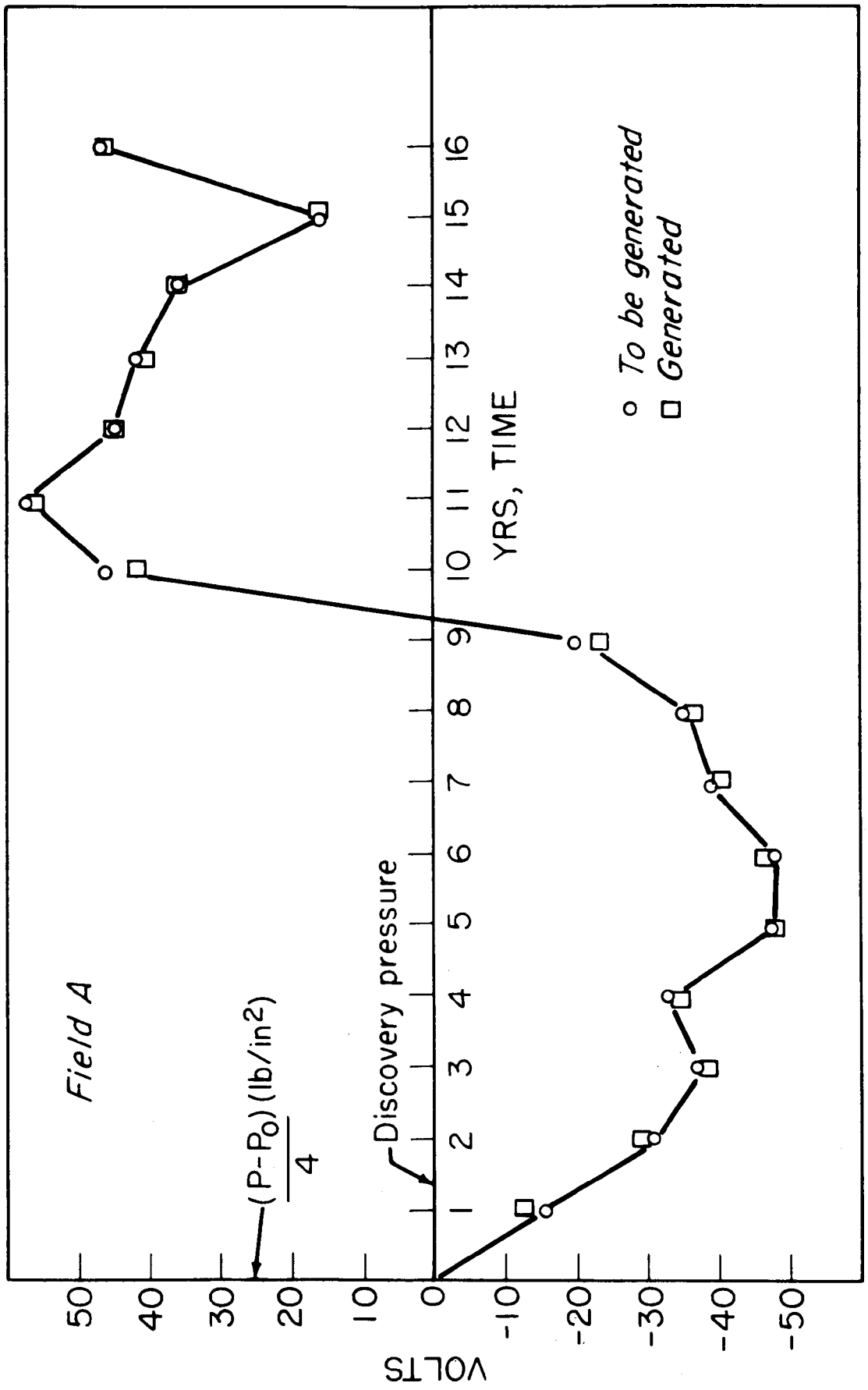


Fig. 9- Specified pressure variation in field A & the generated function

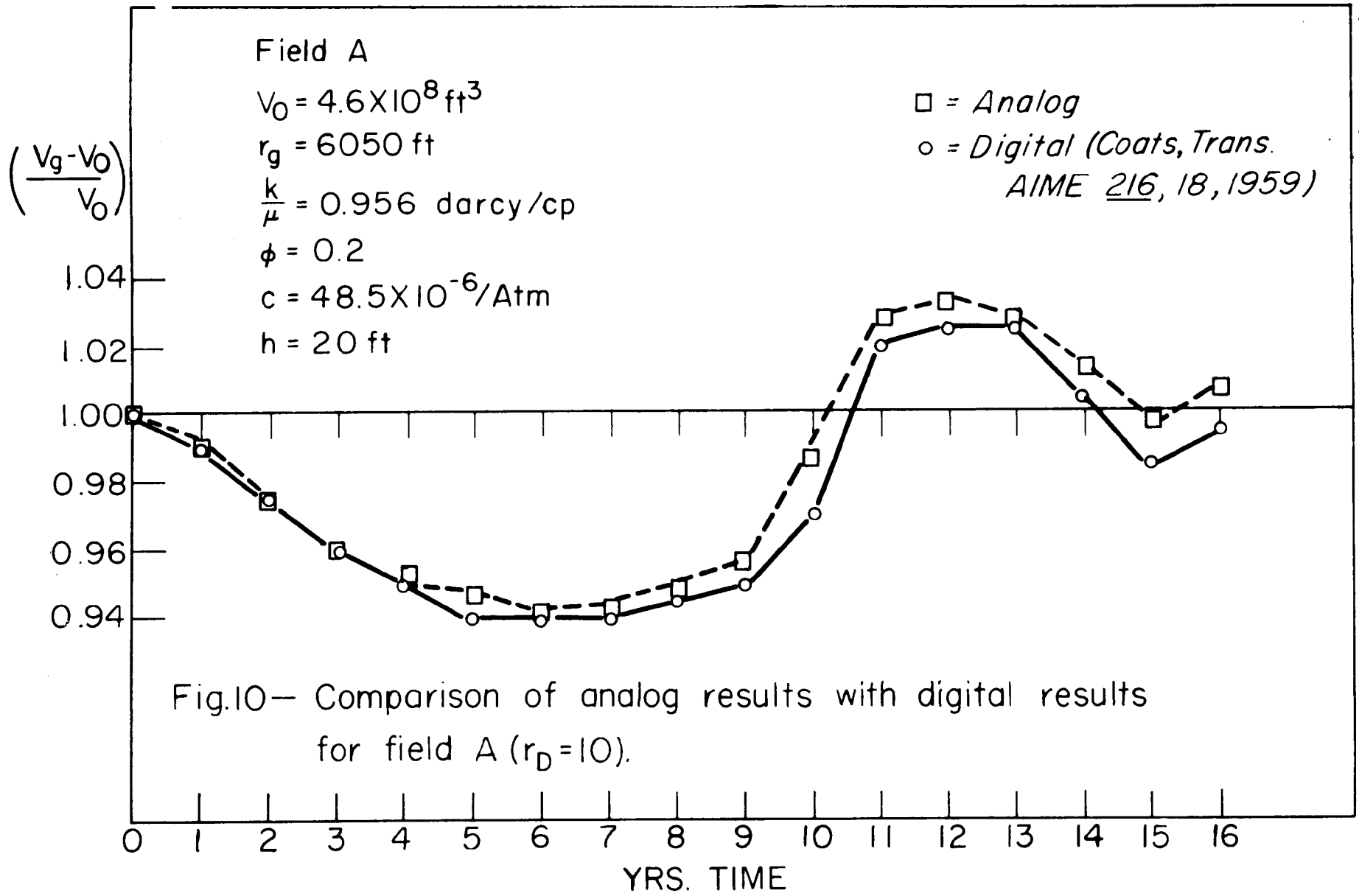


Fig.10— Comparison of analog results with digital results for field A ($r_D = 10$).

Upon substituting equation (20) and simplifying the equation it reduces to equation (22):

$$Q_{tD} = 49.5\, P_0 \sin \omega t_D - \frac{(0.577) P_0 \omega}{(0.0122)^2 + \omega^2} \left\{ \frac{\omega}{0.0122} \sin \omega t_D + \cos \omega t_D - e^{-0.0122 t_D} \right\} \quad (22)$$

$$(t_D > 5, \; r_D = 10)$$

The analog method is tested against the theoretical equation (22) for annual sinusoidal pressure variation.

$$G = 50 \sin \frac{\pi}{6} \theta = 50 \sin (0.0697 t_D) \; \#/in^2$$

The circuit used for this case is given in Figure 46. The potentiometer settings and the component sizes are different than those of Figure 7 because of the fact that the machine time constant K is different. In generating the SIN input, a low frequency oscillator is used. Table I shows the comparison of the analog results with equation (22). The agreement is quite good, and this is just about what one can expect so far as analog accuracy is concerned.

Table I. Comparison of Analog Results with Theoretical Cumulative Flux Function for Sinusoidal Pressure Variation ($t_D = 7.52\, \theta$)

θ, month	Q_{tD}(psi) from Eq. (22)	Q_{tD}(psi) Analog Result
6	633 (efflux)	617
12	-267 (influx)	-275
24	-356.5	-348
36	-386.5	-374
48	-396.2	-396
60	-399.4	-400
120	-401	-

c. Pressure Case of Infinite Aquifer: In simulating an infinite aquifer, the transfer function must be approximated from the solution of constant terminal conditions in tabular form in the literature.[4][12] Since the Q'_{tD} is not available in equation form, a curve fitting must be done in the form of equation (14). Since the approximate form of the equation from the limited aquifer is known, the determination of a suitable transfer function on an electronic differential analyzer by trial and error is no problem. However, it should be kept in mind that a reasonable working circuit can be derived from the transfer function expression. Attention must be given to the double integration term in the transfer function expression of equation (23) - $1/s^2$ term. But this term is identical to that of $1/s$ term, provided that the initial condition of the time derivative of the cumulative flux function is zero. From the practical point of view, to solve actual reservoir problems, the double integration term should not bother us. However, from the theoretical view point, careful attention should be given to the double integration term.

For an infinite aquifer, the Q'_{tD} or P'_{tD} are unbounded functions. However, one can always find the equivalent transfer function expression up to some t_D value depending on the specific problem.

By doing a series of trial and error, and making use of the tables given by Van Everdingen and Hurst[4], the following tranfer function is found to give the adequate simulation for the practical range of time, provided that the pressure variation is not too great. ($r_D = \infty$, $t_D < 5000$, $a = 1$)

$$sf_1(s) = \frac{49.5}{1 + \frac{s}{0.0126}} + \left(\frac{0.266}{s} - \frac{14.2\times10^{-6}}{s^2}\right) e^{-70s} \qquad (23)$$

The circuit is given in Figure 47 while the results are compared with theoretical values in Table II. In equation (23), delayed functions are involved. The delay operation is controlled at amplifier No. 7 in Figure 47. The delayed functions should be avoided if at all possible. It is not only a nuisance to control, but also may disturb other operations.

Table II. Comparison of Analog Results with Theoretical Cumulative Flux Function for Constant Pressure Case, ($r_D = \infty$, $K = 0.1$, $a = 1$)

t_D	(Theoretical, p. 314, Hurst)	Analog Run No. 1	Analog Run No. 2
50	24.82	24	24
100	43.01	43	43
200	75.86	77	77
400	134.8	135	135
800	242.3	240	242
1000	293.1	290	295
1500	413.6	410	420
2000	531.5	530	540
2500	646.6	640	650
3000	759.0	750	770
4000	975.7	960	970

In this circuit, equation (23) requires $P_1 = 0.499$ and $P_3 = 0.1064$. However, the errors of the computer demand that P_1 and P_3 to be 0.531 and 0.113 respectively to give the results in Table II. The infinite aquifer case requires more amplifiers than a limited aquifer case, which is a measure of the complexity of a problem.

The circuit given in Figure 47 has two drawbacks in applying to actual problems: one is the translated or delayed function and the other is the small machine time constant. The small machine time constant means that the machine is running fast; thus making the proper generation of the input signal difficult.

The transfer function expression obtained from $\frac{dQ_{tD}}{dt_D}$ (Figure 29) is shown in equation (24). In equation (24) the Laplace Transform is taken with respect to the actual time in month.

$$sf_1(s) = \frac{.075}{1+\frac{s}{0.8a}} + \frac{2.64}{1+\frac{s}{0.108a}} + \frac{18}{1+\frac{s}{0.01a}} + \frac{0.28a}{s} - \frac{2.4\times10^{-5}a^2}{s^2} \qquad (24)$$

Based on equation (24), the circuit shown in Figure 48 is obtained for $a = 4$ and $K = 5$. A double integration term appears in equation (24) for which no rigorous theoretical proof of the simulation is given as to the initial condition effect. However, at small times the contribution of this term is negligible because of the small coefficient, and the pressure input is also very small for actual problems. This error by double integration is taken care of by changing the coefficients of the lower power terms. The result obtained with $P_7 = 0.238$ from this circuit (Figure 48) is compared with the theoretical constant pressure case solution in Table III.

Table III. Comparison of Analog Results with Theoretical Cumulative Flux Function for Constant Pressure Case, ($r_D = \infty$, $K = 5$, $a = 4$)

t_D	Q'_{tD} (Theoretical, p. 314, Hurst)	Q'_{tD}, Analog
10	7.42	7.5
50	24.82	25
100	43.01	43.7
200	75.86	77
300	105.8	108
400	134.8	135.5
500	162.4	166
600	189.7	189
700	216	217

Table IV Comparison of Analog Results with Theoretical Pressure Change Function for Constant Rate Case, ($r_D = \infty$, $K = 0.1$, $a = 1$)

t_D	P'_{tD} (Theoretical, $r_D = 1$ p. 314, Hurst)	P'_{tD} Analog Run No. 1	P'_{tD} Analog Run No. 2
10	1.65	1.6	1.6
50	2.69	2.5	2.4
100	2.72	2.75	2.7
200	3.064	3.1	3.1
300	3.263	3.3	3.3
500	3.516	3.55	3.55
600	3.608	3.6	3.6
800	3.75	3.8	3.75
1000	3.86	3.85	3.8
1200	3.95	3.95	3.9

d. Rate Case of Infinite Aquifer: The rate case can be handled much the same way as the pressure case. In order to find the pressure change function at $r_D = 1$, the following transfer function was found to give satisfactory unit step response ($a = 1$, $r_D = \infty$) in comparison with the theoretical values of Van Everdingen and Hurst[4]

$$sf'_1(1,s) = \frac{1.253}{1 + \frac{s}{0.0093}} + \frac{1.967}{1 + \frac{s}{0.153}} + \frac{8.97 \times 10^{-4} e^{-1605}}{s} - \frac{5.9 \times 10^{-4} e^{-7805}}{s} \qquad (25)$$

The circuit is given in Figure 49, and the results are given in Table IV.

No further efforts have been made for this case because of the impracticability as the rate data are seldom available. The rate case simulation is not limited to the pressure change function at $r_D = 1$, but can be extended to obtain the pressure change function at other than $r_D = 1$, by making the use of Mortada's solution.[14] Mortada's solution is re-plotted in Figure 11, so that one can obtain accurate solutions as a function of location r_D. The large time solutions can be estimated by extrapolating on a semi-log plot.

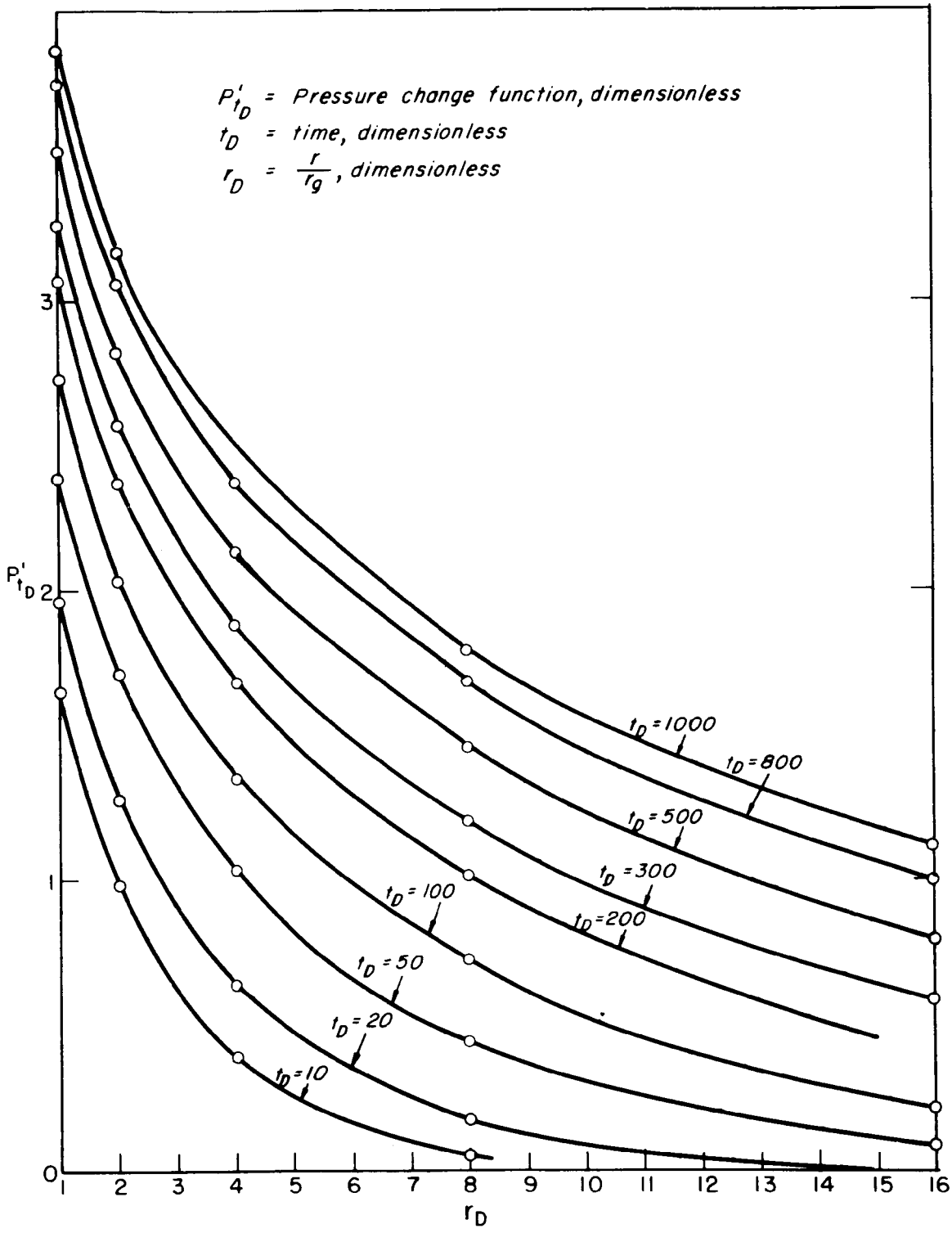


Fig. 11 – Constant rate case solution as a function of location and time ($r_D = \infty$) (original source, Mortada, 1955)

e. Volume Case of Infinite Aquifer: In most any case, the reservior pore volume variation history is available. When one intends to find the pressure change function by feeding in the volume variation, the case is referred to volume case and is a modified rate case.

For the pressure change function at $r_D = 15$ (Figure 11) on an infinite aquifer, the following transfer function is found to be satisfactory:

$$s^2 f_1'(r_D=15, s) = \frac{a}{10^3}\left(2.5 + \frac{0.76}{1+\frac{s}{0.013a}} - \frac{2.33}{1+\frac{s}{0.005a}} - \frac{4.3\times10^{-4}a}{s}\right) \quad (25)$$

The circuit of equation (25) is given for K = 0.5 in Figure 50. The results obtained from Figure 50 are compared with theoretical values of Mortada[14] (or Figure 11) in Table V.

In obtaining the transfer function for this case, $\frac{d P_{RD}'}{d t_D}(r_D, t_D)$ versus t_D is approximated first from the constant terminal rate case solution. It should be pointed out that P'_{tD} is dimensionless while P_{tD} has a dimension of rate.

Table V Comparison of Analog Results with Theoretical Pressure Change Function at $r_D = 15$ for Constant Rate Case (Infinite Aquifer) Using Volume Variation as Input Signal.

t_D	P'_{tD} (Theoretical, Mortada)	P'_{tD} (Analog)
50	0.11	0.11
100	0.23	0.25
200	0.46	0.46
300	0.63	0.62
400	0.75	0.73
500	0.85	0.83
600	0.94	0.93
650	0.98	0.97

IV APPLICATIONS FOR AQUIFER BEHAVIOR STUDY

In the last two chapters analog simulation of gas storage aquifer on an electronic differential analyzer is developed. Using this method as a tool whenever needed, aquifer behavior study is made to give a better understanding of the pressure changes and the reservoir pore volume changes for different types of gas storage fields. For convenience, the study is categorized into a. Isolated field, b. Effect of a fault on unit step responses, c. Interference among two or more fields on a common aquifer, and d. Moving boundary problem.

a. Isolated Field: Under the heading of isolated field, the findings which would be of interest to the practical engineers are discussed. These include the effect of permeability on water return ability for a limited aquifer, the effect of aquifer size on water-return ability, the effect of phase shift in the pressure cycle on water-return ability, the order of magnitude of the error introduced by the flow resistance at the gas-water twilight zone, and the effect of the areal geometry of a gas storage field.

1) Effect of the Permeability on Water-Return Ability for a Limited Aquifer: The amount of influx or efflux from a gas storage field is a function of permeability k, gas field radius r_g, brine viscosity μ, aquifer sand thickness h, aquifer size, and the pressure variation. The general discussion of the reservoir variables is given in a latter chapter, and it is intended to show how the permeability of the water sand affects the flux when the rest of the quantitative variables are kept constant.

The following typical set of values are taken to construct Fig. 12:

ϕ	: 0.18	r_D	: 10
c'	: 7×10^{-6}/psi	Pressure	: Annual Sinusoidal
r_g	: 2000 ft	k	: 0.1 darcy, $t_D = 3.8\,\theta$
μ	: 1 cp	k	0.198 darcy, $t_D = 7.52\,\theta$
h	: 100 ft		

$$W = 2\pi h r_g^2 c' \phi Q_{xD} = 3160 Q_{qD} \text{ Cu. ft.}$$

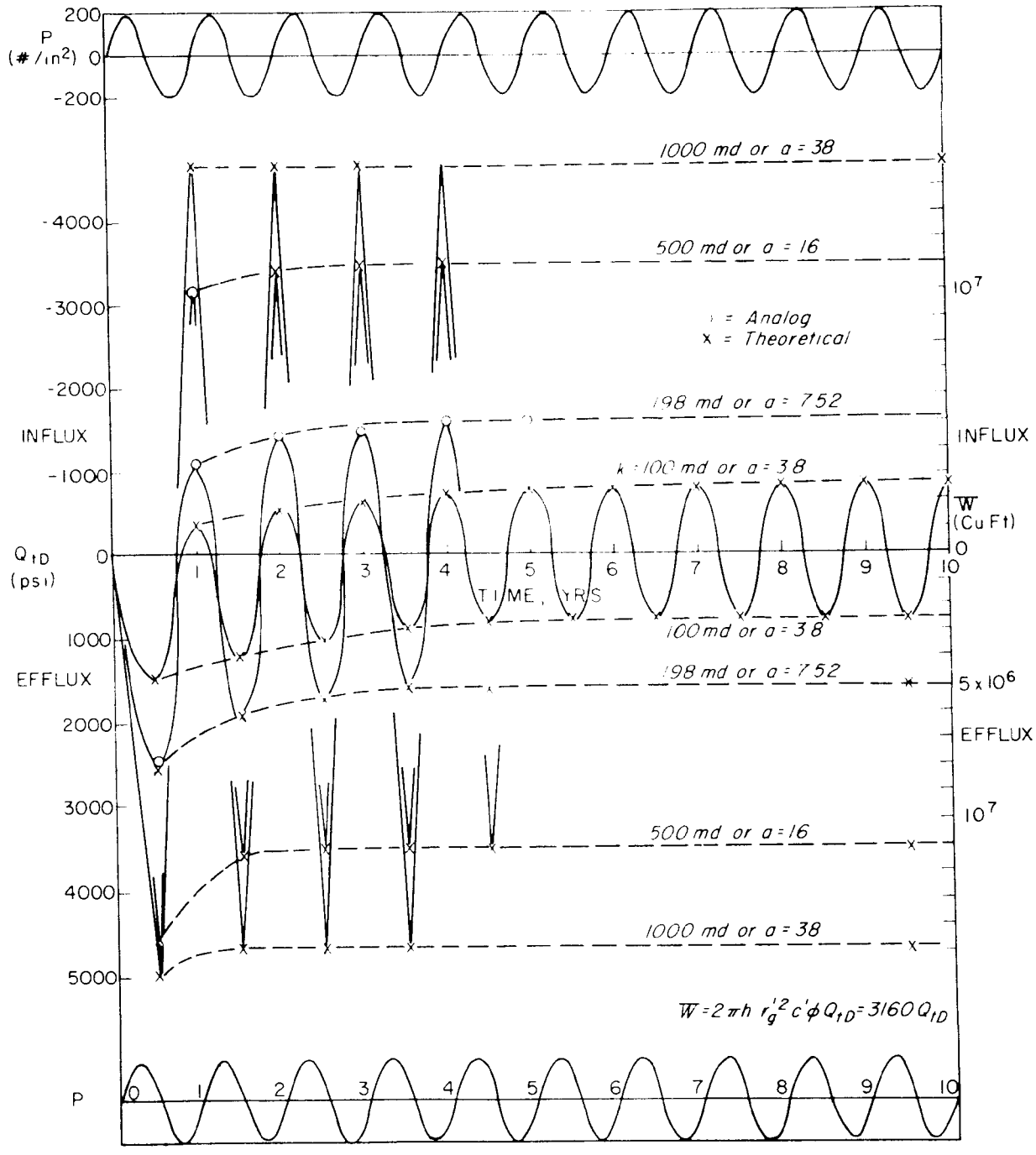


Fig 12- Effect of permeability on Water-return ability for limited aquifer (r_D=10)

Equation (22) is used for Figure 12 and the analog results are plotted also, as a check. From the study, the following conclusions are drawn:

1) For a limited aquifer, complete recovery (maximum and minimum points have the same absolute values) is possible within a period of time.

2) For high values of k, the amplitude becomes bigger, but the amplitude is not a linear function of k.

3) The complete recovery point is reached sooner for higher values of k. In other words, the locus of the peak points is leveling off sooner to a horizontal line for high values of k.

4) The peak points occur when the pressure returns to the discovery pressure or zero pressure, as designated.

ii) Effects of Aquifer Size on Water-Return Ability. With the same values taken as before, a study was made for k = 0.1 darcy to an infinite aquifer and to a limited aquifer of $r_D = 10$. Figure 13 shows the comparison of the extent of flux to the reservoir. For the infinite aquifer, a theoretical equation (28), which is derived below, is used, and the solution has been checked by the analog method using the circuit of Figure 51. The circuit of Figure 51 is much the same as that of Figure 48. It is conclusive from Figure 13 that the curve for the infinite aquifer case sags down, and the recovery is very slow. In fact, the recovery is never completed, and it can only be accomplished with the allowance of infinite time. The absence of the reflected pressure wave is considered to be responsible for the effect. For high permeability, say k = 1 darcy, the recovery is expected to be faster, like in the case of $r_D = 10$. The envelope of the peak points has the shape of the $\frac{dQ'_{tD}}{dt_D}$ versus t_D curve.

Equation (28) has been mathematically derived from equation (7). Equation (7) can be written in another form noting that the initial value of Q'_{tD} is zero:

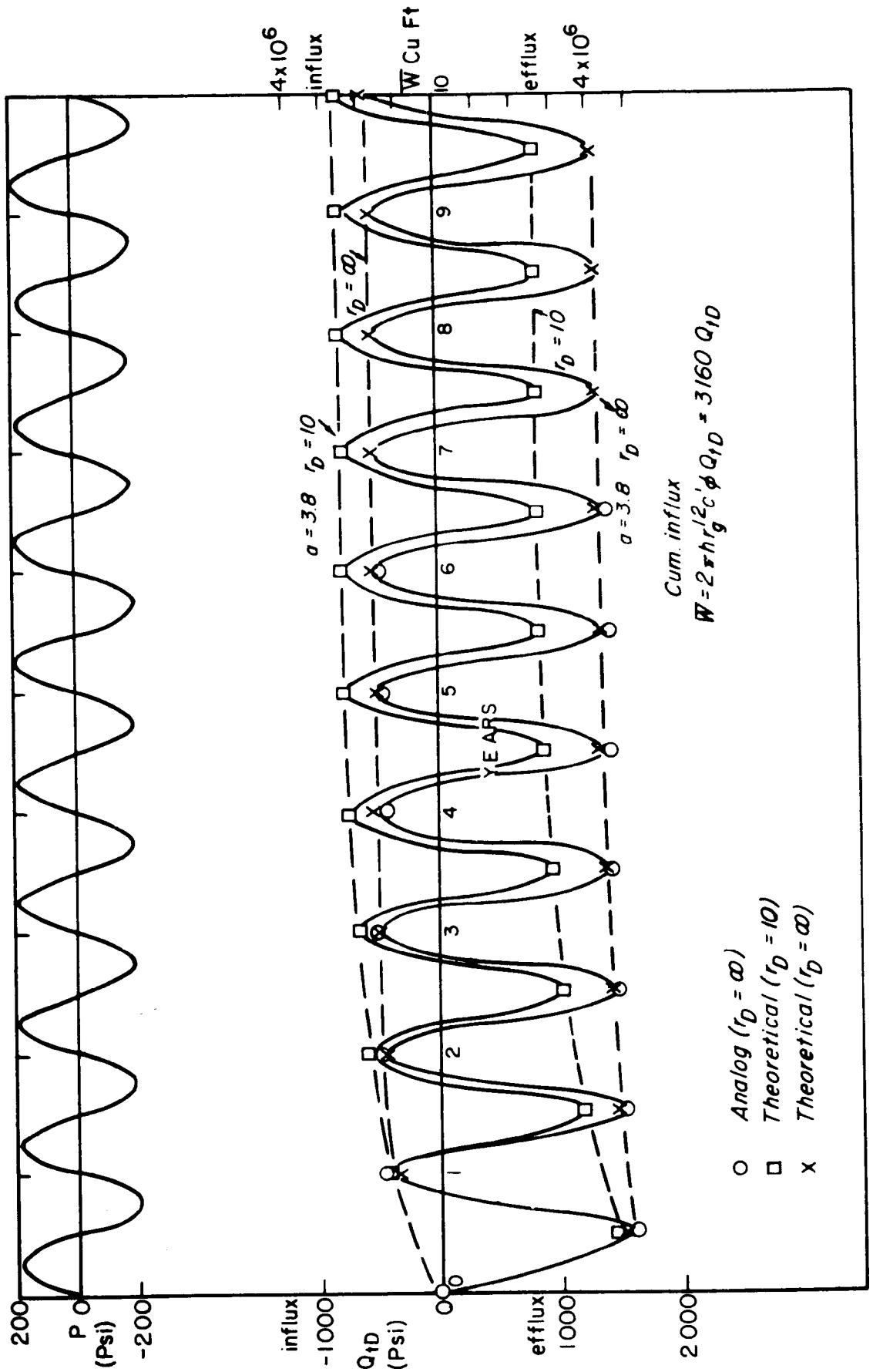


Fig. 13 – Effect of aquifer size on water-return ability

$$Q_{tD} = \int_0^{t_D} G(t_D - \tau) \cdot \left(\frac{dQ'_{tD}}{d\tau}\right) \cdot d\tau$$

For an infinite aquifer the following approximation can be made using the Chatas' table [12] of Q'_{tD} versus t_D:

$$\frac{dQ'_{tD}}{dt_D} = 0.6e^{-0.8t_D} + 0.285e^{-0.108t_D} + 0.18e^{-0.01t_D} + 0.28 - 2.4\times10^{-5}t_D \qquad (27)$$

Equation (27) is the inversion of equation (24). When $G = P_o \sin\omega t_D$, the solution can be written as:

$$Q_{tD} = -\cos\omega t_D\left[\frac{0.28P_o}{\omega} + \frac{0.6\omega P_o}{(0.8)^2+\omega^2} + \frac{0.285\omega P_o}{(0.108)^2+\omega^2} + \frac{0.18\omega P_o}{(0.01)^2+\omega^2}\right]$$

$$+ \sin\omega t_D\left[\frac{0.48P_o}{(0.8)^2+\omega^2} + \frac{(0.108)(0.285)P_o}{(0.108)^2+\omega^2} + \frac{(0.18)(0.01)P_o}{(0.01)^2+\omega^2} + \frac{2.4\times10^{-5}P_o}{\omega^2}\right]$$

$$+ \left(\frac{0.28P_o}{\omega} + \frac{P_o\omega(0.6)e^{-0.8t_D}}{(0.8)^2+\omega^2} + \frac{P_o\omega(0.285)e^{-0.108t_D}}{(0.108)^2+\omega^2}\right.$$

$$\left. + \frac{P_o\omega(0.18)e^{-0.01t_D}}{(0.01)^2+\omega^2} - \frac{2.4\times10^{-5}P_o t_D}{\omega}\right) \qquad (28)$$

This equation gives the cumulative flux when the pressure varies sinusoidally at the gas field. The theoretical points of an infinite aquifer in Fig. 13 are based on this equation.

iii) Effect of Phase Shift in Pressure Cycle on Water-Return Ability: With the same numerical values (k = 0.1 darcy, a = 3.8, $r_D = \infty$), the effect of the phase shift in pressure cycle is shown in Fig. 14. It is noted that the influx or efflux is greatly different upon shifting the phase of the pressure cycle. However, the envelopes or loci of the peak points of different pressure cycles have a definite tendency of forming a curve

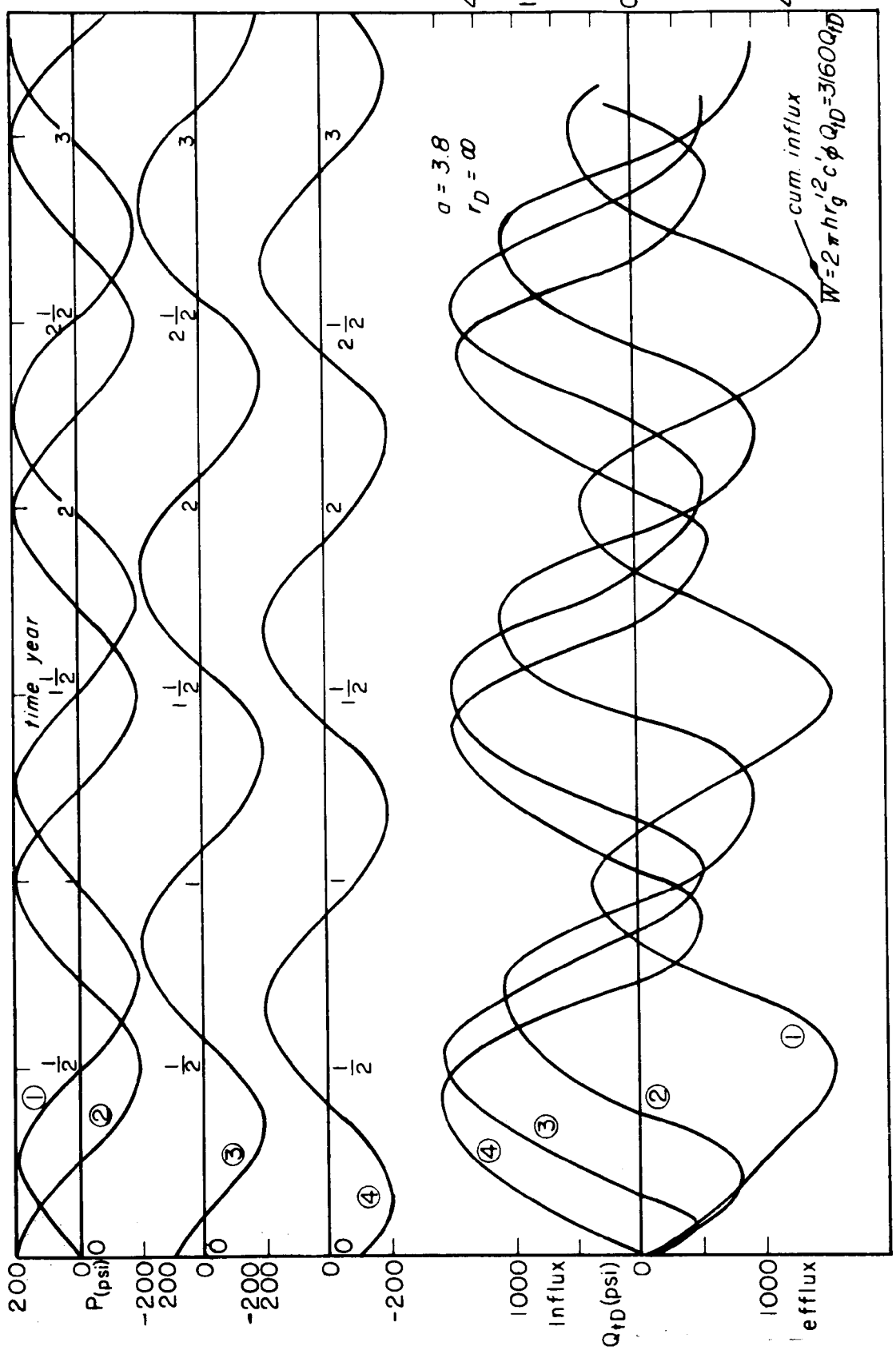


Fig.14 - Effect of phase shift in pressure cycle on water-return ability

pattern. For a certain pressure cycle - e.g. (2), the absolute value of the maximum amplitude is lower than that of another pressure cycle - e.g. (4). The circuit of Fig. 51 is used for the study, and the input sinusoidal function is generated by a low-frequency oscillator.

iv) Effect of Twilight Zone Resistance: At the gas-water interface, it is generally understood that the boundary is not a clearcut line: a twilight zone of gas and water is known to exist at the interface. A consequence of this is that the flow resistance in the twilight zone is different than that of the aquifer. The pictorial sketch of the model is shown in Fig. 15. If the twilight zone thickness is small, one may neglect the compression of the water in this zone and consider it as an incompressible fluid. By making an approximation of $\ln\left(1-\frac{\Delta l}{r_g}\right) \cong \left|\frac{\Delta l}{r_g}\right|$, one can show that the following relationships exist:

$$\frac{dW}{d\theta'} = 2\pi\phi c' r_g^2 h \frac{dQ_{xD}}{d\theta'} = \left(\frac{k}{\mu}\right)_2 \frac{2\pi r_g h}{\Delta l}\left(P'-P_g\right)$$

$$\left(P'-P_g\right) = \frac{\left(\frac{k}{\mu}\right)_1}{\left(\frac{k}{\mu}\right)_2} \frac{\Delta l}{r_g} \frac{dQ_{xD}}{dt_D}$$

In order to see the order of magnitude of the error introduced by the twilight zone resistance, the following numerical values are used:

$$\frac{\Delta l}{r_g} = 1/100.0$$

$$\frac{\left(\frac{k}{\mu}\right)_1}{\left(\frac{k}{\mu}\right)_2} = 3 \; ; \; P' = 1.0; \; r_D = 10$$

$$\frac{dQ'_{xD}}{dt_D} = 0.577\, e^{-0.0122 t_D} \text{ (from eq. (20))}$$

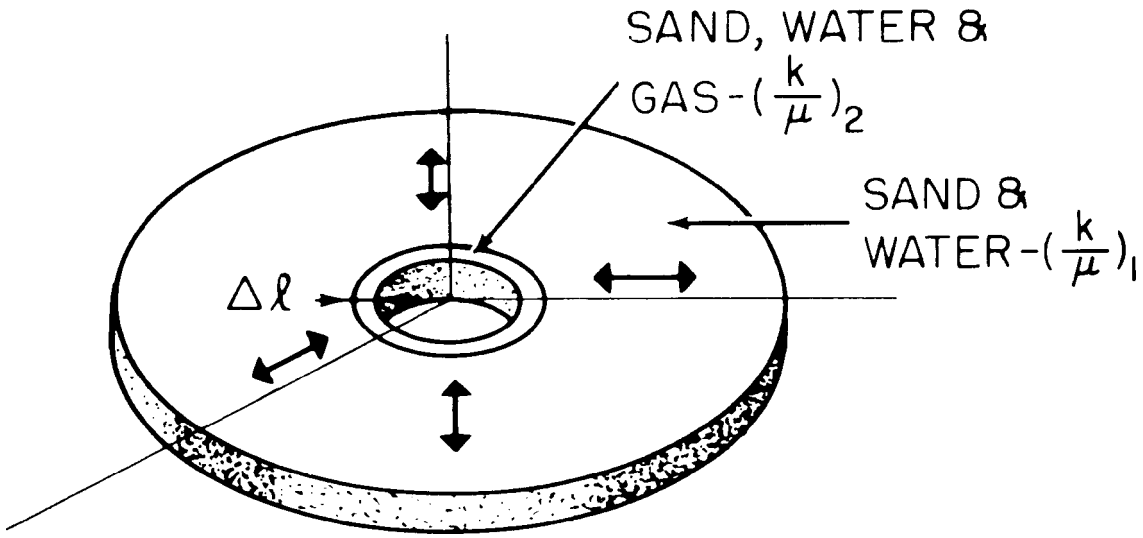


Fig. 15 - Radial flow model with twilight zone resistance

These numbers result:

$$\left(1 - \frac{p}{p_i}\right) = 0.01735\, e^{-0.0122 t_D}$$

The computed values are plotted in Fig. 16. The treatment here is essentially analogous to having a finite heat transfer coefficient at the inner radius rather than an infinite one. If the coefficient is finite, there will be a temperature drop across the film, the thickness of which will correspond to Δl in the reservoir problem. Actually, the thickness of the gas-water twilight zone may be changing as a function of time as well as the flow resistance $\left(\frac{k}{\mu}\right)_2$ due to time-varying saturation effect. However, it is intended here to find out the order of magnitude of the error introduced due to the non-uniformity of the resistance $\left(\frac{k}{\mu}\right)_1 \neq \left(\frac{k}{\mu}\right)_2$ when the twilight zone thickness is small. With the selected numbers, the error to the unit step response never exceeds two percent for the constant terminal pressure case. This is quite small in relation to the errors of the analyzer itself and the accuracy of the data. When the thickness of the twilight zone is not small, and when $\left(\frac{k}{\mu}\right)_2$ cannot be assumed to be constant, then the problem becomes extremely complex, and the discussion for such case is given in a latter chapter of this thesis.

v) Effect of Areal Shape of Reservoir: By making a careful study of interference between the two identical circular reservoirs with the charts given by Mortada[14], a rate case solution with a fault at r_D is prepared as shown in Fig. 19. When one considers the geometry formed by overlapping a set of twin circles as shown in Figure 17, it is noted that the non-circular geometry is a special case of a fault problem which is fully discussed in the following section. Since the center-to-center distance of the twin circles is small, the difference between $P_{t_D}\left(\frac{d}{r_g}-1, t_D\right)$ and $P_{t_D}\left(\frac{d}{r_g}+1, t_D\right)$ becomes great, and the conventional way of averaging the values with center-to-center distance in treating the interference problem becomes incorrect. In preparing Fig. 19 for the small d/r_g values, the limiting values for $d/r_g = 0$ are located first and then the curves are completed. Fig. 19 is useful for non-circular reservoir geometry

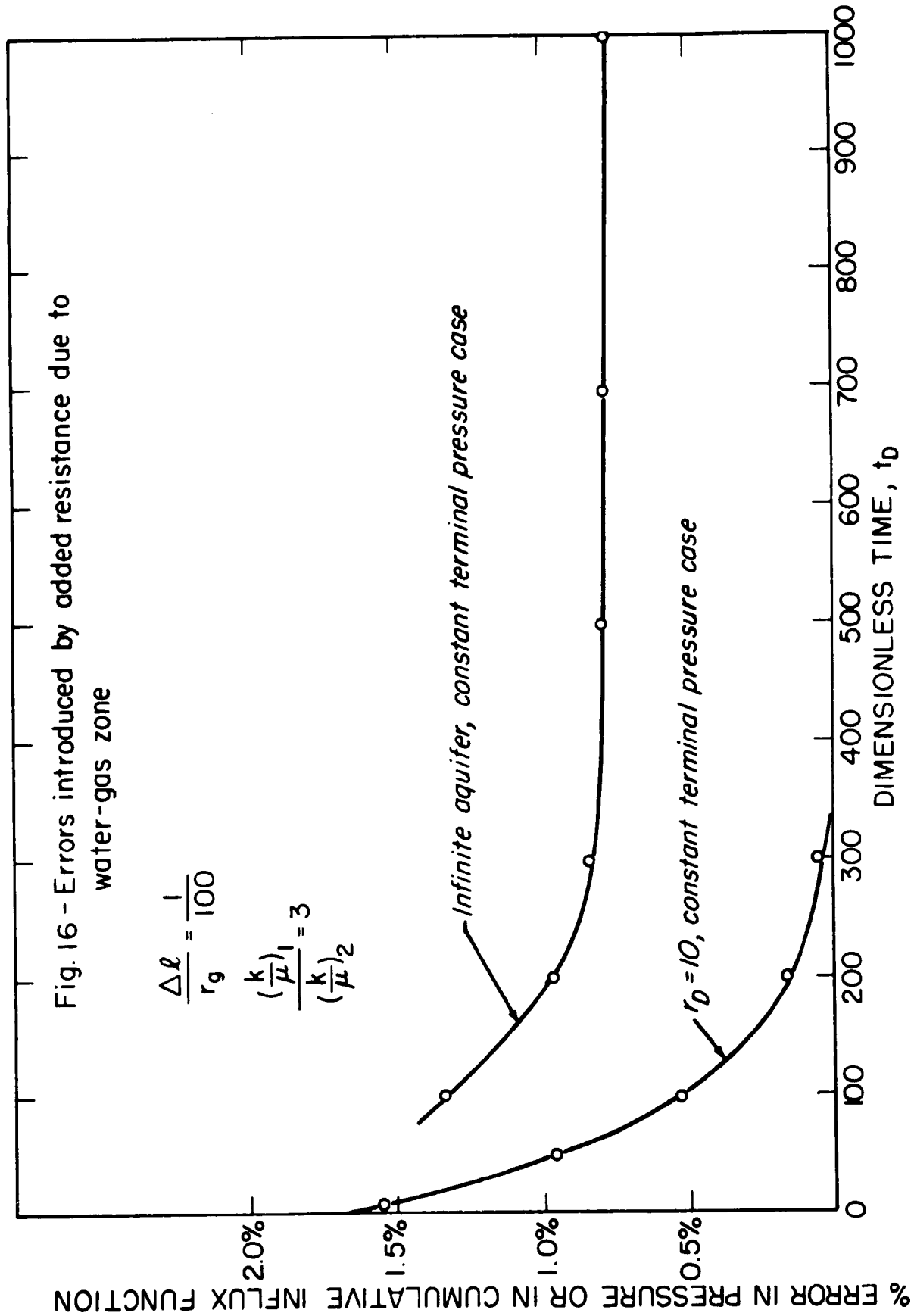


Fig. 16 - Errors introduced by added resistance due to water-gas zone

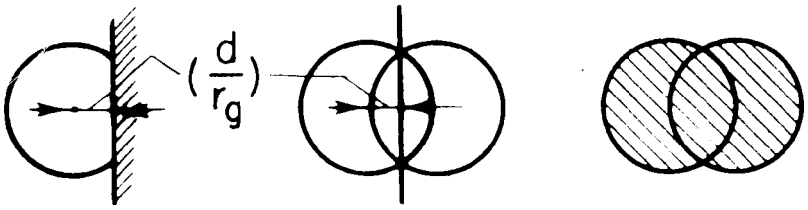


Fig. 17 - A noncircular reservoir model

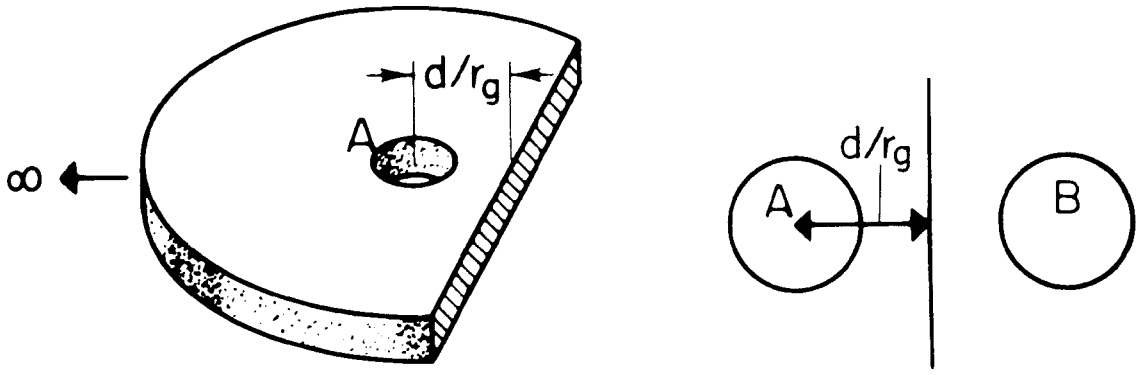


Fig. 18- Radial flow model with a fault at $(\frac{d}{r_g})$

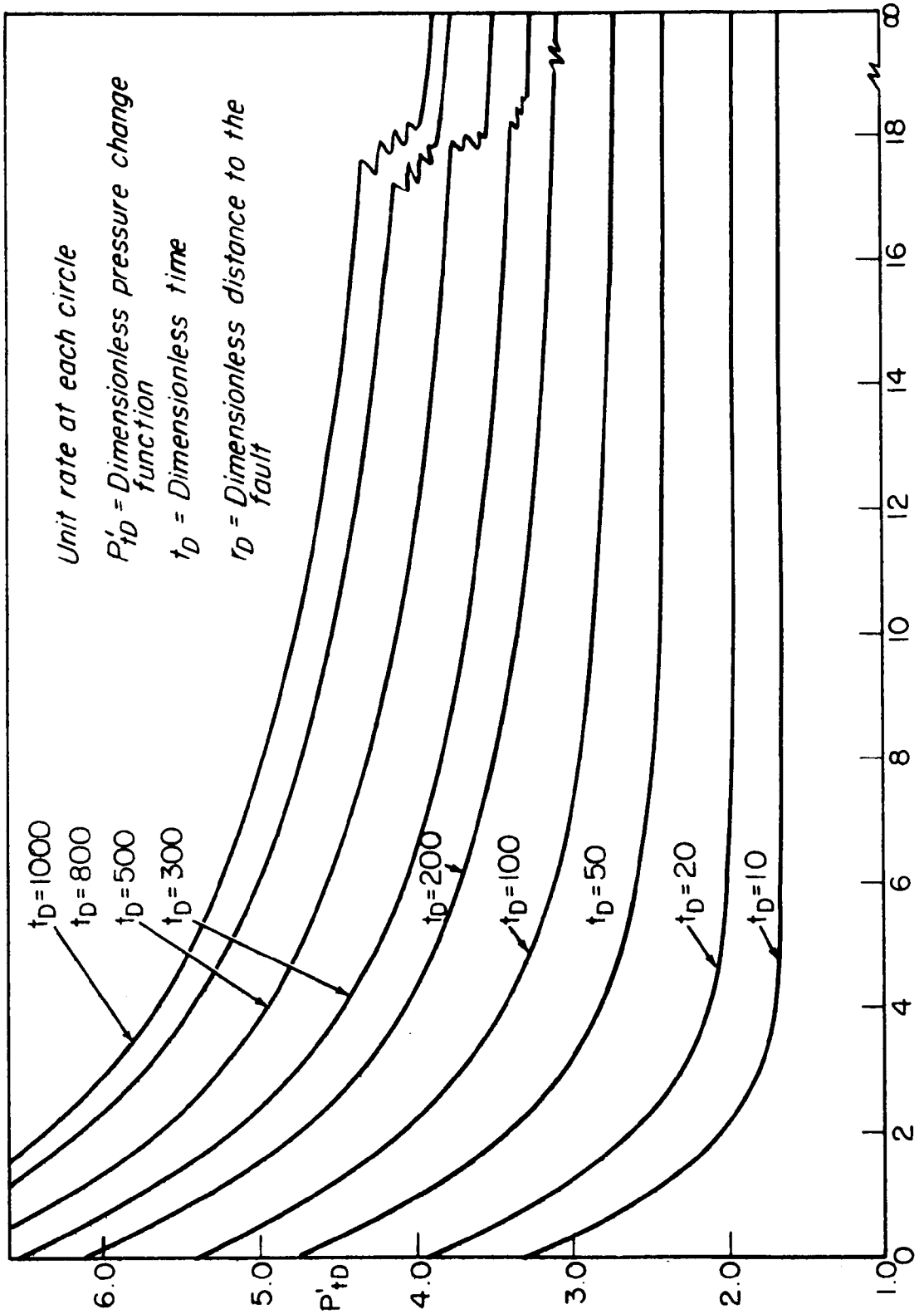


Fig. 19– Constant rate case solution with a fault at r_D

formed by overlapping two identical circles as well as for a fault problem.

In order to see the areal shape effect of the reservoirs, Table VI is made by the use of Fig. 19 to compare the non-circular geometry and the equal-area circular geometry. The comparison shows that if the areal shape is approximated by an equal-area circle, the error in estimating the unit impulse response is small. The conclusion is supported by the further studies made with geometries overlapped by three identical circles on a delta, regardless whether it is pressure case or rate case. However, there is no assurance of this conclusion for the short time range. (less than $t_D < 10$).

b. Effect of a Fault on Unit Step Response: Often an impermeable fault is located in an aquifer and prevents the pressure communication, which, in turn, effects the performance of a gas storage reservoir. Efforts have been made to obtain solutions for the constant terminal rate case with a fault, constant pressure case with a fault, constant rate case for three identical reservoirs on a delta, and constant pressure case for three identical reservoirs on a delta. These cases may be considered as special cases of interference problems or idealized interference studies. The study model is shown in Fig. 18.

i) Constant Terminal Rate Case with a Fault: In handling a fault problem, one needs to consider two identical reservoirs situated 2d distance apart, by making use of the line of symmetry. Since a linear combination of particular solutions to a linear and homogeneous differential equation is a solution to the differential equation, the following equation can be written as suggested by Mortada[14] with respect to equation (5):

$$P_A = P_B = P_{xD\,Aa} + P_{xD\,Ab}$$

$$\text{or } \left(\frac{\mu}{2\pi kh}\right) P_{xDA} = \left(\frac{\mu}{2\pi kh}\right)\left[P_{xD\,Aa} + P_{xD\,Ab}\right] = \left(\frac{\mu}{2\pi kh}\right)\left(P_{xD}(1, t_D) + P_{xD}\left(\frac{2d}{r_g}, t_D\right)\right) \quad (29)$$

Table VI Comparison of Constant Rate Case Solutions to a Non-Circular Geometry (Fig. 17) and an Equal-Area Circular Geometry.

A. $\frac{d}{r_g} = 1/2$, $t_{D\ circle} = \frac{t_{D\ odd}}{(1.267)^2}$, rate = 2 (dimensionless)

$t_{D\ odd}$ $(\frac{d}{r_g} = 1/2)$	P'_{t_D} (non-circular)	P'_{t_D} (circle)
10	2.90	2.92
20	3.52	3.52
50	4.35	4.35
100	4.98	5.01
200	5.73	5.70
300	6.16	6.10
500	6.6	6.6
800	7.1	7.05
1000	7.28	7.27

B. $\frac{d}{r_g} = 1$, $t_{D\ circle} = \frac{t_{D\ odd}}{(1.414)^2}$, rate = 2 (dimensionless)

$t_{D\ odd}$ $(\frac{d}{r_g} = 1)$	P'_{t_D} (non-circular)	P'_{t_D} (circle)
10	2.56	2.72
20	3.16	3.30
50	4.00	4.13
100	4.66	4.77
200	5.35	5.44
300	5.78	5.84
500	6.20	6.34
800	6.70	6.81
1000	6.95	7.03

Here, $P_{tD}(1, t_D)$ and $P_{tD}(\frac{2d}{r_g}, t_D)$ are readily available values in the literature as constant terminal rate case solutions of an isolated reservoir.[4][14] The pressure change function at A in equation (29) is plotted as a function of $\frac{d}{r_g}$ using t_D as a parameter in Fig. 19. So, by knowing a value of $\frac{d}{r_g}$, one can read off the pressure change function for the constant terminal rate case with a fault as a function of time. For an arbitrary rate case,

$$P_{tDA} = (P_{tD})_{Aa} + (P_{tD})_{Ab} = E(t_D)_A \left[s f_1'(s) \right]_{Aa} + E(t_D)_B \left[s f_1'(s) \right]_{Ab}$$

But, $E(t_D)_A = E(t_D)_B$, and therefore,

$$P_{tDA} = E(t_D)_A \cdot s \cdot \left[f_1'(s)_{Aa} + f_1'(s)_{Ab} \right]$$

Once the unit step response is found from Fig. 19, proper transfer function can be set up on an analog computer, following the developed method, to find the solution for the specified terminal rate case.

Equation (29) is only good when the difference between $P_{tD}(\frac{d}{r_g}-1, t_D)$ and $P_{tD}(\frac{d}{r_g}+1, t_D)$ is small, so that the average value can be expressed by $P_{tD}(\frac{d}{r_g}, t_D)$. In order that this would be true, $\frac{d}{r_g}$ must be a reasonably large number.

ii) Constant Terminal Pressure Case with a Fault: The rate case of a fault problem is quite simple; however, the pressure case with a fault becomes more involved and conventionally thought of as a trial and error problem. For this case, equation (29) also applies, even though P_{tDAa} and P_{tDAb} are not readily available by any means.

By combining solutions of the rate case and the pressure case on electronic differential analyzers, a method has been devised to find the solution for the pressure case with a fault without doing a trial and error method. The overall scheme of the operation is sketched in Fig. 20

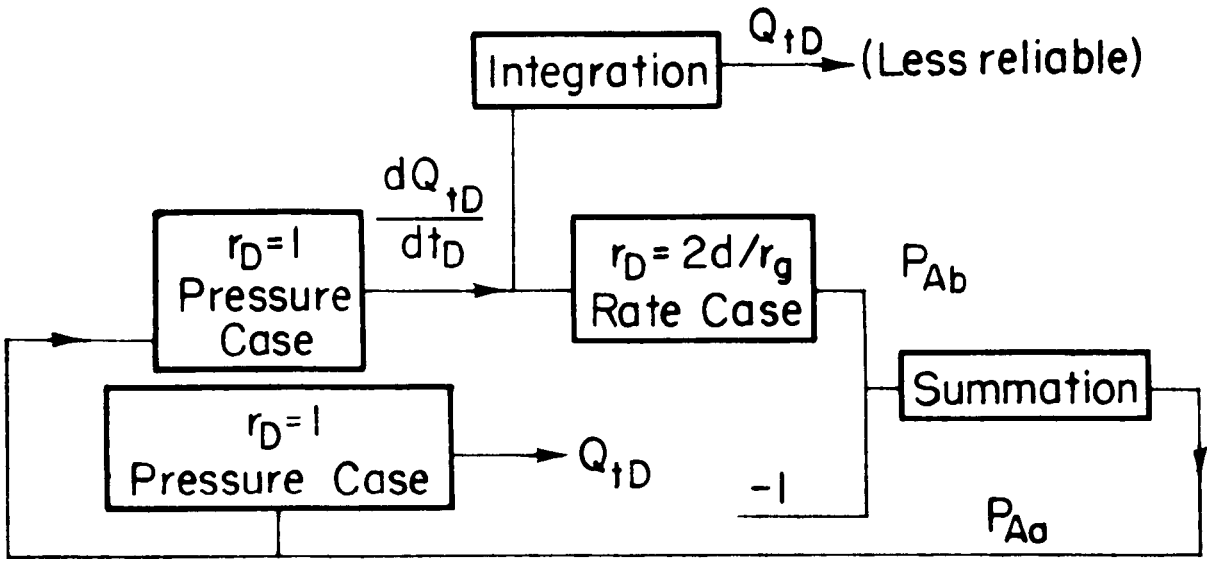


Fig. 20 - Overall operations required for pressure case with a fault in the aquifer

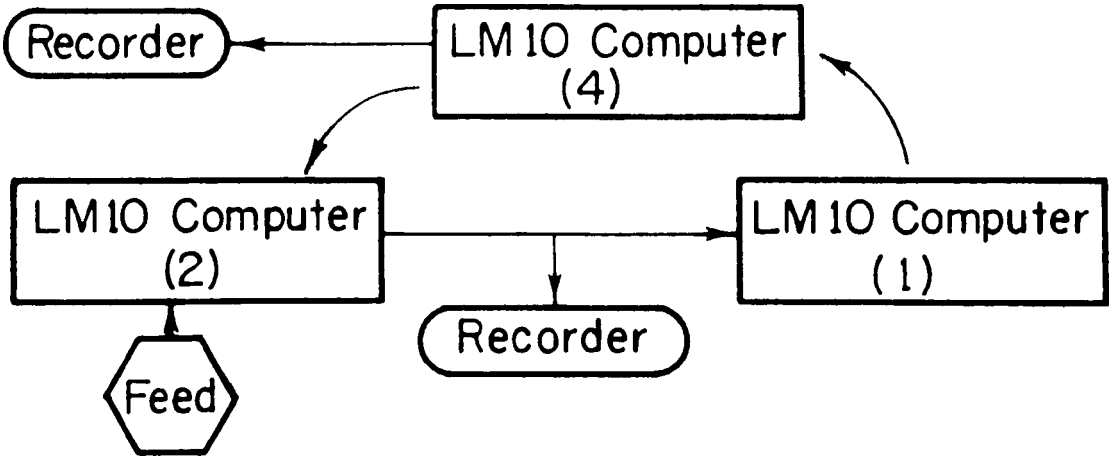


Fig. 21 - Arrangement of equipment for pressure case with a fault in the aquifer

while the equipment arrangements are shown in Fig. 21. By feeding an input signal corresponding to the gas field pressure, the functioning of the whole setup is interlocked to give the desired answer of the problem.

In Fig. 20, $\frac{dQ_{tD}}{dt_D}$ appears, and this means a differentiation operation. On an analog computer, a differentiation operation is impractical because of instability. In order to avoid machine differentiation step, a transfer function, which gives $\frac{dQ_{tD}}{dt_D}$ directly, is set up rather than Q_{tD} transfer function. It can be shown that the following relationship exists for the pressure case, since $Q_{tD}(0) = 0$:

$$\frac{s\,Q_{tD}(s)}{g(s)} = \frac{L\left\{\frac{dQ_{tD}}{dt_D}\right\}}{g(s)} = s^2 f_1(s)$$

where $f_1(s)$ is the Laplace Transform of the cumulative flux function for the constant terminal pressure case. In obtaining $s^2 f_1(s)$, Chatas' table[12] for cumulative flux function for constant pressure case was used. The following transfer function is employed for the experiment (a = 1):

$$s^2 f_1(s) = 1.345 - \frac{2.4 \times 10^{-5}}{s} - \frac{0.6}{1+\frac{s}{0.8}} - \frac{0.25}{1+\frac{s}{0.108}} - \frac{0.18}{1+\frac{s}{0.01}}$$

The circuit for the case when a fault is located at $\frac{d}{r_g} = 2.46/2$ is given in Fig. 52.

In order to construct a complete set of curves for any fault location, independent runs were made at the fault locations of $r_D = 2$, 4, and 8. The circuits used for $r_D = 2$ are given in Figures 53, 54, and 55. The three computer units A, B, and C were coupled and operated simultaneously in order to get the desired solution for a fault problem. Figures 56 and 57 are the circuits of Unit B for $r_D = 4$ and 8, respectively. The same circuits for Units A and C were used for all experiments. The results are plotted in Fig. 22 which shows the constant pressure case solution with a fault.

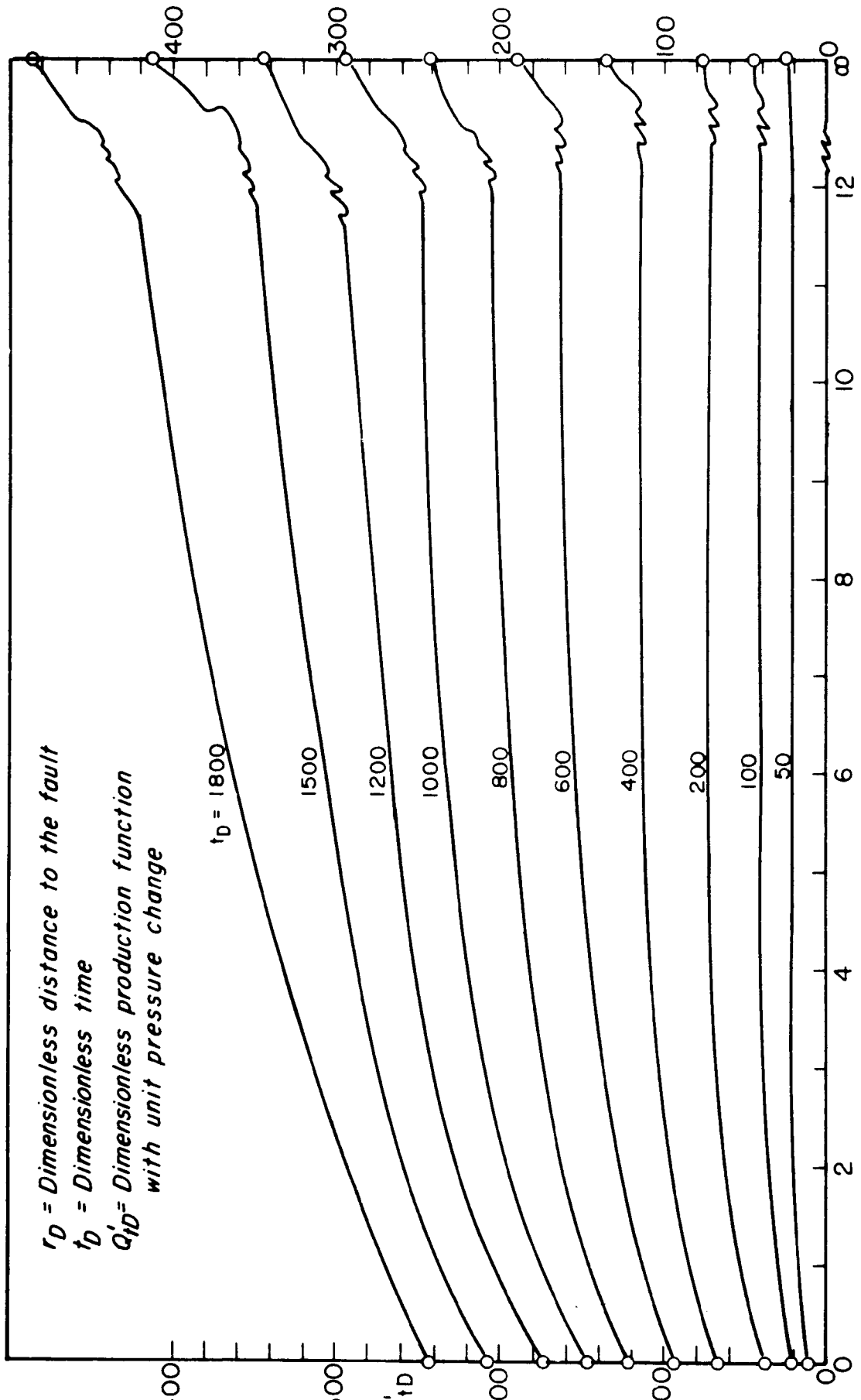


Fig. 22 - Constant pressure case solution with fault at r_D

An alternate method of obtaining the constant terminal pressure case solution with less amount of equipment is to make use of the constant rate case solution with a fault in Figure 19. An overall rate case transfer function with a fault must be obtained from Figure 19. And a time-varying rate input must be generated which gives a constant pressure change output. This method is used to obtain the pressure case solution from volume case solution for a growing disk model which is discussed in detail in a latter chapter.

It can be proven that the overall transfer function (from pressure directly to Q_{tD} for a fault problem) is theoretically a parallel combination of individual effects.

$$\left[s f_1(s)\right]_{overall} = \frac{\left[s f_1(s)\right]_{Aa} \cdot \left[s f_1(s)\right]_{Ab}}{\left[s f_1(s)\right]_{Aa} + \left[s f_1(s)\right]_{Ab}}$$

However, it seems impractical to try to find the overall transfer function from the individual transfer functions because of the complexity involved in the equation.

iii) Three Identical Reservoirs on a Delta: This case is much the same as the fault case because the reservoirs are identical and the distances between the reservoirs are the same. The geometry is sketched in Figure 23. For this case one can write:

$$P_A = P_B = P_C = P_{Aa} + 2P_{Ab} \qquad \text{(dimensionless)}$$

By changing the input resistor to amplifier No. 4 in Figures 54, 56 and 57, which were used for the fault case, from 2 megohms to 1 megohm, the above relationship can easily be simulated. The pressure case solution for three identical reservoirs on a delta is given in Figure 24. The rate case solution can be directly obtained from Mortada's solution[14] and is plotted in Figure 23.

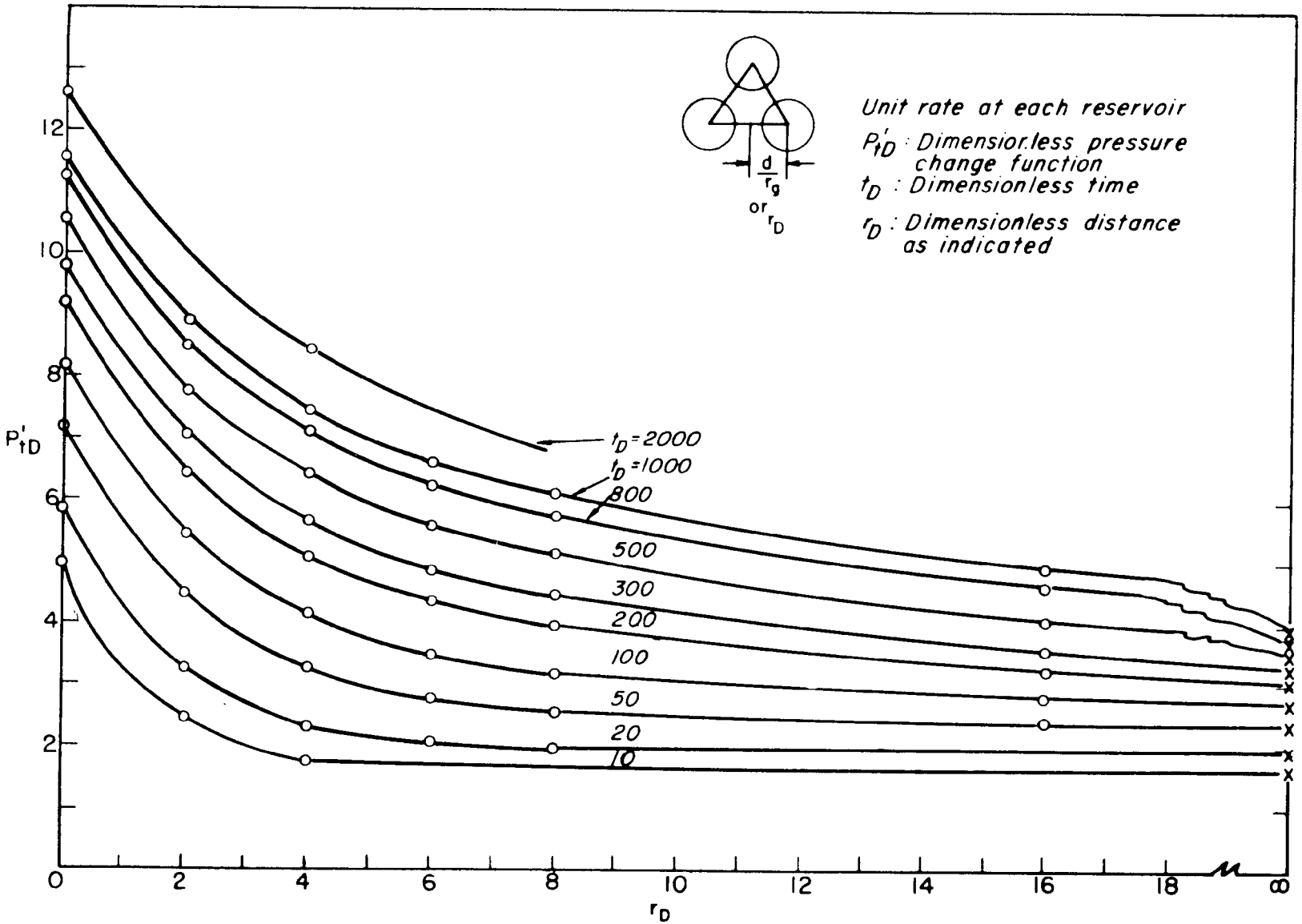


Fig. 23 Constant rate case solution for three identical reservoirs on a delta

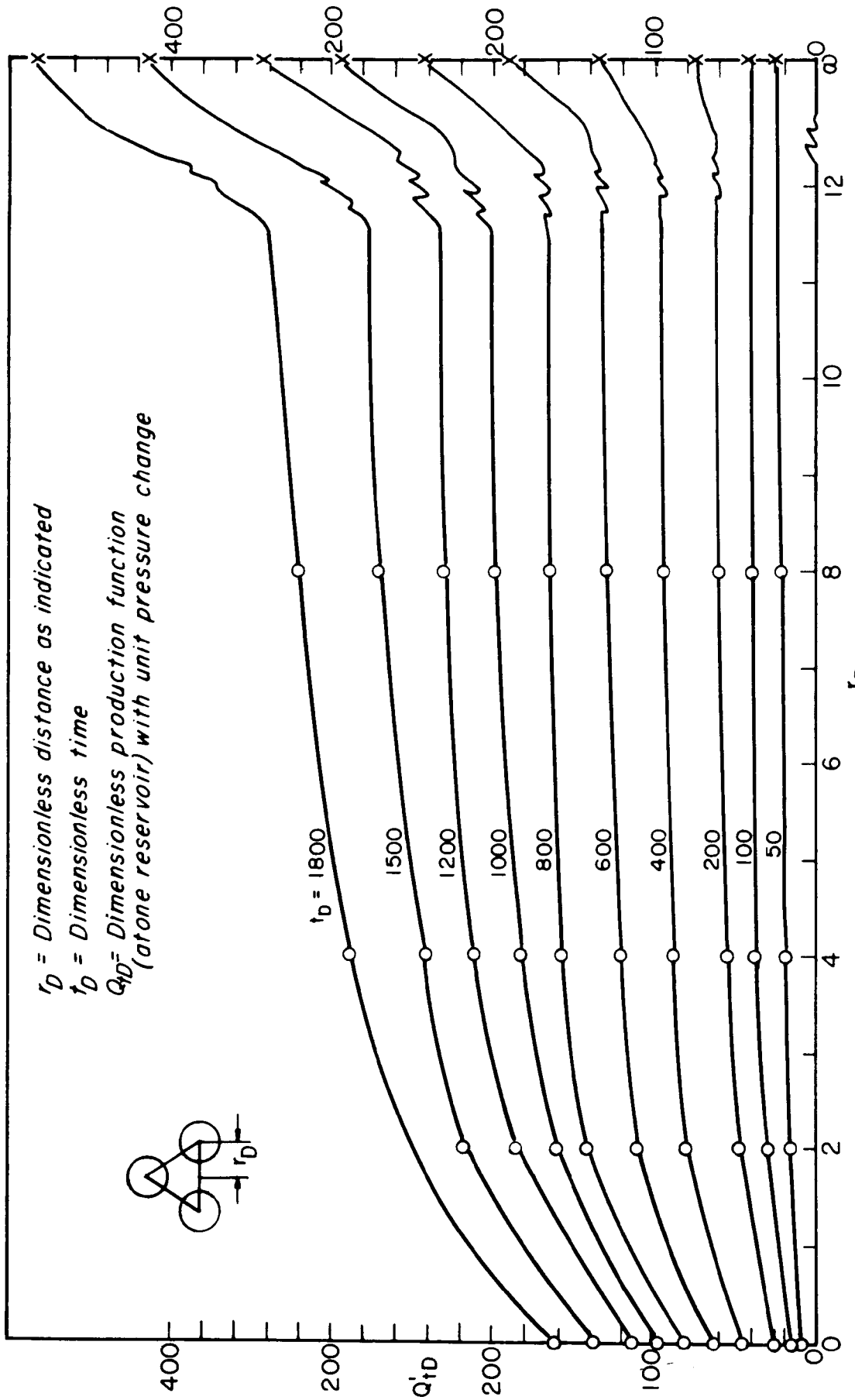


Fig. 24 - Constant pressure case solution for three identical reservoirs on a delta

iv) Use of the Constructed Unit Step Response Curves: Figures 19 and 22 can be used for a fault problem as well as for a reservoir geometry which can be approximated by overlapping two identical circles. Figure 23 and 24 can be used for a reservoir geometry approximated by overlapping three identical circles on a delta. Also, Figures 23 and 24 are useful to triangular shape aquifer geometry.

Above all, the primary purpose of constructing the unit step response curves is to serve as a guide and show how different they are compared to those without a fault.

By the use of the prepared graphs it was found that for a geometry formed by overlapping two identical circles or three identical circles on a delta can be approximated with a circle of equal area without introducing drastic error in getting the unit step response. (see also v. of section a.)

To illustrate the use of the graphs, suppose one considers the following information:

Pressure case

Three identical reservoirs on a delta

$r_D = 1/2$, $t_{D\ odd} = 800$ (dimensionless time calculated based on the radius of the identical circles),

then the following can be found:

Area : 7.0646 (when $r_g = 1$)

Radius of the equal area circle : 1.5

t_D circle : $800/(1.5)^2 = 356$

Q'_{tD} of the circle : 122.1 (reference 4)

$(1.5)^2 (122.1) = \underline{274.5}$ for equal area circle

$Q'_{tD\ odd} = 94$ from Fig. 24

$(3)(94) = \underline{282}$ for three overlapped circles.

c. Interference Among Two or More Fields Situated on a Common Aquifer: The first study of interference among the oil fields was made on an electrical reservoir analyzer to study the East Texas Fields.[11] But the first mathematical interference study was made by Mortada.[14] The application of Mortada's method to gas storage problems was made by Coats

in his thesis.[2] Coats' specific example was the interference of Fields C and D. Coats also studied Field A for which he came up with a good matching job by considering Field A as an isolated field sitting on a limited aquifer of $r_D = 20$.[6]

The purposes of the interference study here are to show how fields C and D actually affected Field A performance, and to show how Field E might have influenced the Field A. The approximate distance from Field A to Fields C, D, and E is $r_D = 15$. The distance may lead to a careless thought of neglecting the Fields C, D, and E. The larger the distance is, the smaller is the interference effect at a certain time, but there is no guarantee that the interference is going to be small at all times. The discussion is made under the subheadings of i) Interference theory, ii) The effect of flux at Field A on Fields C, D, and E, iii) The effect of fluxes at Fields C and D on Field A performance, and iv) The effects of fluxes at Fields C, D, and E on Field A performance.

i) Interference Theory: The basic idea of this theory stems from the fact that the original partial differential equation describing the liquid flow through a porous medium is linear and homogeneous. The same argument for equation (29) in the fault case study can be extended to any number of fields situated on a common aquifer. The pressure drop at a field can be broken down into the contributions attributed by the flux of each individual neighboring field, as well as by its own flux, because the water flux can only be caused at the expense of the pressure change.

ii) The Effect of Flux at Field A on Fields C and D: The Fields C and D were discovered in December 1944, while Field A was discovered in September 1941. The approximate geometry is sketched in Fig. 25. The radii of the three fields are approximated from the contour maps to be 1.43 - 1.55 miles. These three fields all have different pressure-time and volume-time histories.

The approximate volume variation at Field A has been computed from the production and pressure-time data. The volume variation is approximate because of the uncertainty of the original reservoir pore

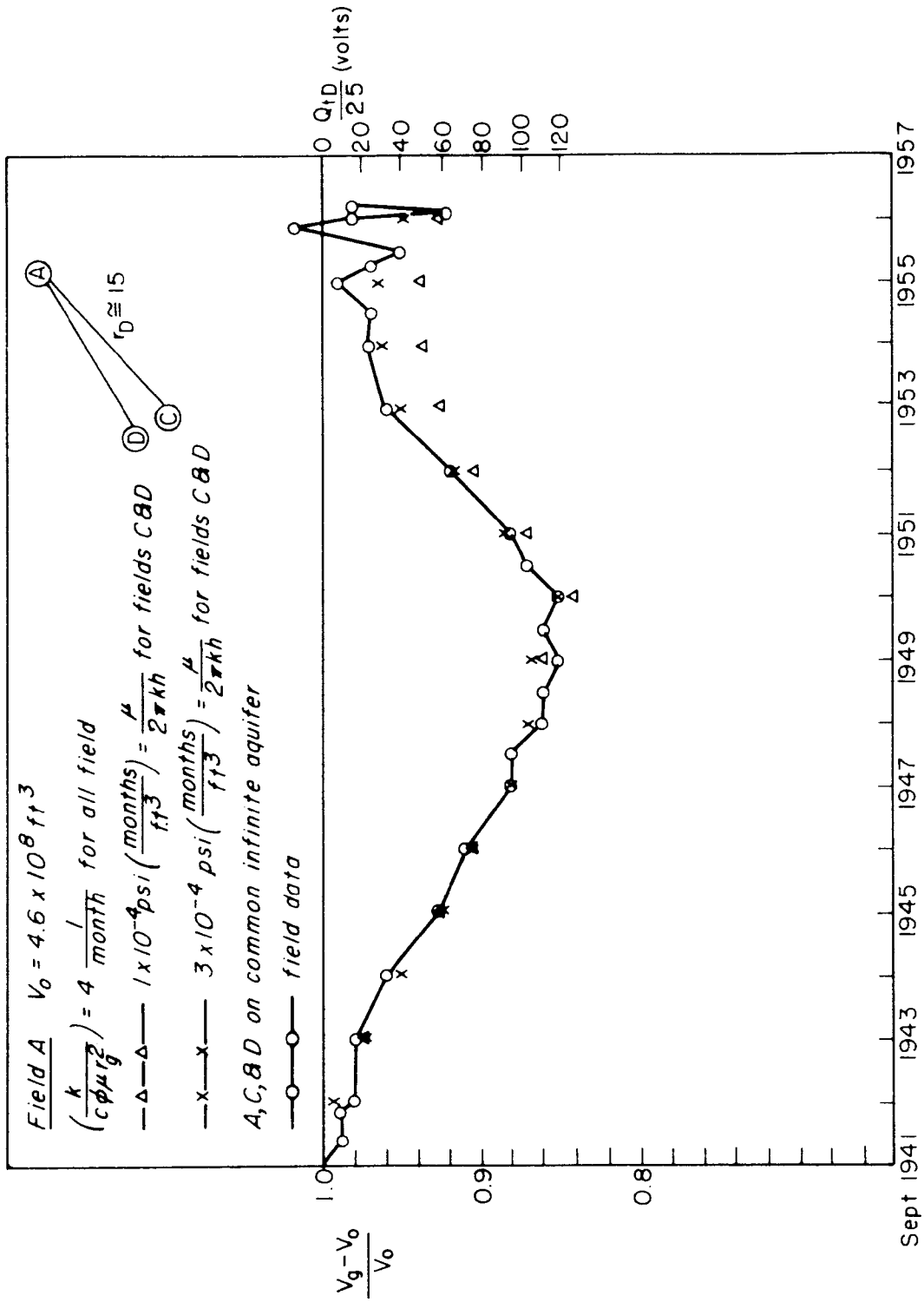


Fig. 25– Reservoir pore volume variation for field A considering the interference of fields C & D

volume estimation. The estimation of the original gas in place is usually made by assuming the pore volume to be constant for a certain period from the discovery date. The pressure decline, plotted against the production, usually gives a constant slope from which the approximate original pore volume can be estimated.

The volume variation of Field A is shown in Fig. 25. Using this volume variation as an input signal, the pressure change function at $r_D = 15$ can be obtained from the circuit given in Fig. 50. The output is the pressure change function from which one can find the extent of the pressure change contributions at Fields C, D, and E by the flux variation at Field A. The percent influences are given in Table VII as a function of time, which has been calculated from the following equation.

$$\% \text{ Influence to D by A} = \frac{P_{DA} \times (100)}{P_D - P_{DA}}$$

where $P_{DA} = b\,(P_{tD})_{DA}$, ($P_{DA}$ is the pressure change in psi at D by A) and P_D is the pressure in field D, taking its discovery pressure as datum.

The extent of the influence is a function of the distance between the fields, the flux variation of the influencing field, and the constants "a" and "b". The reservoir constants a and b are fully discussed in a latter chapter. From the result of this study, one can conclude that the distance between the fields ($r_D = 15$) is certainly not great enough to ignore the existance of the Fields C, D, and E completely.

Table VII. Influence of Field A on Fields C and D, ($a = 4$, $b = 10^{-4}$).

Time	% Influence at D by A	% Influence at C by A
Mar. 1946	36.7	48.3
Sept.	35.7	46.0
M 1947	29.5	35.7
S	28.9	34.2
M 1948	32.5	33.3
S	31.3	-
M 1949	28.2	49.7
S	23.5	-
M 1950	24.4	35.7
S	23	18.8
M 1951	17.7	38.3
S	16.2	12.7
M 1952	10.4	31.6
S	2.5	0
M 1953	1.0	0
S	6.0	4.4
M 1954	10.0	25.1
S	13.9	19.0
M 1955	19.0	19.3
S	14.5	-
M 1956	9.0	5.0
S	7.0	0

iii) The Effects of Fluxes at Fields C and D on Field A Performance: It is shown that Fields C and D may have influenced the performance of Field A. Since the approximate volume variations of Fields C and D are available (Table VIII), the influence of Fields C and D can be found. As was done in the previous case, the volume variations of Fields C and D are used as input signals to find the pressure change functions at Field A using the circuit of Figure 50. The influence is noticeable during the period of June, 1945 - December, 1951. The influence of C to A and that of D to A oppose each other and nearly cancel from 1952. By selecting typical reservoir constants and by using the circuit of Figure 48, the volume variation of Field A is predicted

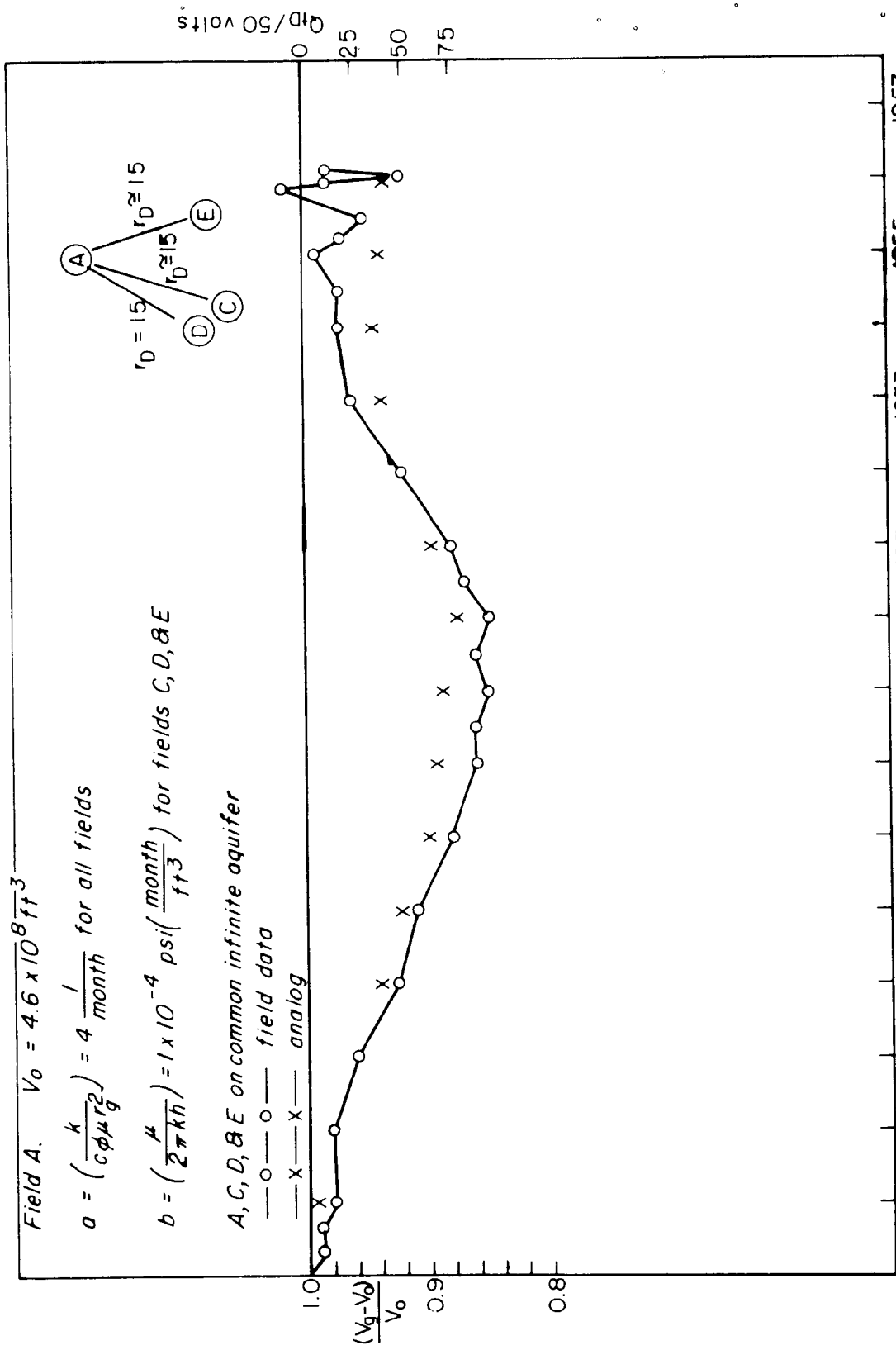


Fig. 26 - Reservoir pore volume variation for field A considering the interference of fields C, D, & E

considering the influence of Fields C and D. The results are plotted in Figure 25 to compare with the actual data. The input to the circuit of Figure 48 is no longer the pressure variations of Field A given in Figure 9. The input must be the pressure contribution at Field A by its own flux which can be found by subtracting the pressure drop due to the interference from other fields. The pressure input signals used to get the flux of Field A is given in Table IX.

This attempt shows that it is possible to do the fair matching job of the actual data by simply forcing the reservoir constants to fit, even though the constants may not be realistic.

iv) The Effects of the Fluxes at Fields C, D, and E to Field A performance: In this study the effect of Field E is included in addition to Fields C and D for which the previous section is devoted. The distance to Fields C, D, and E from A is $r_D = 15$ as shown in Figure 26. The approximate volume variation of Field E is given in Table X. The procedure of the study is the same as that of the previous case. The pressure input is given in Table IX while the result of the volume prediction is plotted in Figure 26 along with the actual data. By properly choosing the reservoir constants, it is expected that the results can be improved.

Table VIII Volume Variations of Fields C and D

Time	Field C		Field D	
	$\frac{V_g}{V_o} - 1$	Volts	$\frac{V_g}{V_o} - 1$	Volts
Dec. 1944	-0.003	-1.5	-	-
Jun. 1945	-0.007	-3.5	-0.056	-11.2
D	-0.001	-0.5	-0.016	- 3.2
J 1946	-0.011	-5.5	-0.032	- 6.4
D	0.003	1.5	-0.05	-10.0
J 1947	-0.02	-10.0	-0.055	-11.0
D	-0.03	-15	-0.063	-12.6
J 1948	-0.031	-15.5	-0.077	-15.4
D	-0.038	-19	-0.089	-17.8

Table VIII (cont'd)

Time	Field C $\frac{V_g}{V_o} - 1$	Field C Volts	Field D $\frac{V_g}{V_o} - 1$	Field D Volts
J 1949	-0.018	- 9	-0.094	-18.8
D	-0.032	-16	-0.11	-22
J 1950	-0.032	-16	-0.12	-24
D	-0.017	8.5	-0.14	-28
J 1951	-0.007	- 3.5	-0.16	-32
D	0.034	17	-0.18	-36
J 1952	0.037	18.5	-0.21	-42
D	0.089	44.5	-0.25	-50
J 1953	0.084	42	-0.24	-48
D	0.105	52.5	-0.25	-50
J 1954	0.088	44	-0.257	-51.4
D	0.124	62	-0.265	-53
J 1955	0.119	59.4	-0.272	-54.4
D	0.102	51	-0.278	-55.6
J 1956	0.106	53	-0.284	-56.8
D	0.07	35	-0.288	-57.6

Table IX Pressure Variations to Find the Cumulative Flux at Field A.

(1) : Pressure input signal ignoring Fields C, D, and E.
(2) : Considering Fields C and D, $a = 4$; $b = 10^{-4}$.
(3) : Considering Fields C and D, $a = 4$; $b = 3 \times 10^{-4}$.
(4) : Considering Fields C, D, and E, $a = 4$; $b = 10^{-4}$.

Time	Well-head Reservoir Pressure, psi	Volts (1)	Volts (2)	Volts (3)	Volts (4)
Sept. 1941	438				
Jan. 1942	419	5	5	5	3.4
Feb.	410	7	7	7	5.4
Mar.	402	9	9	9	7.4
Apr.	397	10.3	10.3	10.3	8.7
May	394	10.5	10.5	10.5	9.0
June	391	11.7	11.7	11.7	10.1
July	389	12.5	12.5	12.5	11.0
Nov.	361	19	19	19	17.4
Dec.	359	20	20	20	18.4

Table IX (cont'd)

Time	Well-head Reservoir Pressure, psi	(1)	(2)	(3)	(4)
Feb. 1943	349	22.5	22.5	22.5	20
Mar.	349	22.5	22.5	22.5	20
Apr.	336	25.5	25.5	25.5	20
June	328	27.5	27.5	27.5	25
July	325	28.5	28.5	28.5	26
Aug.	318	30	30	30	27.5
Sept.	315	30.7	30.7	30.7	28.2
Oct.	313	31.3	31.3	31.3	29
Dec.	308	32.5	32.5	32.5	30
Jan. 1944	304	33.5	33.5	33.5	32
Jun.	290	37	37	37	35.5
Dec.	283.5	36.5	36.5	36.5	35
Jan. 1945	280	37	37	37	32
Aug.	294	34	32	28	29
Sept.	300	33	31	27	28
Nov.	279	40	38	34	35
Jan. 1946	272	41.5	39	35	32
Jun.	253	46.3	43	37	37
Dec.	243	49	46	40	39.5
Jan. 1947	240	49	46	40	39
Jun.	245.5	48	45.5	40	38
Dec.	252	46.5	42	33	36.5
Jan. 1948	255	46	42	34	32.4
Mar.	258.5	45	41	33	31.4
Apr.	273	41.5	37	28	28
Jun.	279.2	40	35	25	26.4
Dec.	298.8	35	30	20	21.4
Jun. 1949	293.9	36	31	21	26.4
Sept.	297.8	35	29.5	18.5	25.4
Dec.	289.4	37	31.5	20.5	27.4

Table IX (cont'd)

Time	Well-head Reservoir Pressure, psi	(1)	(2)	(3)	(4)
Apr. 1950	277.9	40	35.5	26.5	27.5
May	284.6	39	35	27	26.5
Jun.	292.6	36	31.5	22.5	23.5
Jul.	296.3	35	30.5	21.5	22.5
Aug.	299.5	35	30.5	21.5	22.5
Sept.	360.5	20	16	8	7.5
Oct.	436.2	0.5	-3.5	-11.5	-12.0
Nov.	444.4	-1.5	-5.5	-13.5	-14.0
Dec.	434.4	1	-3	-11	-11.5
Jan. 1951	367.5	17.5	13.5	5.5	9.5
Feb.	338.3	25	21	13	17
Mar.	331.7	26.5	22.5	14.5	18.5
Apr.	369.1	17	13	5	9
May	424.7	3.5	0	-7	-4.5
June	504.5	-16.5	-20	-27	-8.5
July	543.3	-21.5	-25	-31	-29.5
Aug.	596.1	-39.5	-42.8	-49.5	-47.5
Sept	622.4	-46	-49	-55	-54
Oct.	634.4	-49	-51	-55	-57
Nov.	584.2	-36.5	-38.5	-42.5	-44.5
Dec.	549.8	-15	-17	-21	-23
Jan. 1952	492.4	-13.5	-15	-18	-18
Feb.	463.4	-6.5	-8	-11	-11
Mar.	457.4	-5	-6	-8	-8
Apr.	470.2	-8	-8	-8	-8
May.	524.8	-28.5	-28.5	-28.5	-28.5
Jun.	582.5	-36.5	-36.5	-36.5	-36.5
Jul.	641.9	-51	-51	-51	-51
Aug.	661.0	-56	-56	-56	-56
Sept.	664.9	-57	-57	-57	-57
Oct.	644.7	-50	-50	-50	-50
Nov.	621.1	-46	-46	-46	-46
Dec.	587.7	-35	-35	-35	-35

Table IX (cont'd)

Time	Well-head Reservoir Pressure, psi	(1)	(2)	(3)	(4)
Jan. 1953	521	-21	-21	-21	-21
Feb.	473	- 9	- 9	- 9	- 9
Mar.	441.6	- 0.8	- 0.8	- 0.8	- 0.8
Apr.	440	- 0.5	- 0.5	- 0.5	- 0.5
May	454.3	- 4	- 4	- 4	- 4
Jun.	465.4	- 7	- 7	- 7	- 7
Jul.	533.1	-24	-24	-24	-24
Aug.	594.	-39	-39	-39	-39
Sept.	616.6	-45	-45	-45	-45
Oct.	627	-48	-48	-48	-48
Nov.	605.5	-42.5	-42.5	-42.5	-42.5
Dec.	549.4	-28	-28	-28	-28
Jan. 1954	476.3	-10	-10	-10	-10
Feb.	433.1	1	1	1	1
Mar.	407.6	7.5	7.5	7.5	7.5
Apr.	417.2	5	5	5	5
May	449.8	- 2.5	- 2.5	- 2.5	- 2.5
Jun.	494.4	-14	-14	-14	-14
Jul.	531.2	-23	-23	-23	-23
Aug.	577.6	-35	-35	-35	-35
Sept.	603.2	-42	-42	-42	-42
Oct.	598	-41	-41	-41	-41
Nov.	559.5	-30	-30	-30	-30
Dec.	467	- 7	- 7	- 7	- 7
Jan. 1955	396.2	10.5	10.5	10.5	10.5
Feb.	332.4	26.5	26.5	26.5	26.5
May	329	27.5	27.5	27.5	27.5
Jun.	409.8	7	7	7	7
Jul.	497.7	-15	-15	-15	-15
Aug.	565.2	-32	-32	-32	-32
Sept.	581.4	-36	-36	-36	-36
Oct.	580.8	-36	-36	-36	-36
Nov.	520	-20.5	-20.5	-20.5	-20.5
Dec.	431.4	2	2	2	2

Table IX (cont'd)

Time	Well-head Reservoir Pressure, psi	(1)	(2)	(3)	(4)
Jan. 1956	375.5	16	16	16	16
Feb.	312.8	31	31	31	31
Mar.	275	41	41	41	41
May	276.6	40	40	40	40
Jun.	329.2	27	27	27	27
Jul.	380.4	14.5	14.5	14.5	14.5
Aug.	434.5	1	1	1	1
Sept.	502.3	-16	-16	-16	-16
Oct.	483	-11	-11	-11	-11
Nov.	497.8	-15	-15	-15	-15
Dec.	466.8	- 7	- 7	- 7	- 7

Table X Volume Variation of Field E

Time	$(\frac{V}{V_0} - 1)$	Volts
Aug. 1935	0	0
Aug. 1942	-0.06	-30
Aug. 1943	-0.06	-30
Jul. 1944	-0.055	-27.5
Feb. 1945	-0.06	-30
Oct. 1945	-0.065	-32.5
Apr. 1946	-0.075	-37.5
Oct. 1946	-0.065	-32.5
Apr. 1947	-0.08	-40
Oct. 1947	-0.055	-27.5
Apr. 1948	-0.095	-47.5
Sept. 1948	-0.08	-40
Mar. 1949	-0.055	-27.5
Oct. 1949	-0.07	-35
Apr. 1950	-0.05	-25
Oct. 1950	-0.075	-37.5
Apr. 1951	-0.05	-25
Sept. 1951	-0.06	-30

Table X (cont'd)

Time	$(\frac{V}{V_o} - 1)$	Volts
Jul. 1952	+0.02	+10
Oct. 1952	-0.045	-22.5
May 1953	-0.015	- 7.5
Nov. 1953	-0.025	-12.5
Apr. 1954	+0.02	+10
Nov. 1954	-0.02	-10
Jul. 1955	+0.08	+40
Oct. 1955	-0.02	-10
Aug. 1956	+0.095	+47.5
Oct. 1956	-0.03	-15

d. Moving Boundary Problems: The problems which we have treated thus far are fixed boundary problems. The gas field radius has been considered to be stationary or constant. Other than the "aquifer gas storage" problems, the constant radius assumption is quite good. However, in the aquifer gas storage, the gas bubble radius is growing from zero to a mile during a certain period of time before a well-developed, and stabilized gas bubble is established.

Some theoretical analysis of the moving boundary problem is offered in this section. The heading is further subdivided into i) Partial differential equation, ii) Approximate solution and performance coefficients of back pressure curve, iii) Use of the instantaneous sources, iv) Unit step responses of growing disk source model for finite aquifer thickness.

i) Partial Differential Equation: For moving boundary problems, which one is referring to aquifer gas storage operations, the gas field radius is changing as a function of time. However, from the derivation of the original differential equation, there have been no restrictions on the gas bubble radius, and the equation (4) must hold true even for a moving boundary problem.

$$\frac{\partial^2 P}{\partial r^2} + \frac{1}{r}\frac{\partial P}{\partial r} = \frac{c\phi\mu}{k}\frac{\partial P}{\partial \theta'} \qquad (4)$$

If one makes a transformation of $r_D = \frac{r}{r_g}$, r_D is not only a function of r, but it is also a function of time because r_g is changing as a function of time. Therefore, the partial differential equation takes the following form:

$$\frac{\partial^2 P}{\partial r_D^2} + \frac{1}{r_D}\frac{\partial P}{\partial r_D} = \frac{c\phi\mu r_g^2}{k}\left(\frac{\partial P}{\partial \theta'} + \frac{\partial P}{\partial r_D}\frac{\partial r_D}{\partial \theta'}\right) \qquad (30)$$

Equation (30) has an extra term added to the radial diffusivity equation (5). When r_g is constant, equation (30) reduces to equation (5). Equation (30) describes the liquid flow through a porous medium when the reservoir radius is growing, and it is a nonlinear partial differential equation as it appears because of the last term. It looks as though the attempt of trying to re-define the dimensionless time to reduce equation (30) to the form of equation (5) is not likely to be successful.

The analog approach to solve a melting slab problem, where heat flow in only one direction is allowed, has been reported, based on a so called "lumped-cell method".[17] Coats' method[2] ignores the last term of equation (30).

ii) Approximate Solution and Performance Coefficient of Back Pressure Curve: Considering a moving boundary model of a horizontal radial plug flow as shown is Figure 27, one can make a rate balance at the boundary at a time θ:

$$\text{Rate (volume/unit time)} = (2\pi\phi r_g)\frac{dr_g}{d\theta}h = \frac{dV_g}{d\theta}$$

$$\because \quad V_g = \phi\pi r_g^2 h$$

$$\text{Rate (volume/unit time)} = 2\pi r_g h \frac{k}{\mu}\left(\frac{\partial P}{\partial r}\right)_{r_g}$$

Equating these two rate expressions:

$$\frac{dr_g}{d\theta} = \frac{k}{\phi\mu}\left(\frac{\partial P}{\partial r}\right)_{r_g}$$

or by writing

$$r_g\left(\frac{\partial P}{\partial r}\right)_{r_g} = \left(\frac{\partial P}{\partial r_D}\right)_1 ,$$

$$\frac{dr_g^2}{d\theta} = \frac{2k}{\phi\mu}\left(\frac{\partial P}{\partial r_D}\right)_1$$

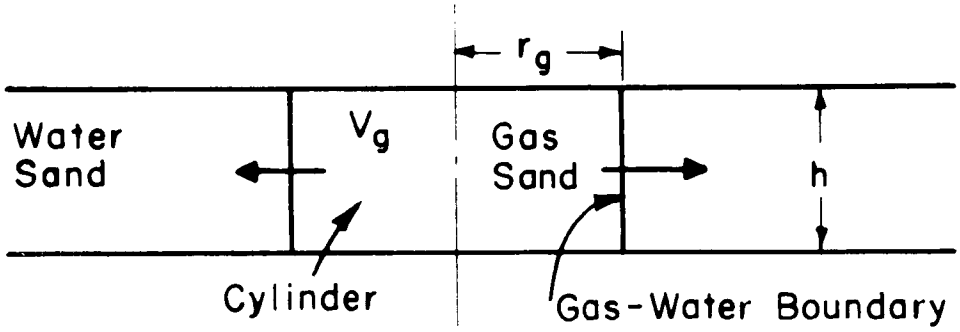


Fig. 27 - Horizontal radial plug flow moving boundary model.

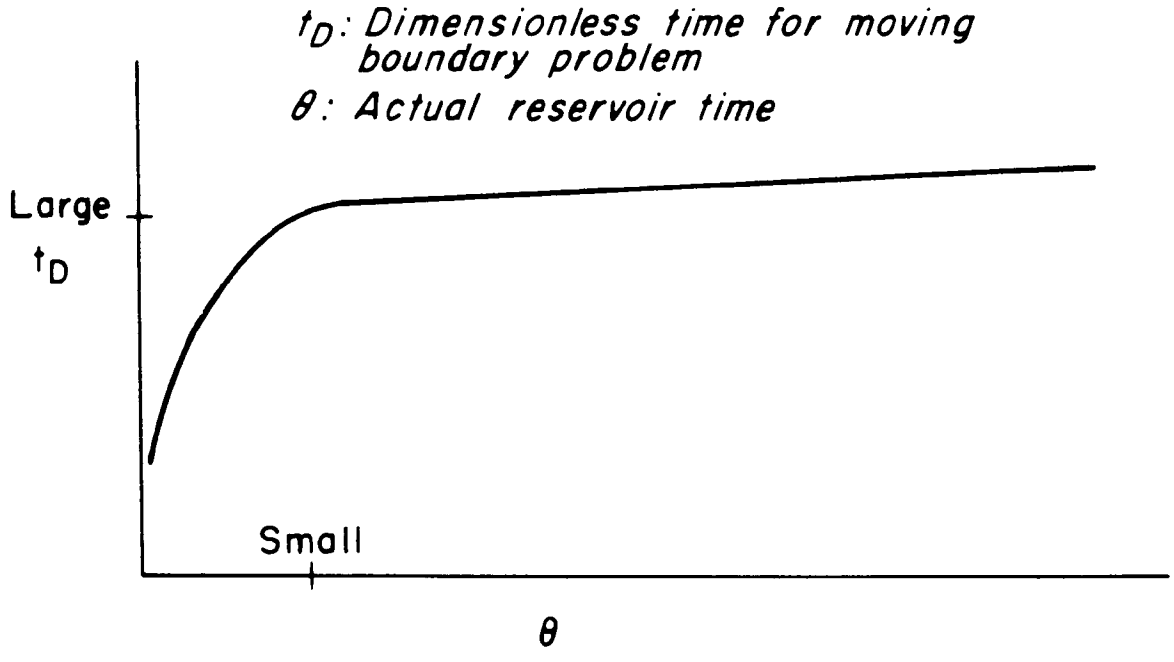


Fig. 28 - Moving boundary dimensionless time versus actual time.

Finally, it gives the following form:

$$r_g^2 - (+0) = \frac{2k}{\phi\mu}\int_{+0}^{\theta}\left(\frac{\partial P}{\partial r_D}\right)_1 d\theta \qquad (31)$$

It turns out that, for a moving boundary problem applicable for gas storage operations, the value of dimensionless time becomes large (order of thousands) after a short period of time as illustrated in Figure 28. The dimensionless time in Figure 28 has a different meaning than that of the fixed boundary problems.[2] From our experience, it is also noted that the pressure gradient at the reservoir levels off at the large dimensionless time portion as shown in Figure 29. $\left(\frac{\partial P}{\partial r_D}\right)_1$ is a direct measure of the water flux at the gas-water interface, and it should be directly proportional to the performance coefficient of the well-known back pressure equation:[13]

$$Q = C\left(P_f^2 - P_s^2\right)$$

The proportionality constant " C " actually changes according to Figure 29, but the change at the large time portion is very small, and people accepted the idea of its constancy.

By taking the following numbers:

$$\left(\frac{\partial P'}{\partial r_D}\right)_1 = 0.203$$

$$P = 50/14.7 \text{ atm (constant)}$$

$$\phi = 0.2$$

$$\frac{k}{\mu} = 1.0 \text{ darcy/cp}$$

the following simple equation is obtained:

$$r_g' \cong 1.395 \times 10^{-2}\,\theta^{1/2} \qquad (32)$$

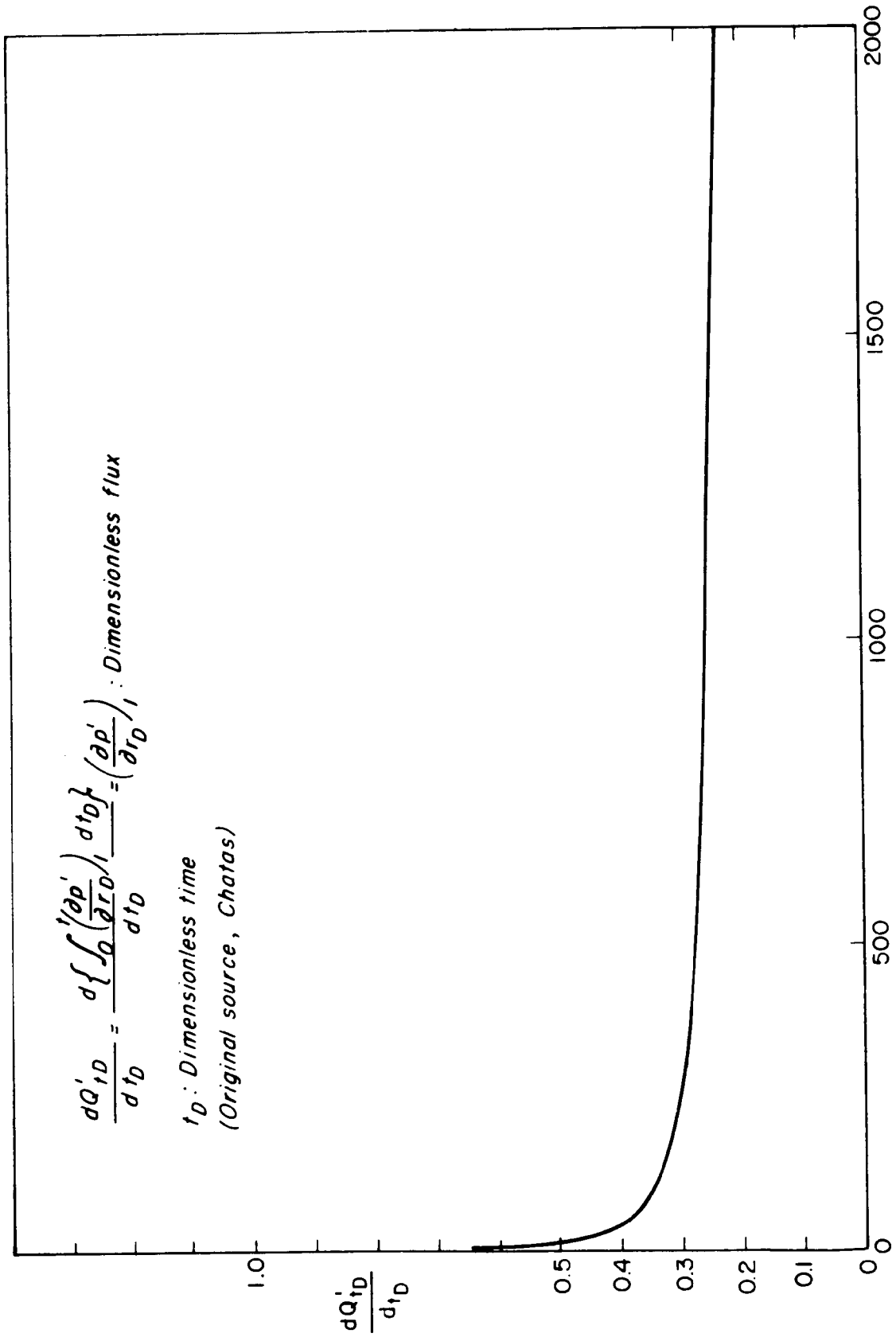


Fig. 29-Pressure gradient at the reservoir versus dimensionless time.

From equation (32) one can easily show that the t_D's for the moving boundary problem are actually big numbers (see also the growing disk model study in a latter section). Even though this has been a bias estimate, it is an indication that the assumption is not critical. Using this method, Figure 30 is constructed. It must be pointed out that the method is reasonable only when the short time effect can be ignored.

The approximate solution for the gas bubble growth with $\frac{k}{\mu} = 1.0$ darcy/cp in Figure 30 is compared in Figure 31 with the gas bubble growth computed by assuming fixed gas bubble radii of 100 ft and 500 ft. When a fixed radius is assumed, the radius of the gas bubble is calculated from:

$$r_g' = \sqrt{\frac{V_g 10^6}{\phi \pi h}} = \sqrt{\frac{2\pi h c' \phi r_{g\,fixed}^2 (\Delta P) Q'_{tD}}{\phi \pi h}}$$

Where Q'_{tD} is read from the Van Everdingen and Hurst table [4] by knowing $t_D = \frac{k}{c \phi \mu r_{g\,fixed}^2}$.

It is interesting to note that equation (32) has a similar expression as that of the drainage radius [13] reported in the literature. The physical interpretation of this similarity is that the gas bubble growth takes place much the same way as the drainage radius propagation. It must be pointed out that the drainage radius concept and equation (32) are the results of studying the strictly radial plug flow model.

iii) Use of the Instantaneous Sources: In the early part of this section for moving boundary problems, it was shown that the Van Everdingen and Hurst table [4] can not be used theoretically, and that the rigorous analytical attempt to solve equation (30) is hopeless.

An alternate approach is taken here, using the instantaneous sources. Some analytical solutions to different shapes of moving sources which may be useful to aquifer gas storage problems are derived. The solutions are developed by the use of the instantaneous point source solution given by

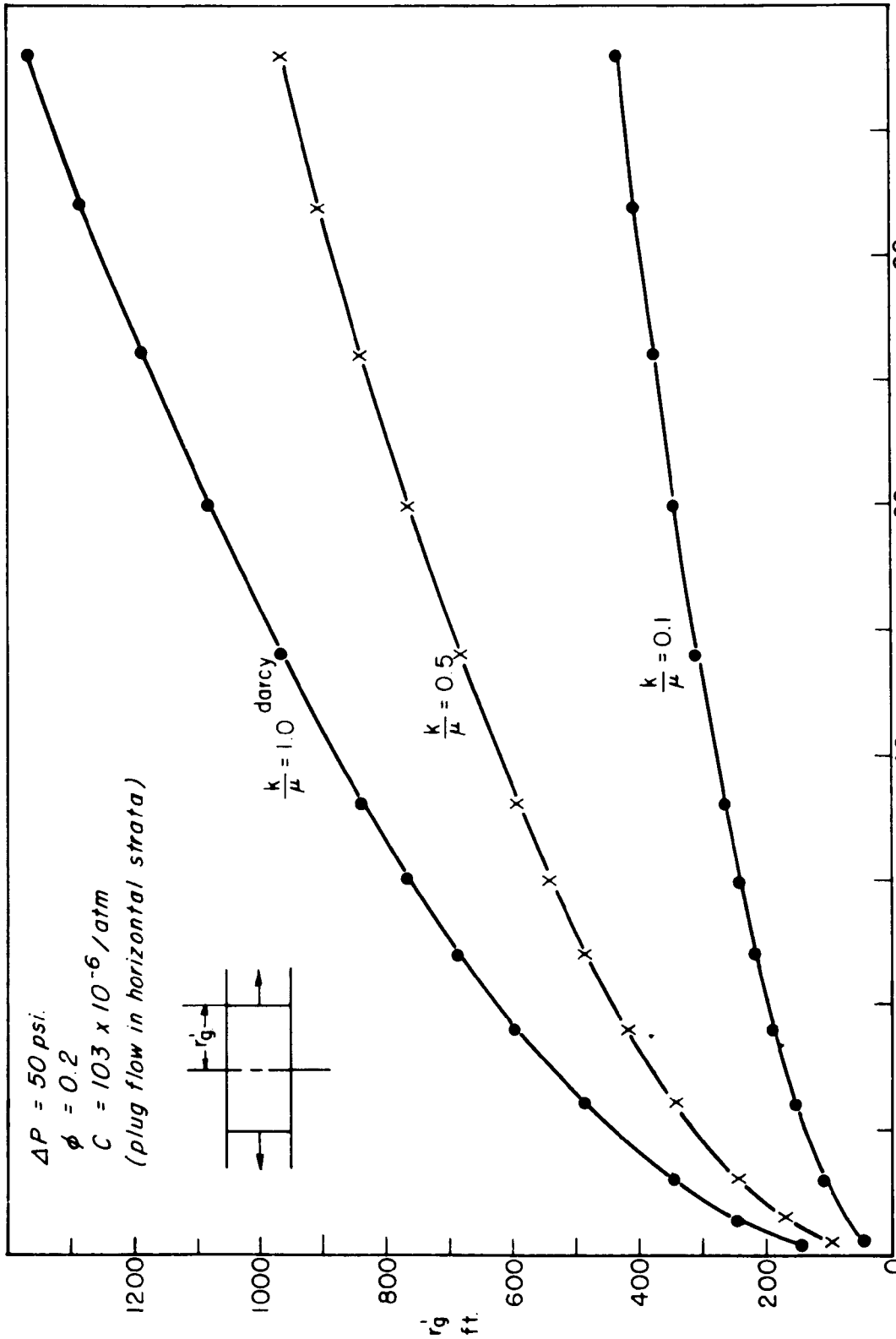


Fig.30 - Approximate gas bubble growth with time for constant pressure case of infinite aquifer

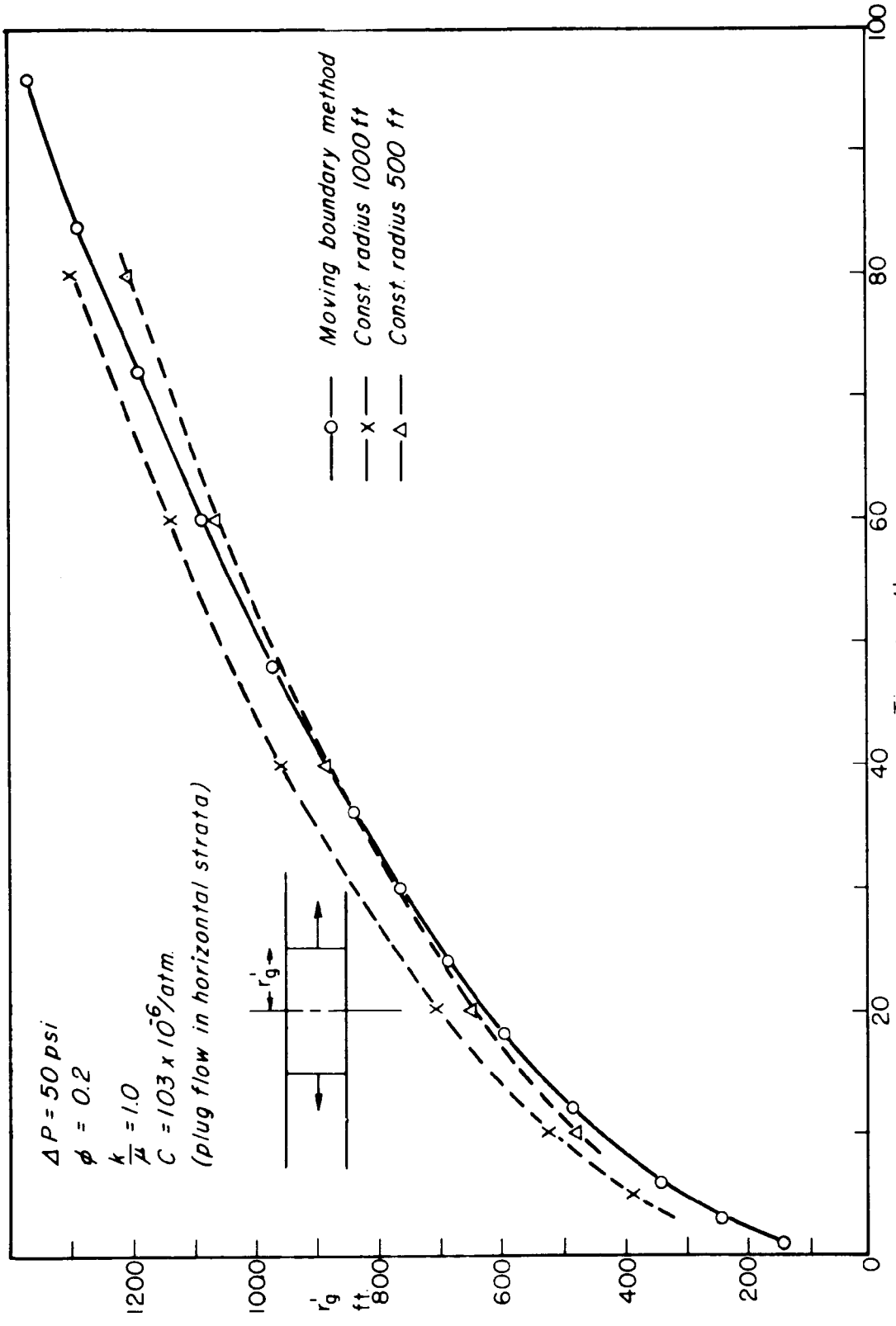


Fig. 31 – Approximate gas bubble growth with time for constant pressure case (for fixed or growing radius)

Carslaw and Jaeger.[15] Recently, Ramey[19] and also Bailey and Larkin[18] have used similar solution of this kind for the application to the thermal oil recovery process. In the thermal recovery process, the heat conduction in the underground combustion is much the same as the flow of liquid through a porous medium, and the basic governing differential equation is identical.

(A) Instantaneous Point and Line Source: The instantaneous point source or sink solution was first offered by Carslaw and Jaeger in their book.[15] This solution can be modified to the flow of liquid through a porbus medium. The partial differential equation (diffusivity equation) in three dimensional cartesian coordinates is:

$$\frac{\partial^2 p}{\partial x^2} + \frac{\partial^2 p}{\partial y^2} + \frac{\partial^2 p}{\partial z^2} = \frac{c\phi\mu}{k} \frac{\partial p}{\partial \theta'} \tag{33}$$

and is satisfied by:

$$\varrho = \frac{q}{8\phi\left[\pi\left(\frac{k}{c\phi\mu}\right)\theta\right]^{3/2}} \cdot e^{-\frac{\{(x-x')^2+(y-y')^2+(z-z')^2\}}{4\left(\frac{k}{c\phi\mu}\right)\theta}} \tag{34}$$

where ϱ = density of water

q = mass withdrawn, lb.

(x', y', z') = location of source

The solution (34) may be considered as the density change in the infinite three dimensional water-sand body due to a quantity of mass q strength instantaneously withdrawn at $\theta = 0$ at a point (x', y', z'). This solution is called the instantaneous point source solution. It is a highly imaginative case but is quite useful in developing more important solutions to complicated source problems.

Upon distributing a series of instantaneous point sources of ($q_1 dz'$) strength along the line z' (Figure 32), and integrating from - ∞ to + ∞, the instantaneous line source solution can be obtained:

$$\rho = \frac{q_1}{4\pi\phi\left(\frac{k}{c\phi\mu}\right)\theta} \cdot e^{-\frac{\{(x-x')^2 + (y-y')^2\}}{4\left(\frac{k}{c\phi\mu}\right)\theta}} \qquad (35)$$

where q_1 = mass withdrawn per unit depth (z direction), lb/ft. This solution is the radial flow solution where the fluid is withdrawn at the infinitely long line uniformly and instantaneously.

(B) Uniform Cylindrical Surface Source Moving Radially (Radial Flow). A uniform cylindrical surface source can be synthesized from equation (35), by expressing

$$(x-x')^2 + (y-y')^2 = r^2 + r_g^2 - 2 r r_g (\theta_A - \theta_A') \;;$$

distributing the line sources around the circle of radius r_g of strength ($q_2 r_g d\theta_A$); and integrating from zero to 2π. The instantaneous cylindrical surface source solution becomes:

$$\rho = \frac{q_3}{2\phi\left(\frac{k}{c\phi\mu}\right)\theta} \cdot e^{\frac{-(r^2+r_g^2)}{4\left(\frac{k}{c\phi\mu}\right)\theta}} \cdot I_0\left(\frac{r r_g}{2\left(\frac{k}{c\phi\mu}\right)\theta}\right) \qquad (36)$$

where $q_3 = 2\pi r_g q_2$ lb/ft depth

I_0 = Bessel function of the 1st kind of an imaginary argument and zero order.

So far, we have developed the source geometry by integrating in the sequence from point - line - cylindrical surface, (Figure 33). Time effect must be considered in order to obtain a continuous source, but with

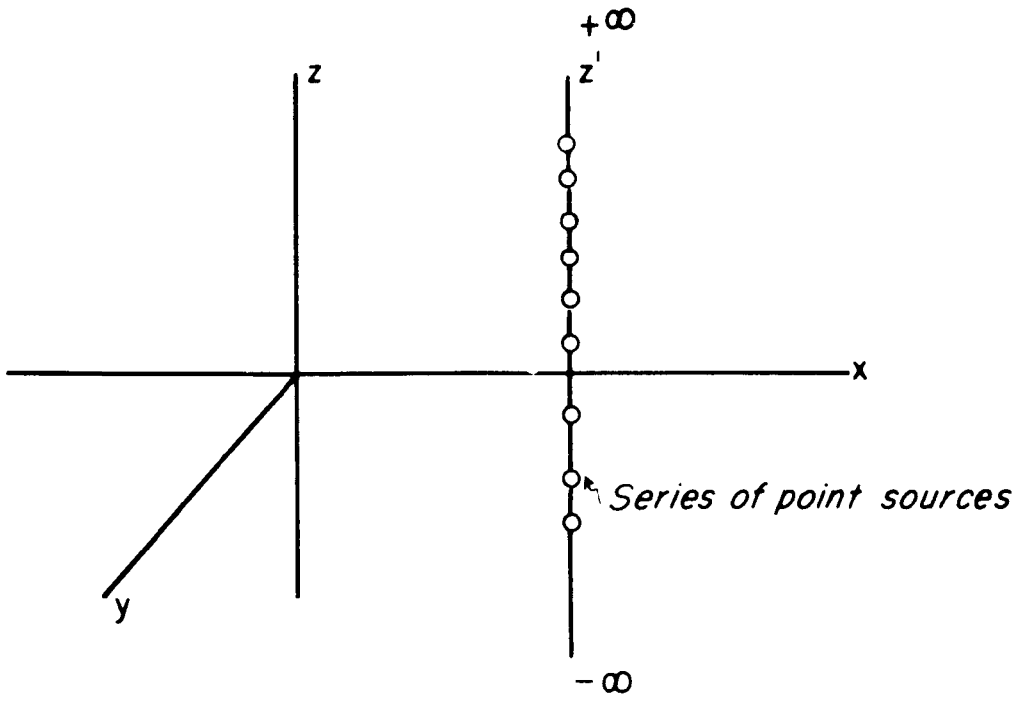


Fig 32- Line source from point sources

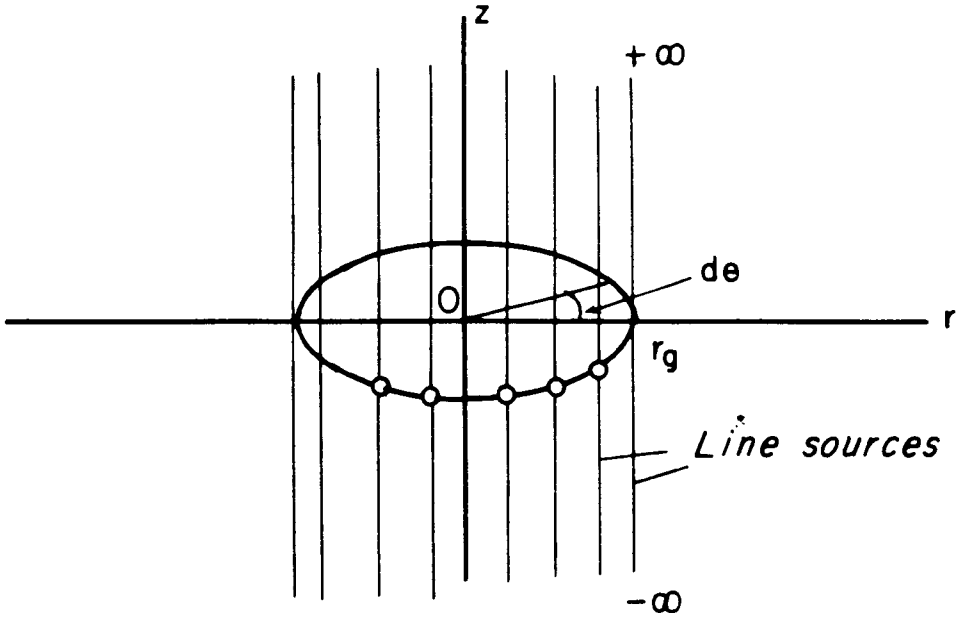


Fig. 33- Uniform cylindrical surface source from line sources

time varying q_3 rate and r_g. One can impose a desired continuous source or sink by a number of instantaneous sources of the proper strength in the correct sequence of time. This, in essence, is the superpositon of the different pressure or density effect with time varying mass rate per unit depth. In doing so, one is also free to choose the radius r_g as a function of time because we did not put any restrictions on r_g in the course of developing equation (37).

$$-(\rho-\rho_o) = \frac{1}{2\phi\left(\frac{k}{c\phi\mu}\right)} \int_0^\theta \frac{q_4 \cdot e^{\frac{-(r^2+r_g^2)}{4\left(\frac{k}{c\phi\mu}\right)(\theta-\tau)}}}{(\theta-\tau)} \cdot I_o\left(\frac{r\,r_g}{2\left(\frac{k}{c\phi\mu}\right)(\theta-\tau)}\right) d\tau \qquad (37)$$

where q_4 = mass rate per unit depth, lb/day-ft. Equation (37) is the solution for strictly radial flow on an aquifer with arbitrary mass flux when the uniform pressure cylindrical surface is moving radially. Muskat's book[3] (p. 688) gives the identical equation but did not mention its validity for a moving source.

When one assumes an aquifer gas storage model to be strictly radial flow and uniform sand thickness in a horizontal strata, the volume of the gas space is (Figure 27)·

$$V_g = \phi \pi r_g^2 h$$

or

$$r_g = \left(\frac{V_g}{\phi \pi h}\right)^{1/2}$$

upon substituting,

$$\rho \cong \rho_o\left[1-c(p_o-p)\right] \; ; \quad q \cong \rho_{Av}\frac{dV_g}{d\theta} \; ; \quad \frac{\rho_{Av}}{\rho_o} \cong 1.0$$

the solution to the model as shown in Figure 27 becomes:

$$(P_g - P_{og}) \cong \frac{\mu}{2kh} \int_0^{\theta} \frac{\frac{dV_g}{d\tau} \cdot e^{\frac{-V_g}{2\pi\phi h\left(\frac{k}{c\phi\mu}\right)(\theta-\tau)}} \cdot I_o\left[\frac{V_g}{2\pi\phi h\left(\frac{k}{c\phi\mu}\right)(\theta-\tau)}\right] d\tau}{(\theta-\tau)} \quad (38)$$

where P_{og} is the reservoir pressure at the time equals zero. The relationship between V_g, P_g, and θ of the gas bubble is described by equation (38).

(C) Ring Source Moving Radially: By distributing a series of instantaneous point sources around a circle, equation (34) can be converted to a solution for the instantaneous ring source (Figure 34):

$$\rho = \frac{q}{8\phi\left(\pi\left(\frac{k}{c\phi\mu}\right)\theta\right)^{3/2}} \cdot e^{\frac{-(r^2 + r_g^2 + z^2)}{4\left(\frac{k}{c\phi\mu}\right)\theta}} \cdot I_o\left[\frac{r\, r_g}{2\left(\frac{k}{c\phi\mu}\right)\theta}\right]$$

where q = mass withdrawn, lb. For the moving ring source, the solution becomes at z = 0:

$$\rho = \frac{1}{8\phi\left(\pi\left(\frac{k}{c\phi\mu}\right)\right)^{3/2}} \int_0^{\theta} \frac{q_5 \cdot e^{\frac{-(r^2 + r_g^2)}{4\left(\frac{k}{c\phi\mu}\right)(\theta-\tau)}} \cdot I_o\left[\frac{r\, r_g}{2\left(\frac{k}{c\phi\mu}\right)(\theta-\tau)}\right] d\tau}{(\theta-\tau)^{3/2}} \quad (39)$$

where q_5 = mass flux, lb/day.

For an aquifer gas storage, if the shape of the cap rock structure is assumed to be parabolic, there is a relationship between r_g and V_g (Figure 35):

$$V_g = S_F\, r_g^4$$

where S_F is a constant, or $\frac{\phi \pi}{2 S_f}$ & $S_f = \frac{r_g^2}{y_g}$.

With the same approximations made for equation (38), the solution becomes for the moving ring source model as shown in Figures34 and 35:

$$(P_g - P_{og}) \cong \frac{1}{4\phi C\left(\pi \frac{k}{c\phi\mu}\right)^{3/2}} \int_0^\theta \frac{\left(\frac{dV_g}{d\tau}\right) \cdot e^{\frac{-\left(\frac{V_g}{S_F}\right)^{1/2}}{2\left(\frac{k}{c\phi\mu}\right)(\theta-\tau)}}}{(\theta-\tau)^{3/2}} \cdot I_o\left[\frac{\left(\frac{V_g}{S_F}\right)^{1/2}}{2\left(\frac{k}{c\phi\mu}\right)(\theta-\tau)}\right] d\tau \quad (40)$$

(D) Nonuniform Cylindrical Surface Source Moving Radially: (Flow in all directions) Solution for a ring source can be used to give a nonuniform cylindrical surface source of finite length in an aquifer or infinite depth. The instantaneous solution becomes:

$$\rho = \frac{q_3}{8\pi\phi\left(\frac{k}{c\phi\mu}\right)\theta} \cdot e^{\frac{-(r^2+r_g^2)}{4\left(\frac{k}{c\phi\mu}\right)\theta}} \cdot I_o\left[\frac{r\, r_g}{2\left(\frac{k}{c\phi\mu}\right)\theta}\right]\left[erf\left(\frac{h-z}{2\left(\frac{k\theta}{c\phi\mu}\right)^{1/2}}\right) + erf\left(\frac{h+z}{2\left(\frac{k\theta}{c\phi\mu}\right)^{1/2}}\right)\right] \quad (41)$$

where q_3 = lb/ft depth.

For radially moving source:

$$\rho = \frac{1}{8\pi\left(\frac{k}{c\phi\mu}\right)} \int_0^\theta \frac{q_4}{(\theta-\tau)} \cdot e^{\frac{-(r^2+r_g^2)}{4\left(\frac{k}{c\phi\mu}\right)(\theta-\tau)}} \cdot I_o\left[\frac{r\, r_g}{2\left(\frac{k}{c\phi\mu}\right)(\theta-\tau)}\right]\left[erf\left(\frac{h-z}{2\left(\frac{k}{c\phi\mu}(\theta-\tau)\right)^{1/2}}\right) + erf\left(\frac{h+z}{2\left(\frac{k}{c\phi\mu}(\theta-\tau)\right)^{1/2}}\right)\right] d\tau \quad (42)$$

where q_4 = flux per unit depth.

If one considers a model of aquifer gas storage as shown in Figure 36, the solution becomes, with parabolic gas cap shape:

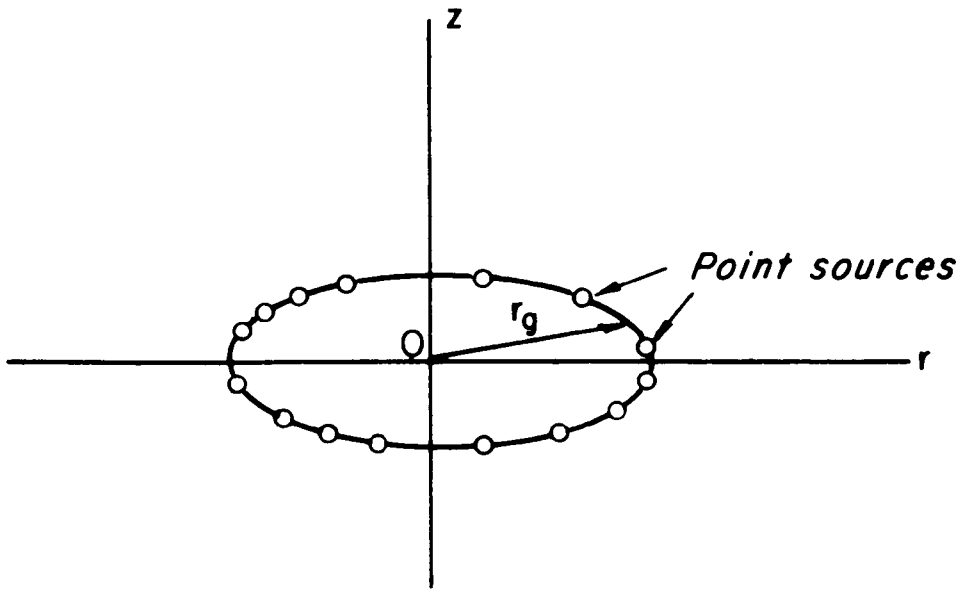


Fig. 34 - Ring source from point sources

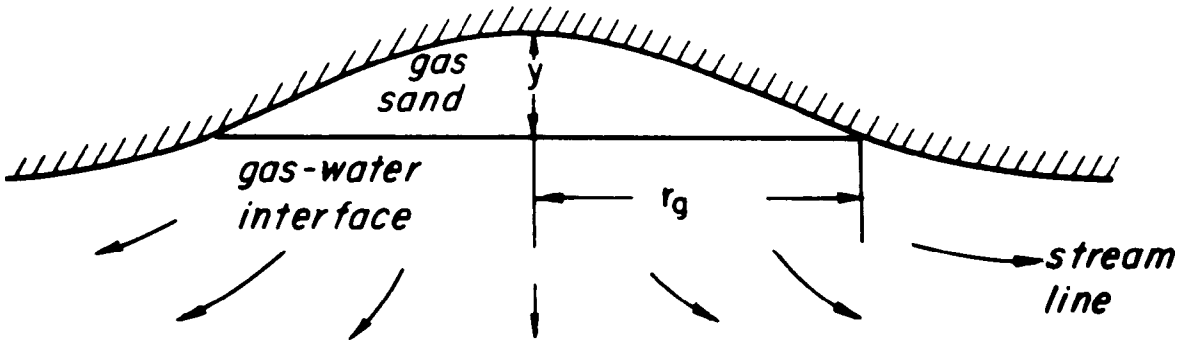


Fig. 35- Shape of the gas cap rock

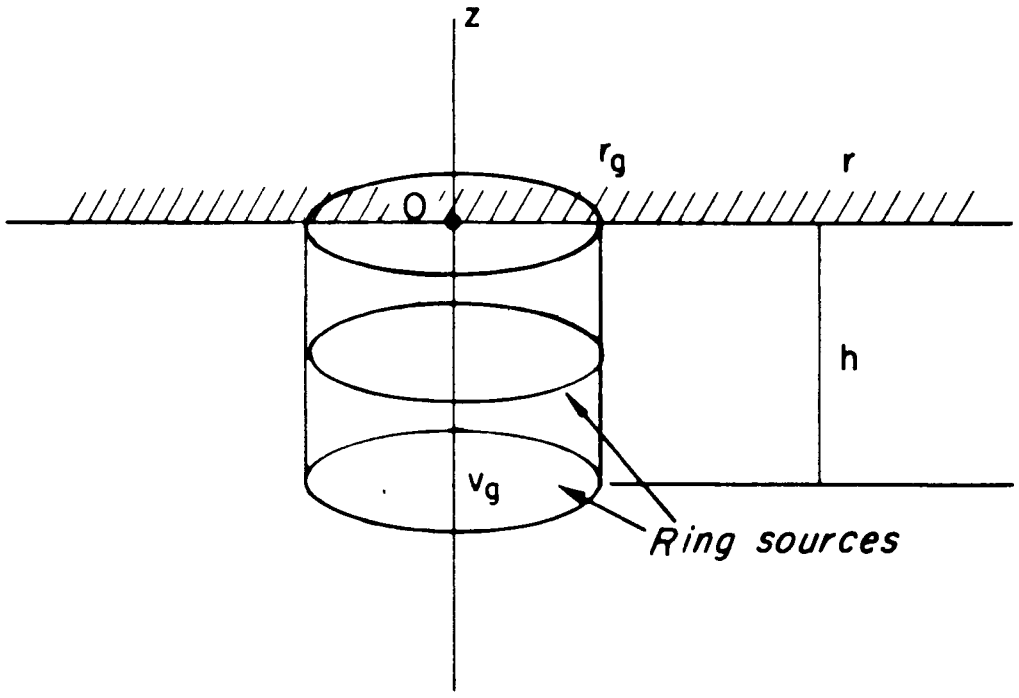


Fig. 36 - Nonuniform cyclindrical surface source from ring sources

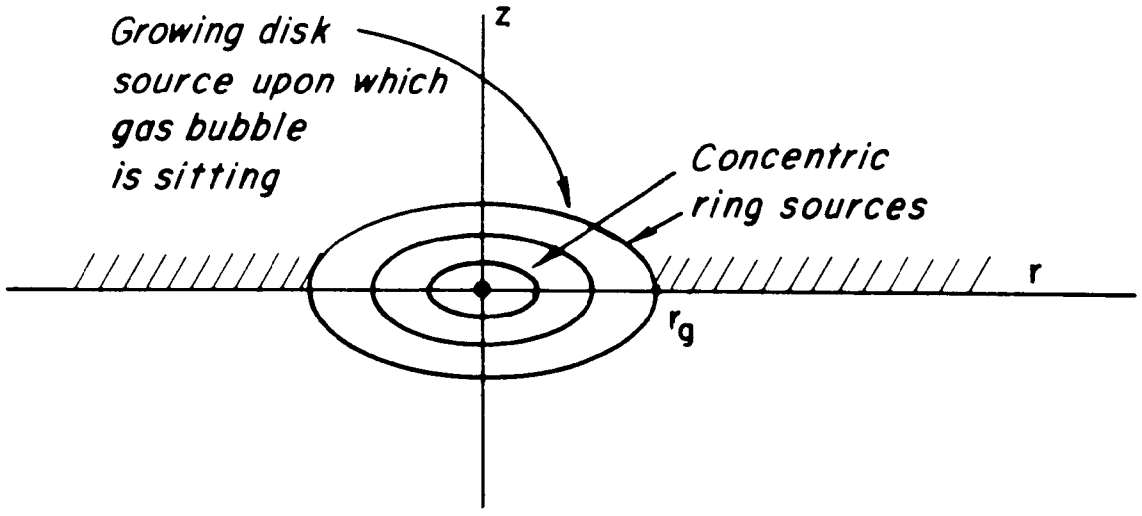


Fig. 37- Disk source from concentric ring sources

$$(P_g - P_{og}) = \frac{\mu}{2\pi kh}\int_0^{\theta} \frac{\left(\frac{dV_g}{d\tau}\right)\cdot e^{\frac{-\left(\frac{V_g}{S_F}\right)^{1/2}}{2\left(\frac{k}{c\phi\mu}\right)(\theta-\tau)}}}{(\theta-\tau)} \cdot I_o\left[\frac{\left(\frac{V_g}{S_F}\right)^{1/2}}{2\left(\frac{k}{c\phi\mu}\right)(\theta-\tau)}\right]\left[erf\left(\frac{h}{2\left(\frac{k}{c\phi\mu}(\theta-\tau)\right)^{1/2}}\right)\right] d\tau \qquad (43)$$

(E) Radially Growing Disk Source on an Infinite Aquifer of Infinite Thickness By placing a number of concentric rings in the x-y plane, and integrating from zero to r_g, the instantaneous disk solution can be obtained.

$$p = \frac{q_6 r_g}{2\phi\left(\pi\frac{k\theta}{c\phi\mu}\right)^{1/2}} \cdot e^{\frac{-z^2}{4\left(\frac{k}{c\phi\mu}\right)\theta}} \cdot \int_0^{\infty} e^{-\left(\frac{k\theta\lambda^2}{c\phi\mu}\right)} \cdot J_o(\lambda r)\cdot J_1(\lambda r_g)\, d\lambda \qquad (44)$$

where q_6 = mass withdrawn/unit area. At z = 0 and r = 0, when the disk radius is increasing, the solution becomes

$$p = \frac{1}{2\phi\left[\pi\frac{k}{c\phi\mu}\right]^{1/2}} \int_0^{\theta} \frac{q_7}{(\theta-\tau)^{1/2}}\left[1 - e^{\frac{-r_g^2}{4\left[\frac{k(\theta-\tau)}{c\phi\mu}\right]}}\right] d\tau \qquad (45)$$

where q_7 = flux per unit area.

For an aquifer gas storage model as shown in Figure 37 with parabolic gas cap shape, the solution is:

$$(P_g - P_{og}) = \frac{1}{c\phi\,\pi^{3/2}\left(\frac{k}{c\phi\mu}\right)^{1/2}} \int_0^{\theta} \frac{\left(\frac{dV_g}{d\tau}\right)\left(\frac{V_g}{S_F}\right)^{-1/2}}{(\theta-\tau)^{1/2}}\left[1 - e^{\frac{-\left(\frac{V_g}{S_F}\right)^{1/2}}{4\left(\frac{k}{c\phi\mu}\right)(\theta-\tau)}}\right] d\tau \qquad (46)$$

Here, P_g is the pressure at the center of the disk.

(F) Solutions for Finite Thickness of Aquifer Sand: So far, the solutions given are for an aquifer of infinite sand thickness; but infinite thickness of an aquifer sand is unrealistic. The aquifer sand (or the Marshal sand) has a thickness of 20 - 200 feet. For the 200 ft. thick sand, it would be improper to neglect the vertical pressure distribution (which means the flow is not radial), therefore, it is improper to consider it as an infinite thickness. In order to handle this, the problem of finite thickness must be considered. By considering identical sources in z direction every 2h distance apart, one concludes:

$$\rho_{\substack{\text{finite}\\ z=0}} = \rho_{\substack{\text{infinite}\\ z=0}} + 2\rho_{\substack{\text{infinite}\\ z=2h}} + 2\rho_{\substack{\text{infinite}\\ z=4h}} + \text{-------} \qquad (47)$$

With equation (47) one can modify equation (40) to give a solution for ring source moving radially on a finite aquifer thickness.

$$P_g \cong P_{og} + \frac{1}{4\phi c\left[\frac{\pi k}{c\phi\mu}\right]^{3/2}} \int_0^{\theta} \frac{\left(\frac{dV_g}{d\tau}\right)}{(\theta-\tau)^{3/2}} \cdot I_o\left\{\frac{\left(\frac{V_g}{S_F}\right)^{1/2}}{2\left(\frac{k}{c\phi\mu}\right)(\theta-\tau)}\right\} \cdot e^{\frac{-\left(\frac{V_g}{S_F}\right)^{1/2}}{2\left(\frac{k}{c\phi\mu}\right)(\theta-\tau)}} \cdot \left(1 + 2e^{\frac{-h^2}{\left(\frac{k}{c\phi\mu}\right)(\theta-\tau)}} + 2e^{\frac{-4h^2}{\left(\frac{k}{c\phi\mu}\right)(\theta-\tau)}}\right) d\tau \qquad (48)$$

One can also develop a solution from equation (46) for radially growing disk source on a finite aquifer thickness:

$$P_g = P_{og} + \frac{1}{c\phi\pi^{3/2}\left(\frac{k}{c\phi\mu}\right)^{1/2}} \int_0^{\theta} \frac{\frac{dV_g}{d\tau}\left(\frac{V_g}{S_F}\right)^{-\frac{1}{2}}}{(\theta-\tau)^{1/2}} \left(1 - e^{\frac{-\left(\frac{V_g}{S_F}\right)^{1/2}}{4\left(\frac{k}{c\phi\mu}\right)(\theta-\tau)}}\right) \cdot$$

$$\cdot \left(1 + 2e^{\frac{-h^2}{\frac{k}{c\phi\mu}(\theta-\tau)}} + 2e^{\frac{-4h^2}{\frac{k}{c\phi\mu}(\theta-\tau)}} + \ldots\right) d\tau \quad (49)$$

Further work on the theoretical analysis of a moving boundary problem is made with equation (49), since the aquifer gas storage can perhaps be described better with this growing disk source model of a finite aquifer thickness.

iv) Unit Step Responses of Growing Disk Source Model of a Finite Aquifer Thickness:

(A) Unit Volume Step Response: The mathematical solution for the rate case is shown to be equation (49) as the details are given under the previous heading. Equation (49) is definitely nonlinear as it appears.

If one defines $t_D = \frac{k\theta}{c\phi\mu h^2}$, equation (49) becomes:

$$P_g = P_{og} + \frac{2\sqrt{S_F}\left(\frac{k}{c\phi\mu h^2}\right)^{1/2}}{c\phi\pi^{3/2}\left(\frac{k}{c\phi\mu}\right)^{1/2}} \int_0^{t_D} \frac{\frac{d\left(V_g^{1/2}\right)}{d\tau}}{(t_D-\tau)^{1/2}} \cdot$$

$$\cdot \left(1 - e^{-\frac{\left(\frac{V_g}{S_F}\right)^{1/2}/h^2}{4(t_D-\tau)}}\right)\left(1 + 2e^{-\frac{1}{(t_D-\tau)}} + 2e^{-\frac{4}{(t_D-\tau)}} + \ldots\right] d\tau$$

But one can approximate.

$$e^{\frac{-\left(\frac{V_g}{S_F}\right)^{1/2}/h^2}{4t_D}} \cong 1 - \frac{\left(\frac{V_g}{S_F}\right)^{1/2}/h^2}{4t_D}$$

because $\frac{1}{\left(\frac{4k\theta}{c\phi\mu r_g^2}\right)}$ is small - e.g. 1/10,000. (See (B))

So, equation (49) reduces to equation (50):

$$P_g = P_{og} + \frac{1}{4c\phi\pi^{3/2}h^3}\int_0^{t_D} \frac{\left(\frac{dV_g}{d\tau}\right)}{(t_D-\tau)^{3/2}}\left(1+2e^{-\frac{1}{(t_D-\tau)}}+2e^{-\frac{4}{(t_D-\tau)}}+\cdots\right)d\tau \quad (50)$$

Equation (50) has the form of equation (11), for which analog simulation method is developed. If one defines the unit volume step response for the pressure change function as P''_{tD}, equation (50) can be written:

$$P_g = P_{og} + \frac{1}{4c\phi\pi^{3/2}h^3}\int_0^{t_D}\left(\frac{dV_g}{d\tau}\right)\cdot P''_{t_D}(t_D-\tau)\,d\tau \quad (51)$$

The unit volume step response P''_{tD} is computed and is given in Table XI.

Table XI. Unit Volume Step Response to get Pressure Change Function For Growing Disk of Finite Aquifer Thickness.

t_D	P''_{tD} (Eq. (50))	P''_{tD} (Analog Check)
0.1	31.6	
0.5	3.59	
1.0	1.773	
5.0	0.354	
10	0.1772	
50	0.03545	
100	0.01773	
200	0.00877	
500	0.003545	0.0037
800	0.00218	
1000	0.001815	0.00185
1300	0.00138	
2000	0.00104	0.00105
3000	0.000782	0.0008
4000	0.000647	

(B) Unit Pressure Step Response: In the preceeding discussion the unit volume step response has been shown for the growing disk model of a finite aquifer thickness. There is no reason to think that Q''_{tD} (the unit pressure step response) does not exist. In obtaining the pressure case solution from the rate or volume case solution, the developed analog method is quite powerful.

With a new definition of the dimensionless time for the growing disk model, the constant "a" is actually found to be large. For example:

$$\frac{k}{\mu} = 0.2 \text{ darcy/cp}$$

$$\phi = 0.16$$

$$c = 100 \times 10^{-6} \text{ 1/atm}$$

$$h = 500 \text{ ft.}$$

$$t_D = \frac{k\theta}{c\phi\mu h^2} = a\theta = 140\ \theta$$

$$\text{or } a = 140 (1/\text{month})$$

This secures the validity of the approximation that was made in the preceding discussion, even though the solution obtained for the small time range is not reliable.

For the analog simulation the following transfer function is obtained from Table XI, ignoring the small time portion of the solution.

$$s f_1''(s) = 10^{-2}\left(4.358 - \frac{3.83}{1+\frac{s}{.01085a}} - \frac{4.5\times10^{-4}a}{s} + \frac{2\times10^{-7}a^2}{s^2}\right) \qquad (52)$$

In equation (52) a double integration term appears for which no real theoretical justification for analog simulation is given as to its initial conditions. However, this should not change the qualitative analysis of the unit pressure step response. A circuit to get pressure change function, using the volume as input for the growing disk model of a finite aquifer thickness, is given in Figure 58. Some corrections have been made to the potentiometer settings of P_5 and P_7. With $P_5 = 0.1952$ and $P_7 = 0.1338$, the unit step response for the constant volume case is checked by the analog method and is added to Table XI for comparison. With the same circuit of Figure 58, the constant pressure case solution is obtained. In doing this, the input (volume variation) is manually controlled in such a

manner that the output pressure change function would be a constant at all times. The constant pressure case solution thus obtained for the growing disk model is shown in Figure 38. The Q''_{tD} in Figure 38 is much the same as Q'_{tD}, and upon multiplying Q''_{tD} by a constant, the volume of the gas bubble can be obtained. The linearity of the curve at the large time portion must be particularly noted.

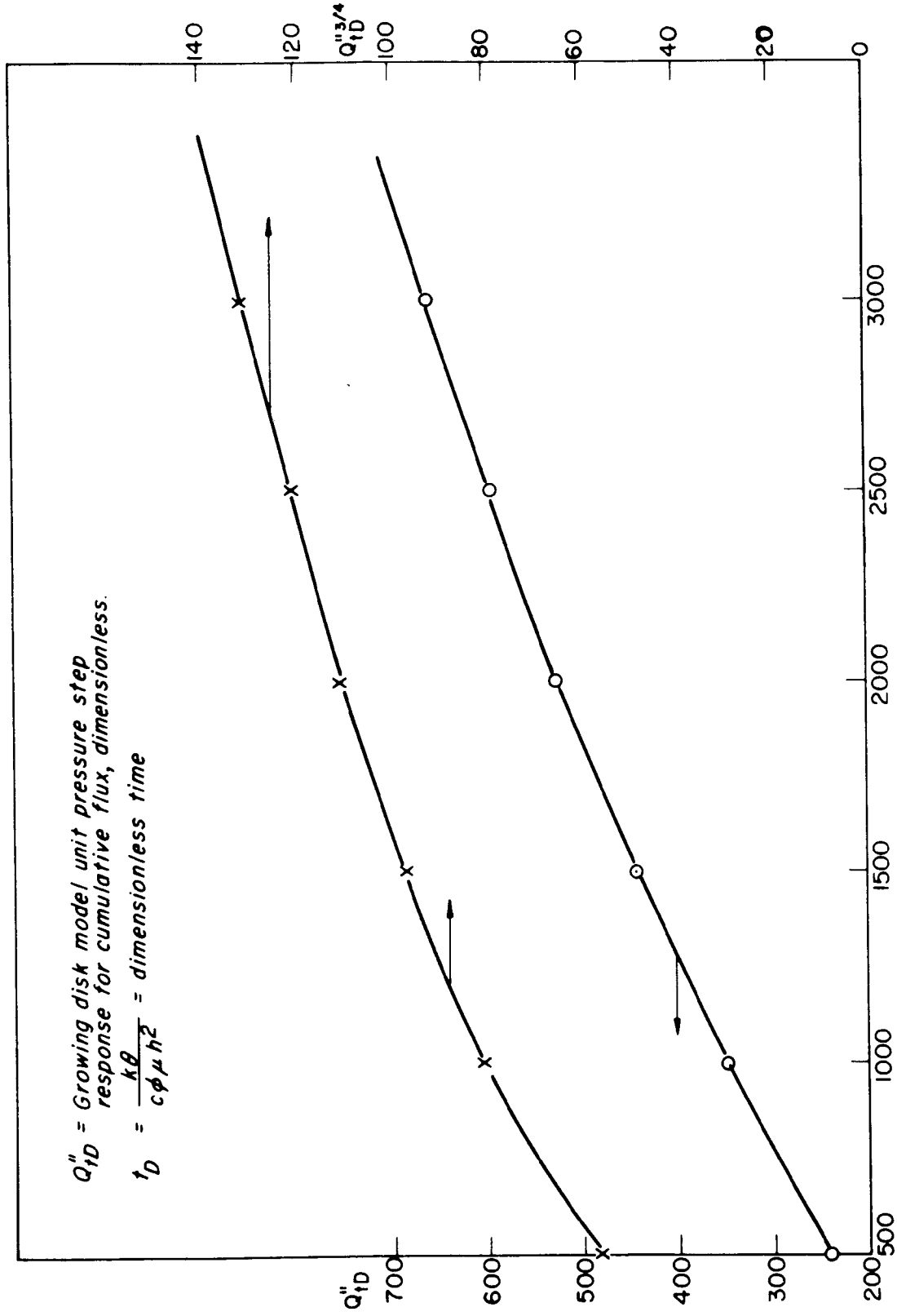


Fig. 38 – Constant pressure case solution to growing disk model of finite aquifer thickness

V ANALYSIS OF RESERVOIR VARIABLES

As an approach for the determination of the water flux to a gas storage reservoir, a theoretical study model has been set up. By making a series of assumptions, one obtains a unit step response of the system. Then, it is further assumed that the system has a linear response characteristic so that one can use the superposition principle to handle the arbitrary time-varying boundary conditions. However, after one's effort and experience with reservoir variables, one should be aware of the uncertainties of the physical constants, and the drastic assumptions one made during the model study.

The purpose of this chapter is to discuss the reservoir variables, and to point out what are the key variables which one ought to juggle to fit the actual data or to correlate.

The basic assumption we make for the reservoir engineering study to handle the time-varying boundary conditions is that the system response characteristic is of linear nature. By system response being linear, it is meant that the basic partial differential equation governing the physical system and its boundary conditions are linear. The system linearity assumption is good for the usual reservoir engineering problems. The probable exceptions to this statement are: a) moving boundary or aquifer gas storage problems during the short period from the initiation of the gas bubble, b) time-varying gas saturation effect in the aquifer, and c) time-varying reservoir constants. These exceptional cases introduce extreme complexity of the theoretical analysis, and such analysis may be hardly worthy of the effort, even though in some cases the theoretical analysis is possible. The special cases of handling some nonlinear problems are discussed in Chapter VII. For the present discussion linearity of the system response is assumed throughout.

The number of variables, that fix the reservoir system of a constant bubble radius to give one water flux versus time curve, is enormous. These are: (for fixed radius)

1) Pressure variation (or rate variation or volume variation).
2) Aquifer size, areal reservoir geometry, aquifer geometry, nonuniform flow resistance in radial direction, etc.
3) k, c, ϕ, μ, and r_g (for fixed radius)
4) μ and h

Either pressure, rate or volume must be known, in any case, because it is the input signal and the first variable. The specification of gas injection is equivalent to specifying pressure, rate or volume, so far as the system variables are concerned.

The second variable is the unit step response curve. Depending upon the size and geometry of the aquifer, there is only one unit step response curve for a linear system. This is illustrated in Figure 39.

Third variable is a group of constants which interprets the reservoir time into the dimensionless time. This constant has the expression of the following:

$$a = \frac{k}{c\phi\mu r_g^2} \qquad (1/\text{month})$$

The range of this constant "a" is 0.5 - 20 (1/month) for a fully developed or constant radius gas storage reservoir.

The fourth or the last variable is a group of constants which relates the pressure change function (dimensionless) into actual pressure change in psi, and has the following mathematical expression:

$$b = \frac{\mu}{2\pi k h} \qquad (\text{psi-month/cu ft})$$

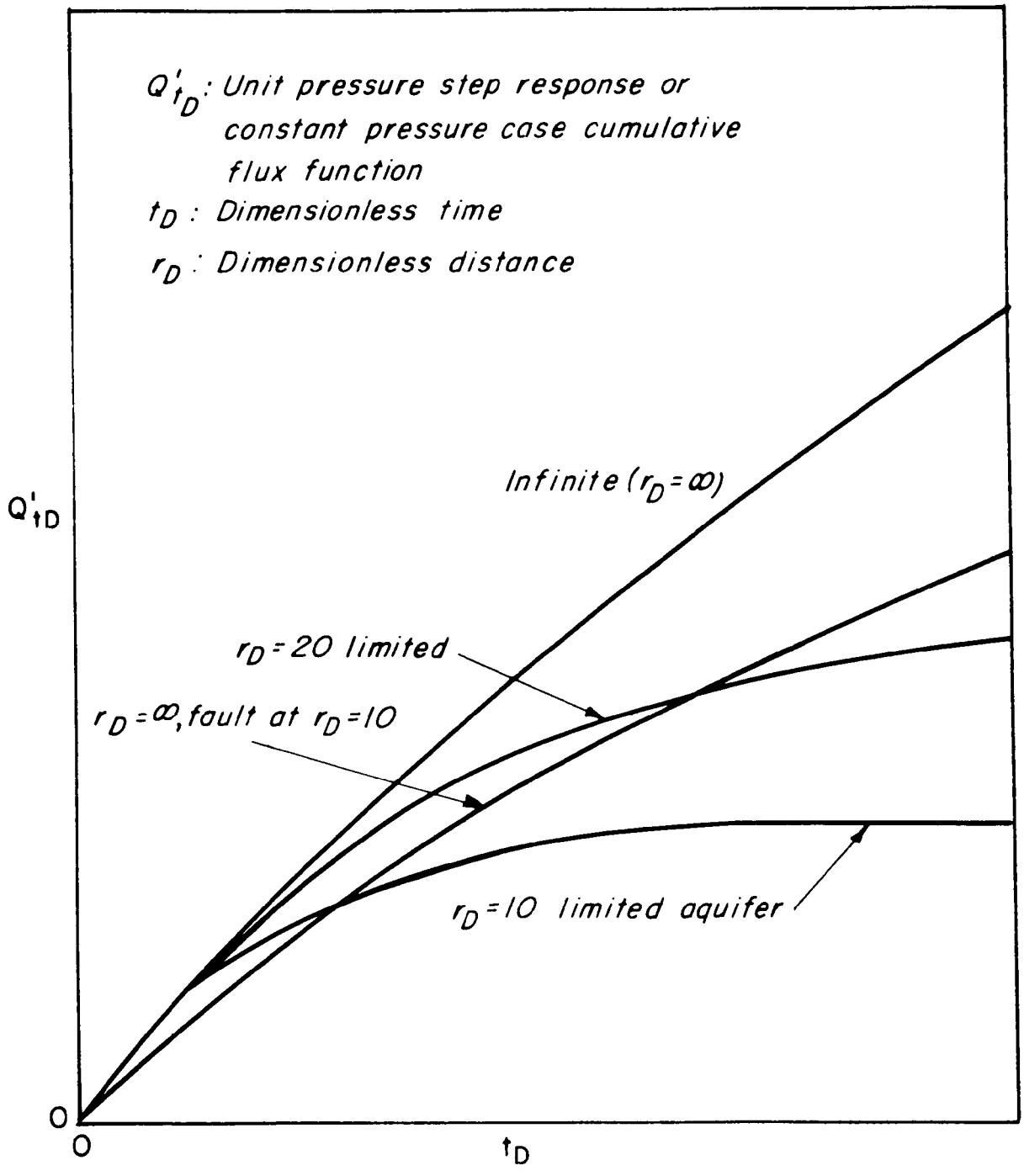


Fig. 39-Illustration of unit pressure step response curves.

The practical range of this constant "b" is 5×10^{-4} - 5×10^{-6} (psi-month/cu ft).

Thus, the constant radius reservoir system response is a function of four basic variables:

1) Input signal (pressure, or rate or volume variation)
2) Unit step response curve (Figure 39)
3) Reservoir constant "a"
4) Reservoir constant "b"

The aquifer theory requires the following two relationships at any time θ among the four variables.

$$(V_g - V_c) = W = \frac{Q_{xD}(G, a)}{ab} \quad \text{for pressure case} \qquad (53)$$

$$(P_g - P_{cg}) = b \cdot P_{xD}(E, a) \quad \text{for rate case} \qquad (54)$$

In equation (53), since it is a pressure case, one still has three more variables to choose in order to fix the system; and there is only one equation, which leaves two degrees of freedom. Also, in equation (54) there are two degrees of freedom. However, the unit step responses for the pressure case and the rate case are not independent.

Therefore, one can conclude that there are two degrees of uncertainty remaining which must be specified, based on some sort of logical deduction; that is, the picked numbers must be realistic, and the unit step curve should have some theoretical support. Once one can pin down the range of these variables, usually he is likely to find that some of the variables are relatively insensitive.

Because of two degrees of uncertainty, one should not be surprised to see that a good matching can be done with different sets of variables and logical deductions. Also, one may find that a logical set

of variables gives a worse result than the unrealistic set of variables: This has been the case in the interference study of the Fields A, C, D, and E.

For a moving boundary problem an additional fifth variable must be added to describe the shape of the gas cap rock. This variable is called shape factor and is designated by S_F in this thesis.

The theoretical study of the aquifer behavior serves as a guide to show how the different numbers give the responses, and serves as a basis for the sort of unit step curve to be picked. And the rest is nothing more than a correlation of the actual data, or trial and error for a good matching job. The aquifer theory is a means to explain why the actual data are correlated in a certain fashion.

When there is no study model and one is only interested in correlating the performance of a gas storage field without going through the use of the aquifer properties - constants "a" and "b", and the geometry of the aquifer, one can rewrite equations (53) and (54) in the following form

$$(V_g - V_o) = Q_\theta(G) \qquad \text{for pressure case} \qquad (53)'$$

$$(P_g - P_{og}) = P_\theta(E) \qquad \text{for rate case} \qquad (54)'$$

In these equations the newly defined unit step responses are $\left(\frac{Q'_{tD}(\theta)}{ab}\right)$ and $\left(b\,P'_{tD}(\theta)\right)$ respectively, and these are functions of actual time rather than dimensionless time. Q_θ and P_θ have the same meaning as those of Q_{tD} and P_{tD} except the fact the unit step responses are redefined. These new definitions of the unit step responses reduced the effective variables of the reservoir system from four to two:

1) Newly defined unit step response curve.

2) Input signal (pressure, or rate or volume variation).

For a given case, there is only one variable; and the system is completely fixed since we have one equation for each case.

In the recent publication of Hutchinson[25] during the progress of this thesis he named $\left(b R'_{FD}(\theta)\right)$ as "resistance function". The central idea of the Resistance Function also prevails in this thesis, even though more extensive and intensive theoretical analysis is made.

The established newly defined unit step responses are good only to a particular field like the pure correlation charts (work of 1957) given in the paper[5] (in which the rate of the pressure change, the pressure level, and the rate or flux of a particular field are correlated for large time).

VI THEORETICAL CORRELATION OF AQUIFER GAS STORAGE PERFORMANCE

In the preceeding chapter, the role of correlation for the prediction of gas storage reservoir volume variation is pointed out; and at the end of Chapter IV, the theoretical unit step responses for a growing disk model of the finite aquifer thickness are given. In this chapter, an example is given as to how these logical deductions are actually applied to handle an aquifer gas storage problem. One may call this method a semi-empirical method because the method has theoretical grounds.

a. Cylindrical Flux Area with Linear Cumulative Flux Function:

In the argument with Figure 29, a point was made that $\left(\frac{\partial P'}{\partial r_D}\right)_1$ does not change much at large t_D values. Also it was pointed out that the dimensionless time for aquifer gas storage problems is actually large. Therefore, the small time effect should be equally weighted at all times and can be ignored. With this reasoning, one can logically assume the following relationship:

$$r_g\left(\frac{\partial P}{\partial r}\right)_{r_g} \cong A \cdot G(\theta) \tag{55}$$

where A is a constant, and G is pressure. What this essentially amounts to is picking a unit step response curve, the slope of which is logically deduced to be a straight line at the large time portion. The relationship can be expressed in terms of a transfer function in the conventional manner, as follows:

$$\frac{Q_{x0}(s)}{g(s)} \cong \text{constant} \cong s f_1(s)$$

Here, $f_1(s)$ is the Laplace Transform of the unit step response and $sf_1(s)$ is the Laplace Transform of the slope of the unit step response curve.

When cylindrical flux area is considered, one can immediately write the following equation:

$$\frac{dV_g}{d\theta} \cong \left\{ AG(\theta) \right\} \frac{k}{\mu} 2\pi h = A' G(\theta)$$

or

$$V_g = A' \int_0^\theta G(\theta)\, d\theta = A' S_1(\theta) \tag{56}$$

where A' is a constant and

$$S_1 = \int_0^\theta G(\theta)\, d\theta$$

The argument narrows down to say that a plot of V_g versus $S_1(\theta)$ is a straight line. Figure 40 shows the plot. As expected, the correlation is not bad at the large times. The data used here are from Field B, which is an aquifer gas storage field.

In equation (56) only one constant appears. This constant is a combination of the unit step response curve, and reservoir constants "a" and "b". The reservoir system is completely fixed in equation (56) by logically deducing the unit step response characteristic as expressed in equation (55). The correlation in Figure 40 can be improved by the modification of equation (55) or with a different flux area.

b. Cylindrical Flux Area with Quadratic Cumulative Flux Function: The next attempt is to try a quadratic unit pressure response for the system:

$$r_g \left(\frac{\partial P'}{\partial r} \right)_{r_g} \cong C_1 + C_2 \theta \tag{57}$$

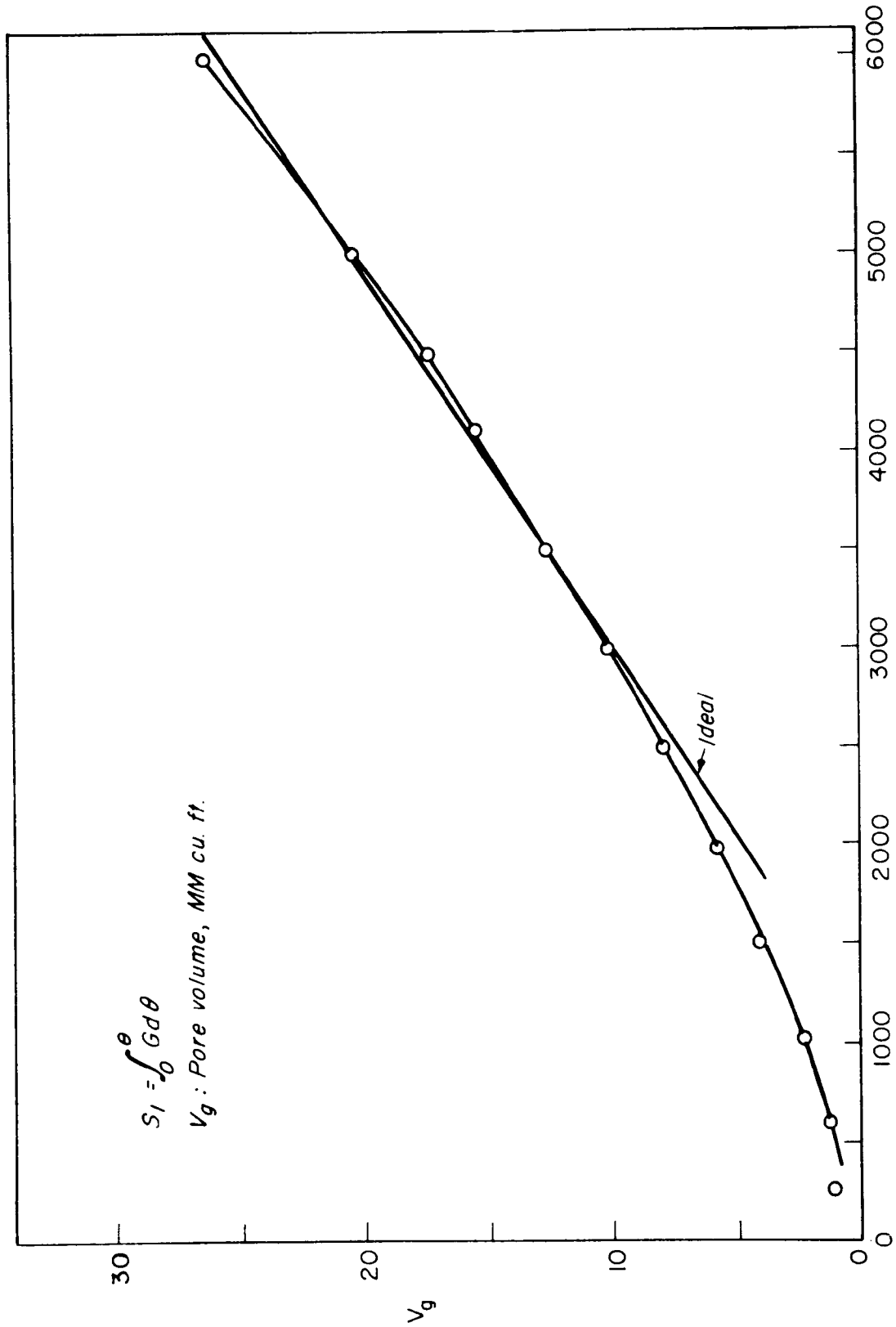


Fig. 40- Reservoir pore volume versus time integral of pressure for field B.

where C_1 and C_2 are constants which depend upon the shape of the gas cap rock sturcutre, physical reservoir constant "a", and the unit step response curve. Again assuming the linearity of the system response one obtains:

$$L\left[r_g\left(\frac{\partial P}{\partial r}\right)_{r_g}\right] = g(s)\cdot s\cdot L\left[r_g\left(\frac{\partial P'}{\partial r}\right)_{r_g}\right] = s\,g(s)\left[\frac{C_1}{s} + \frac{C_2}{s^2}\right]$$

And this gives:

$$\frac{r_g\left(\frac{\partial P}{\partial r}\right)_{r_g}}{G(\theta)} = C_1 + \frac{C_2}{D}$$

where D is the differential operator. By combining with the rate balance equation, the following equation is derived:

$$D V_g \cong \frac{k}{\mu} 2\pi h \left\{ C_1 + \frac{C_2}{D} \right\} G(\theta)$$

or

$$V_g = \left(C_1 \frac{k}{\mu} 2\pi h\right) S_1 + \left(C_2 \frac{k}{\mu} 2\pi h\right) S_2 = A_1 S_1 + B_1 S_2 \qquad (58)$$

where $S_2 = \int_0^\theta \int_0^\theta G\, d\theta\, d\theta$, and A_1 and B_1 are constants (depending upon the unit step response, constants "a" and "b", and S_F).

The method is applied for Field B, and A_1 and B_1 are determined with the data at the time equals 34th and 44th week from the

initiation of the gas bubble growth. The approximate correlation equation is:

$$V_g = 1.500 \times 10^{-3} S_1 + 1.615 \times 10^{-4} S_2 \qquad (59)$$

In equation (59) the unit of V_g is in MM cu ft and S_1 and S_2 are in psi-wk and psi-$(wk)^2$, respectively. The result of equation (59) is plotted in Figure 41 with the field data to show the good correlation. It is quite doubtful whether a rigorous solution to equation (30) can match field data any better than that of Figure 41 because of the uncertainties involved in the postulation of the simplified study model such as.

1) The shape of the rock structure.
2) The vertical pressure distribution because of the thick water sand.
3) The shape of the gas-water interface while the gas bubble is growing. Water coning effect may very well take place.
4) Uncertainties of the aquifer geometry and properties.

c. Disk Flux Area with A Cumultive Flux Function: At the end of Chapter IV, considerable amount of theoretical study was made on the growing disk model of finite aquifer thickness because of its importance to aquifer gas storage field. The unit step responses are obtained for the growing disk model. Careful attention to the unit pressure response must be called for, which is presented in Figure 38. The Q'_{tD} versus t_D curve is very close to a straightline. Suppose one can assume that the average value of the gas bubble radius times the pressure gradient at the gas water interface is a constant, or

$$r_g \left(\frac{\partial P'}{\partial z}\right)_{z=0} \cong C_1 \qquad (60)$$

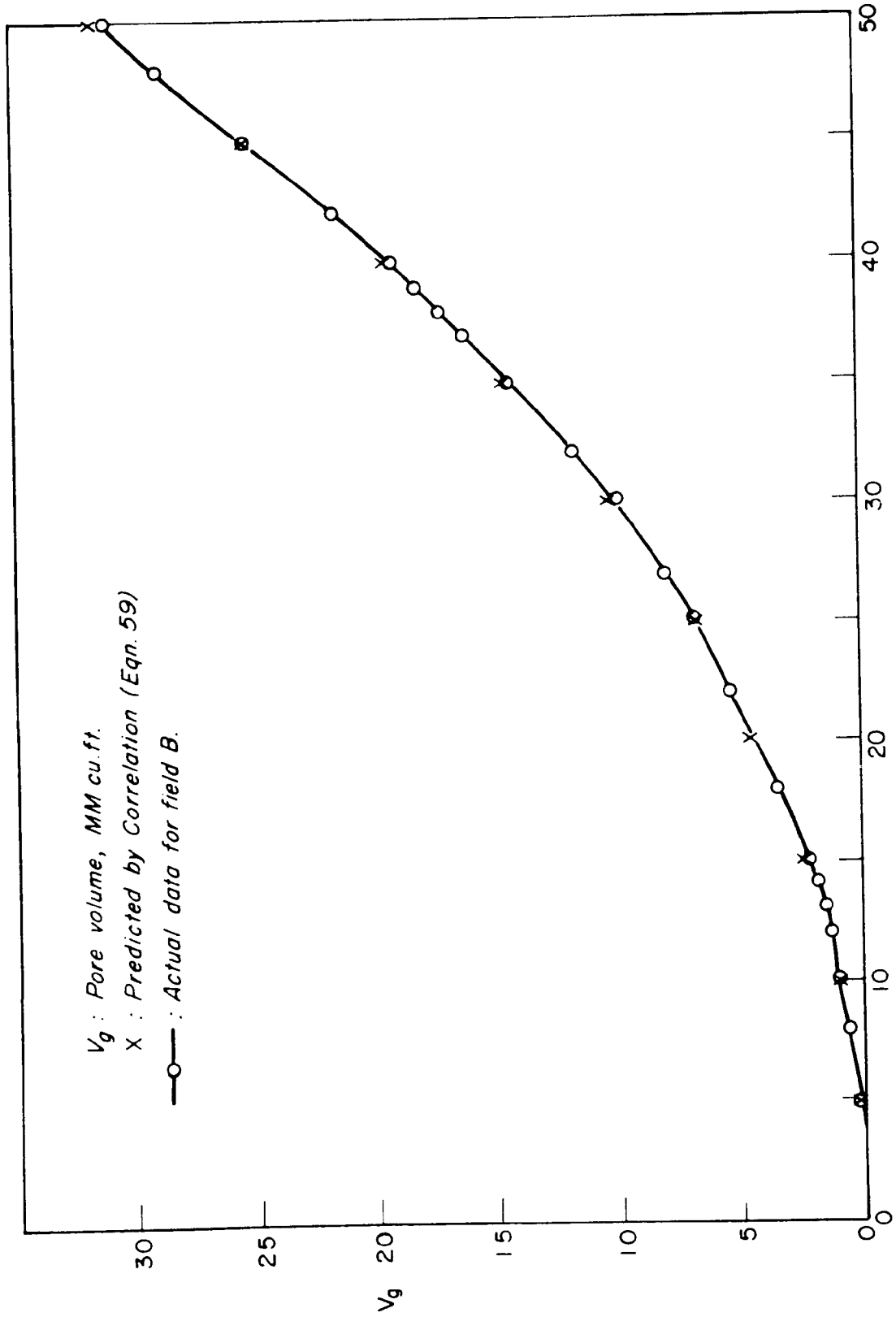


Fig. 41 - Gas reservoir pore volume variation for field B.

Again assuming linear system response, and the gas cap shape to be parabolic, the following relationships are found:

$$V_g = S_F r_g^4$$

$$r_g \left(\frac{\partial P}{\partial z}\right)_{z=0} = C_1 P$$

$$\frac{dV_g}{d\theta} = \pi r_g^2 \frac{k}{\mu}\left(\frac{\partial P}{\partial z}\right)_{z=0} = 4 S_F r_g^3 \frac{dr_g}{d\theta}$$

$$r_g^3 = \frac{3\pi C_1 k}{4 S_F \mu}\int_0^\theta P\, d\theta$$

or simply

$$V_g = A_1 S_1^{4/3} \tag{61}$$

This equation demands that a plot of $Q''^{3/4}_{tD}$ versus t_D is a straightline (Figure 38). This equation also says that a plot of V_g versus S_1 gives a straight line on log-log paper. Figure 42 shows this plot for Field B. The slope of the curve in this case should be 4/3, theoretically or 1.333; but instead, the slope is found to be 1.37 from the actual data correlation. It gives a remarkable correlation, as expected, when the small time data are excluded. The correlation equation for Field B is:

$$V_g = 1.75 \times 10^{-4} S_1^{1.37} \tag{62}$$

Once the correlation curve or the performance curve is established, as shown in Figure 42, the future predictions can easily be made based on this curve. By knowing the gas injection-production schedule from the 30th week, the predictions of the pore volume variation and the

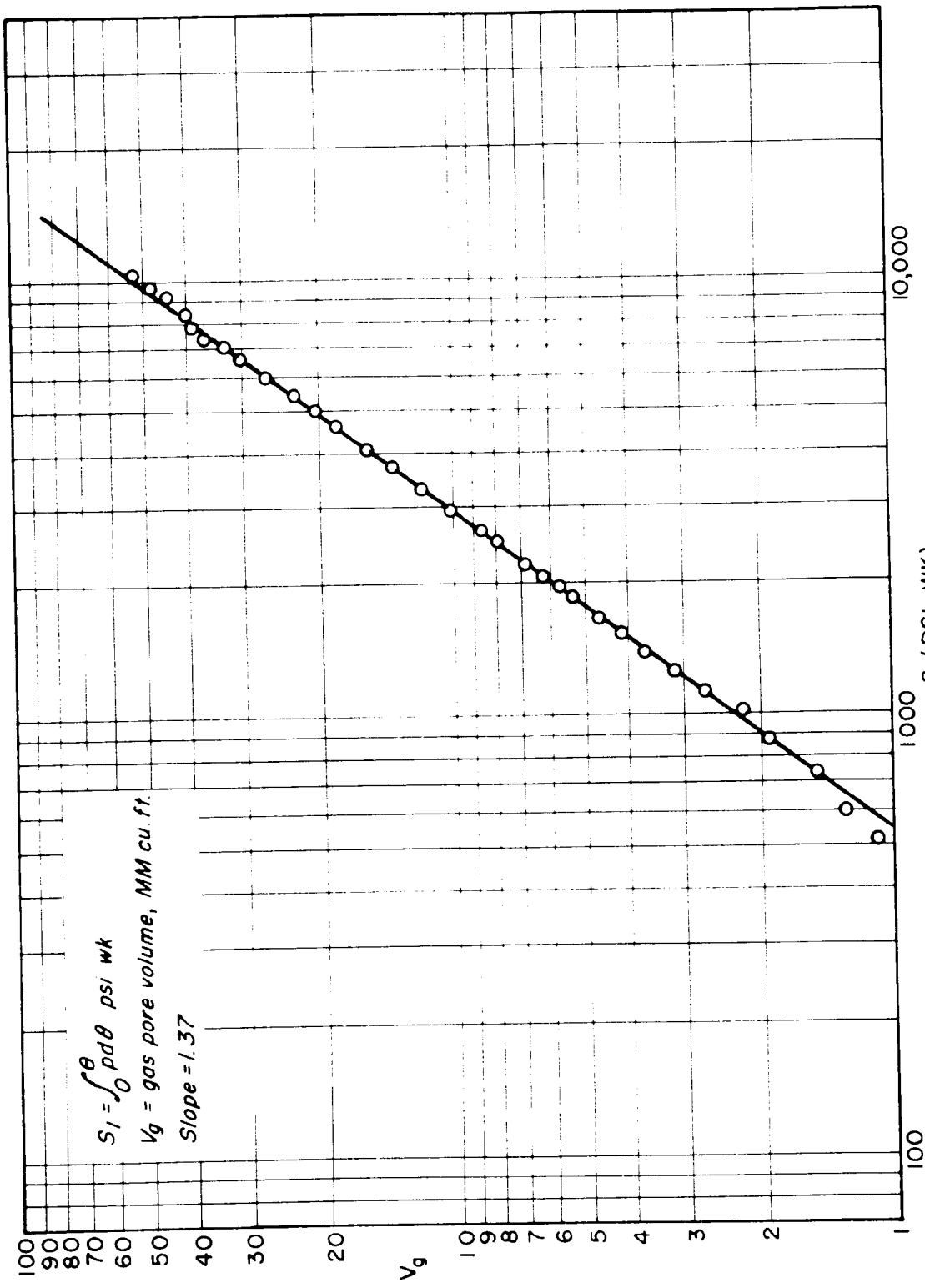


Fig. 42-Aquifer gas storage performance curve for field B.

pressure variation are made using Figure 42; and the predicted results are plotted along with the actual data in Figures 43 and 44 respectively. The volume variation is predicted within 4 percent error. This small error is magnified for the pressure prediction, giving as high an error as 50 psi since the reservoir pressure is over 1000 psia. However, this should not bother us because the volume prediction is of more concern to the practical engineers.

Whenever equation (60) is a valid approximation, it can be shown that the correlation form of equation (62) is generally true, even for the case when there is a gas-water twilight zone for which the simplifying assumptions apply, as discussed in Chapter IV.

By making a theoretical analysis of the unit step response characteristics of a reservoir system, a theoretical correlation equation is derived. From the actual field data, the good correlation is shown, as expected from the theory.

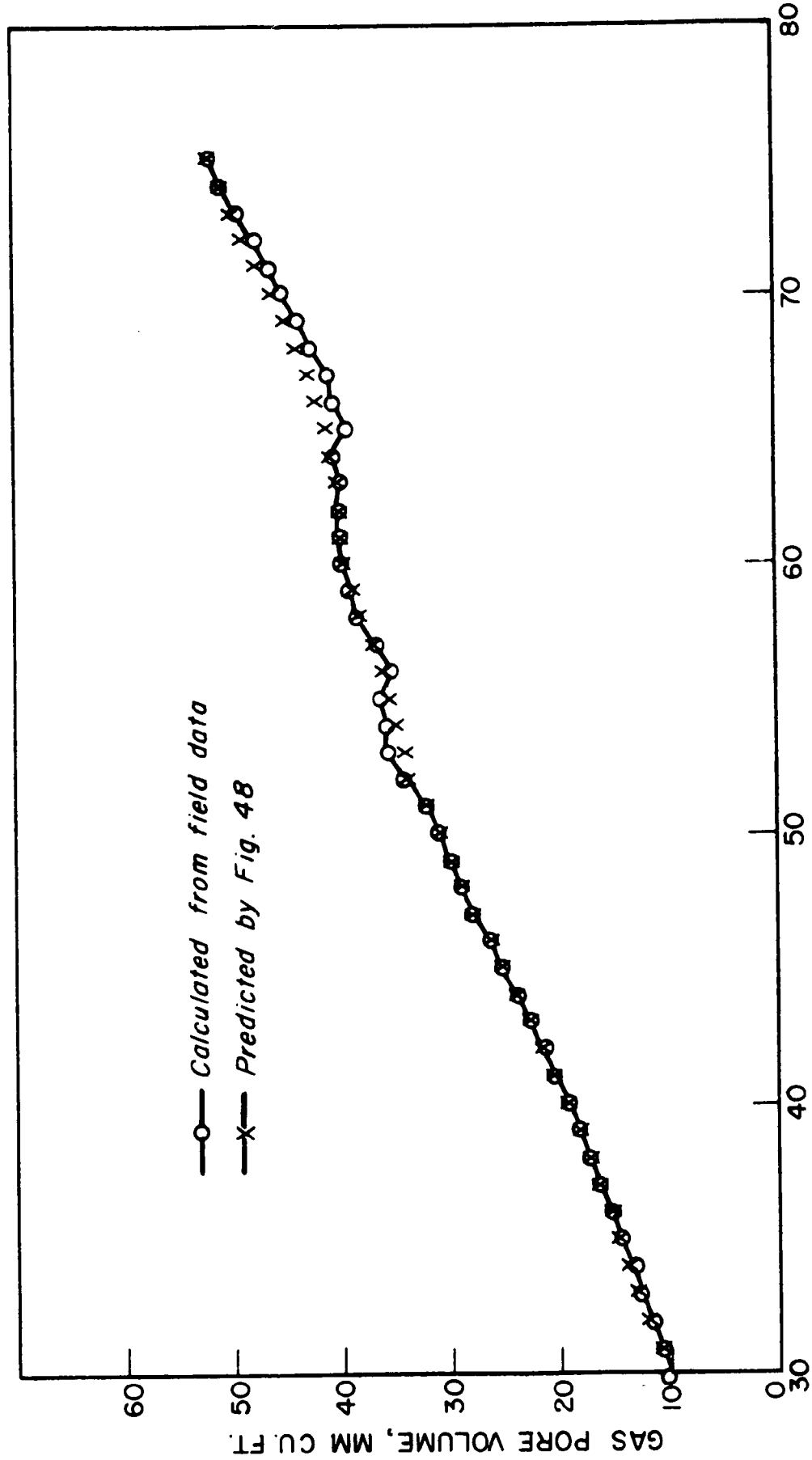


Fig. 43- Comparison between field B data & predicted pore volume.

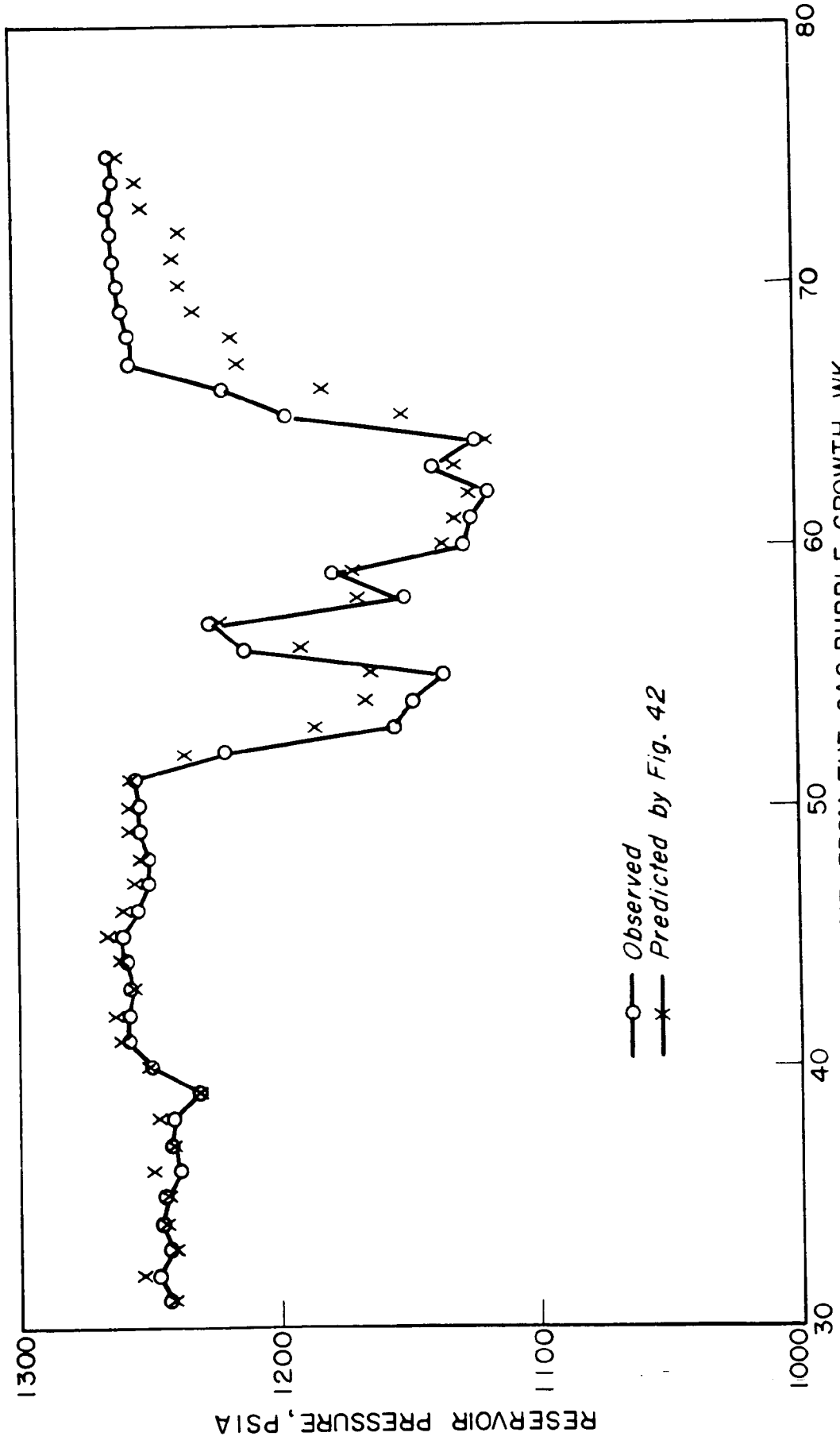


Fig. 44 - Comparison between observed & predicted pressure for field B.

VII OTHER USES OF ELECTRONIC DIFFERENTIAL ANALYZER FOR RESERVOIR ENGINEERING PROBLEMS

In this chapter, the possible uses of an electronic differential analyzer to solve other special reservoir engineering problems are discussed. Under each heading a distinct idea is presented which may be applied to a particular reservoir problem.

a. Computation of Convolution Integrals: In the first part of this thesis, a theoretical development is made to show that the analog simulation, based on simulation equation (8), is equivalent to the computation of a convolution integral continuously. This integral is often called a superposition integral, Faltung integral or Duhamel integral. The mathematical history of this integral is given by Gardner and Barnes.[20]

The computation of a convolution integral is often encountered in other reservoir engineering problems. For instance, the constant rate case solution, derived for continuous cylindrical source by convoluting the instantaneous cylindrical source solution, is a convolution integral. The convolution integral can be computed on an electronic differential analyzer by setting up the proper transfer function as done in this thesis. The equivalent solutions to Mortada's charts[14] and Van Everdingen and Hurst[4] table can be obtained from the instantaneous cylindrical surface source solution. Once the rate case solution is known, the pressure case solution can be found by the method described under the heading "Unit Pressure Step Response of Growing Disk Source" (Chapter IV).

b. Gas Content as Input Signal: Thus far, the studies were made using pressure or volume as machine input signals. Occasionally, the gas content is specified rather than the pressure or volume variation of a gas storage reservoir. In such a case, one can always do successive trial and error computations with some assumed pressure variation as an input signal (for example, the pressure calculated from the gas content assuming a constant volume). The gas content specified case is a modified pressure specified case.

The alternate method is to feed in the gas content as an input signal. Starting from the basic equation of the state of the gas, one can write:

$$P = \frac{\mathcal{Z} n R T}{V_g} = \frac{(1+AP)(n)(RT)}{V_o\left(1-\frac{Q_{xp}}{abV_o}\right)}$$

$$\cong \frac{RT}{V_o}(1+AP)(n)\left(1+\frac{Q_{xp}}{abV_o}\right)$$

$$P \cong \frac{RT}{V_o}\left(1+\frac{Q_{xp}}{abV_o}+nA\right)n \qquad (63)$$

So, the modified pressure case with gas content as an input signal can be simulated, based on equation (63). A general circuit for the simulation is given in Figure 59.

c. Effect of Gas Flow Resistance to Water Flux: The gas flow resistance in the stray sand has been neglected in this thesis; and the average gas storage reservoir pressure is considered to be the pressure at the gas-water interface. It is common understanding that the gas-water interface is not fully segregated; but the pressure at this interface is the terminal pressure which causes the water flux. The cross sectional view of a gas storage reservoir is shown in Figure 45.

In the present discussion it is shown how one can handle gas flow resistance to find water flux for an idealized situation where a column of gas is sitting on an infinite aquifer.

The flow of gas through a porous medium is described[24] by equation (64):

$$\frac{\partial^2 P^2}{\partial x^2} = \frac{2\phi\mu}{k}\frac{\partial P}{\partial \theta'} \qquad (64)$$

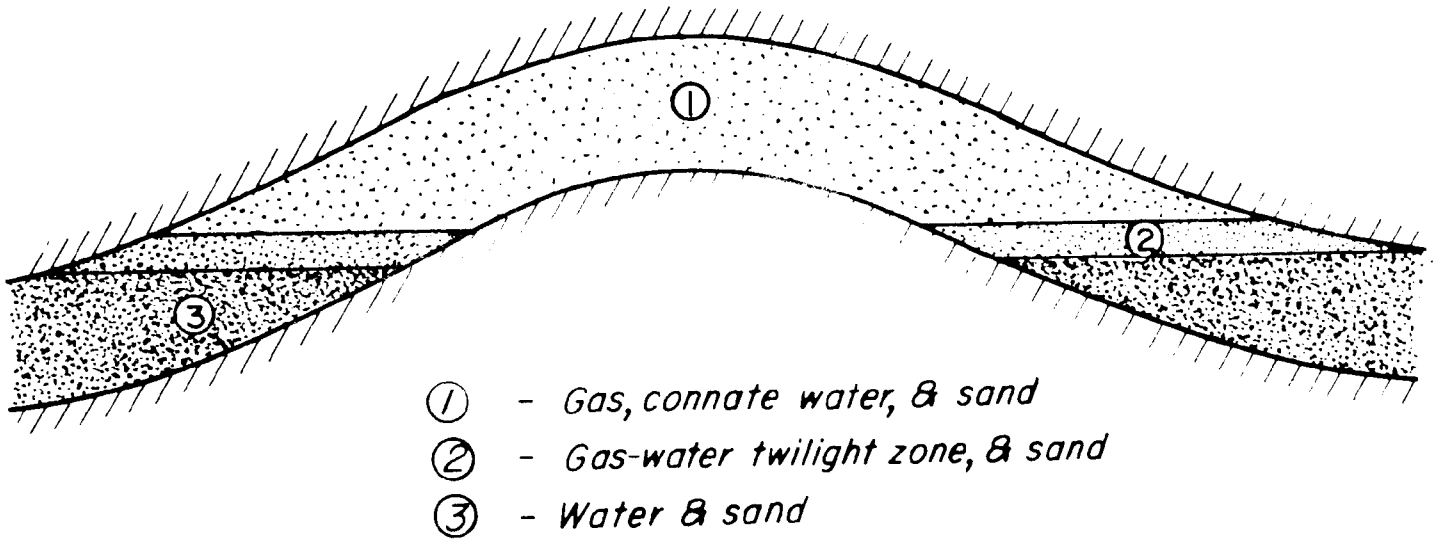


Fig. 45- Cross sectional view of a gas storage reservoir

This equation can be derived from the equation of continuity, Darcy's equation, and the gas law equation. Some questions arise as to the validity of Darcy's equation in the actual cases, but no better equation has yet been offered. The general simulation of the linear gas flow effect to water flux is shown in Figure 60 for the pressure case. The pressure at the top of the gas column is specified in order to find the flux at the interface. The gas flow equation is simulated, based on the finite difference approximations in the space coordinate, while the liquid flow is handled by setting up the transfer function as done in the thesis.

d. Time-Varying Twilight Zone Resistance: In Chapter IV the twilight zone and film resistance concept is given for a case when the gas water twilight zone is not thick. Even though the magnitude of such a twilight zone resistance and the flow mechanics are not known, it is likely that the twilight zone resistance is changing significantly as a function of time. More specifically, the twilight zone resistance may be a function of cumulative flux and flux. So, the pressure across the twilight zone can be expressed as follows.

$$P' = P_g - A Q_{xD} - B \frac{dQ_{xD}}{dt_D} \tag{65}$$

where A and B are constants. The true terminal boundary pressure that causes the water flow in and out of a gas storage reservoir is P' rather than the average bottom-hole gas reservoir pressure P_g. One should be aware of the fact that all the terms in equation (65) are functions of time. This equation can be simulated on an electronic differential analyzer. The general circuit for such simulation is given in Figure 61, where the input signal is still the gas reservoir pressure.

e. Effect of a Thick Twilight Zone: The gas water twilight zone may be thick, so that the compression of the water within the zone is not negligible and the permeability varies with location and time. A simultaneous solution to the diffusivity equation and the gas-liquid two phase flow equation is necessary to handle the thick twilight zone. However, the mechanics of the two-phase displacement for predicting the saturation variation with location and time is not yet known.

A general circuit is given in Figure 62 for the direct simulation of a thick gas-water twilight zone to get the water flux when the gas bubble pressure is given. In this circuit the twilight zone is divided into a number of linear increments, which may have different permeabilities. (An RC type simulation is required here). The permeability variation with location must be pre-determined from the two-phase flow study.

As for the RC type simulation[7], one can show that the electrical capacitors are functions of porosity, compressibility, and the formation volume of the cell, while the resistors are functions of viscosity, permeability, and thickness of aquifer sand or Marshal sand.

f. Oil Field Pressure Decline from Production Data: The pressure decline study of an oil field is more complicated than that of an aquifer water flow rate specified case. Recently Hurst[26] has published a new chart to handle the oil field pressure decline for constant oil production rate case. The arbitrary oil production can be handled using the new Hurst's chart[26] by setting up a transfer function on an electronic differential analyzer as done in this thesis.

A careful study reveals that there is an alternate method which does not necessitate the new chart. The usual constant rate case solution[4] can be used to handle the arbitrary oil production rate case in simulating an aquifer-oil field system on an electronic differential analyzer.

For an undersaturated oil field, the aquifer water flux can be

incorporated with the material balance equation in the following manner:

$$\text{Cumulative water flux} = \left(AN_p - BP \right)$$

where A and B are constants and N_p is the cumulative oil production. The simulation of this equation to obtain the pressure decline from the oil production data is shown in Figure 63. In Figure 63 the circuit that goes in the block representation is the same as that of volume case in this thesis. The extension of this idea can be applied to saturated oil reservoirs, considering the gas liberated from solution.

The method can also be applied to oil field interference studies. A general circuit for oil field interference is given in Figure 64.

VIII APPLICATIONS TO OTHER CHEMICAL ENGINEERING TRANSIENT PROBLEMS

The transient system response study, made with gas storage reservoir problems in this thesis, can be extended to other chemical engineering transient problems of linear response characteristics. For a linear system, the separate solutions, obtained by using each driving force alone, can be added to obtain a composite solution with all the driving forces present. This principle of adding solutions is called "the Principle of Superposition." The pressure, temperature, concentration, fugacity, etc., can be the driving force of the linear transient system analysis. By knowing the unit step response curve, the response with arbitrary driving force can be found by following the developed method. The reverse procedure can be taken to find the unit step response. In fact, this is a way of checking the linearity of the system when two or more independent sets of data are available. The system may not necessarily be one which follows the diffusivity equation. Any system of linear characteristics can be analyzed. Some typical transient problems of interest are presented.

a. Reactor. An example is picked for a one-stage or continuous reactor problem. When two sets of data are available, one can determine whether the system response is linear or not, by the method of analysis. If these two sets of data are satisfied by the same unit step response function, the system can be thought of as a linear system. Once the unit impulse response is found, the same circuit can be used to find the output reactor concentration for any time-varying feed input to the reactor. Obviously, for such studies all the rest of the system variables must be kept constant - e.g. temperature, and pressure of the reactor.

Thus, for any time-varying charge to the reactor, the product concentration can be predicted without knowing much of the kinetics and other complicated theoretical understanding of the transient behavior of

the system, provided that the rest of the variables of the system are held constant.

b. Wetted Wall Column: In a wetted wall column the radial diffusion of a component takes place. When the velocity distribution is known as a function of radius, the unit impulse response if fairly well known: the product concentration of a component is known for a given feed. And the problem narrows down to the reactor problem, except for the fact that a physical transfer operation takes place instead of a chemical reaction. The product concentration can be found for any given time-varying feed input if the system is linear. In this analysis, the response is not governed by the diffusivity equation; and the temperature and the total pressure of the column is assumed to be constant.

For a fixed feed one can choose to study the output and the temperature effect. For this case, the diffusivity equation holds[27]. By knowing the theoretical constant temperature case solution, one can find the solution for the case when the temperature of the column wall changes as a function of height, setting up a proper transfer function based on the unit impulse response, and feeding in the corresponding vapor pressure variation as a function of time dictated by the temperature change.

c. Jacketed Heating Vessel: Often it is possible, by studying heat transfer, that the heating curve can be obtained theoretically for an idealized temperature of the heat source, for a jacketed heating vessel. In any event theoretically, or experimentally, the constant temperature source heating curve can be obtained. Here again, the time-varying temperature and the heating curve can be analyzed if the system can be assumed to be linear. By obtaining independent sets of data, the pseudo-linearity of the system can be checked. If the unit impulse response curve is established, the heating curve can be found for any time-varying temperature without knowing the full details of the heat transfer mechanics.

d. Flow Through a Complex Piping System: The efflux at the outlet of a complex piping system and the pressure variation at the inlet can be studied. First of all, the pseudo-linearity of the system response must be secured by taking two independent sets of data, showing the inlet pressure versus the efflux as a function of time. In doing so, one will be able to establish the proper transfer function which can be used to predict the efflux with any time-varying inlet pressure, if the system is linear.

These examples are typical problems to which one can extend the transient linear system analysis technique. Other than the examples described, the heat conduction problems and the mass diffusion problems are much the same as those of aquifer water flow through a porous medium.

IX SUMMARY AND CONCLUSION

1) A method of simulating an aquifer on a general purpose electronic differential analyzer is developed to handle arbitrary time-varying terminal conditions for the determination of the variation in size or the pressure of a gas storage reservoir adjacent to an aquifer. The solutions with constant terminal conditions to the radial diffusivity equation given in the literature, are used to set up the proper transfer functions. Once a suitable circuit gives the reliable unit step response, the same circuit can be used for any arbitrary input case by feeding the arbitrary time-varying terminal conditions. The output is essentially the result of the computation of a convolution integral. The input signal may be pressure, water flux, or volume variation of a gas storage reservoir.

2) The developed method is employed to make basic studies of theoretical unit step cases. Whenever possible, the results of the developed analog method are compared with the theoretical solutions. The basic studies indicate that the accuracy obtained by the developed simulation method is well within the range usually required for typical gas storage operations, and can be justified in the light of the basic assumptions made in the mathematical formulation of the actual problem. The present work was done on the Sterling Model LM 10 electronic differential analyzers.

Upon making the basic studies and securing the reliability of the developed method, the aquifer beha vior study is made, using the simulation method as a tool whenever needed.

3) For an isolated gas storage field, study is made on the various effects on water return-ability, in which the practical engineers may be interested; specifically, studies are made on the effects of permeability for a limited aquifer, the effect of aquifer size, the effect of phase shift

in the pressure cycle, the order of magnitude of error introduced by the flow resistance at the gas-water twilight zone when the zone is not thick, and the effect of the areal geometry of a gas storage field. The effects are shown in figures and tables.

4) Effect of a fault on unit step responses is studied. The solutions to constant rate and pressure cases are given in figures so that one can read off immediately the unit step responses as a function of time and location of a fault. A fault is referred to as an infinitely long impermeable rock structure on an infinite aquifer. Also, charts are prepared for the unit step responses when three identical circular fields are located on a delta. These idealized studies are to serve as a guide and to give better understanding of the shapes of the unit step response curves for different cases.

5) The interference effect of Fields C, D, and E toward Field A is investigated. The performance of Field A was considered as an isolated field on a limited aquifer by previous investigator.[2] The present study shows that the data-matching job is somewhat flexible because of the large number of the variables which dominate the system. There is a strong need for correlation of the data departing slightly from the purely theoretical analysis.

6) The moving boundary problem is studied theoretically. An approximate method to find the qualitative unit pressure step response is given. This method neglects the small time effect and makes use of the fact that the dimensionless time for moving boundary problems encountered in aquifer gas storage operations is in the order of thousands, where the pressure gradient at the gas field does not change much as a function of time. The use of an instantaneous source for moving boundary problems is discussed, and the analytical solutions are given to different shapes of moving sources which may apply to aquifer gas storage operations.

7) Analytical solutions to growing disk source model are obtained. First, the unit volume step response is computed from the mathematical analysis. Then, the unit pressure step response is determined by employing the developed simulation method, assuming the system is linear. This assumption should be good if the small time is excluded when the gas bubble growth is very rapid. The qualitative analysis shows that the unit pressure step response curve is approximately a straightline at the normal time ranges of aquifer gas storage operations.

8) A general discussion of the reservoir variables is given. The analysis of the variables and the experience with the aquifer behavior study, lead to an understanding of the significance of the theoretical correlation method. The newly defined unit step responses are equivalent to the "resistance function" recently mentioned by Hutchinson[24] for the terminal rate case.

9) A theoretical correlation method to predict the performance of an aquifer gas storage is developed. The method is applied to Field B. The method is proven to give an excellent correlation which is later used to predict the performance of Field B. The predicted values agree very closely with the actual field data.

10) Other possible uses of electronic differential analyzer for reservoir engineering problems are given. These include computation of convolution integral, gas content as input signal, effect of gas flow resistance on water flux, time-varying twilight zone, effect of a thick twilight zone, and oil field pressure decline from production data.

11) The transient system analysis technique developed in connection with reservoir engineering problems is not limited to the diffusivity equation alone, but can be applied to any linear system. Some typical applications to chemical engineering transient problems are given. When more than two independent sets of response data are available, it is possible to find some sort of unit impulse response of the system. Such

pseudolinear unit impulse response or the correlation function can then be used to obtain the response for any time-varying forcing function or driving function.

In brief, the general aquifer behavior is studied, using the developed analog simulation method as a tool, to improve the understanding of the gas storage reservoir-aquifer performance. Efforts have been made to consider the various effects and the special cases that one encounters during the study of a gas storage problem. The ability of an electronic differential analyzer is fully shown; and it is proven to be an inexpensive tool to study reservoir engineering problems. In the course of the theoretical study and the experience with aquifer variables, the significance of the correlation idea is doubly pointed out with theoretical support and logical deductions.

Two areas of research are created from the present study which need future investigator's attention.

1) The basic assumption we have made in the study is the linear characteristic of reservoir system - the fact that we were able to write convolution integral mathematically. Depending upon the system, and how the problem is handled, the degree of nonlinearity can be greatly different; and its significance can be different also. The moving boundary problems and the effect of two-phase zone are subjected to the question of nonlinearity. So far as aquifer storage problems are concerned, one can safely assume a linear system response if the short time analysis is excluded, to secure an engineering answer. The degree of nonlinearity due to two-phase zone effect is not known. The nonlinearity study of these effects should be of good academic interest, even though it may not pay off to improve the engineering answer.

2) Some reservoir problems related to the relative saturation effect are given in this thesis; and some general circuits to handle such problems are presented. The questions remain: a) how thick is the

appreciable low-permeability zone (gas-water twilight zone)? b) how does the permeability vary as a function of location for a fixed radius gas storage field? c) does the permeability change much as function of time for fully developed gas storage reservoir? and d) how does the permeability vary as functions of time and location for a growing gas bubble? The quantitative and qualitative answers to these questions are important. In the absence of these data, the best one can do is to assume a linear system and to find the unit impulse response function or correlation function by trial and error, which gives a good correlation of the actual data. Here again, one should not expect to improve much on the engineering answer obtainable from the method described above.

APPENDIX

APPENDIX I

An Example of Derivation for an Aquifer Simulation Circuit from Transfer Function Expression

In order to show the detail derivation for a simulation circuit from the transfer function expression, an example calculation is shown here. The basic principles involved in obtaining the circuits are unique to all other circuits presented in this thesis with the exceptions of Figures 59, 60, 61, and 62.

a. Basic Features of Electronic Differential Analyzer: Before any attempt to show how the numbers are selected in an analog circuit, it would be well to describe some basic features of an electronic differential analyzer, to understand the symbols used in the circuit. Referring to Figure 7, there are four symbols that must be explained. First, the most important components are the high-gain DC amplifiers or operational amplifiers which are designated by the triangular shapes. It is these amplifiers that become summers or integrators or simulate each term in the transfer function expression. The second symbol is the circle which designates a potentiometer. The potentiometer is able to multiply by a constant less than unity which is set by a dial. The potentiometer setting is written in or by the circle. The third and fourth symbols are for resistors and for capacitors which need no explanations.

The input to the machine is at the left, and the output is at the right, since current flows from left to right by convention.

Since the dependent variable is always time on analog computer, a machine time constant K plays an important role in relating the actual time and the machine running time. The details are explained as the calculation is carried out.

b. Pressure Case of a Limited Aquifer. In the early part of the thesis, a transfer function expression for $r_D = 10$ is found to be the following:

$$s\bar{f}_1(s) = 2.2\left\{1 + \frac{21.5}{1 + \frac{s}{0.0122a}}\right\} \qquad (21)$$

Equation (21) is a combination of equations (15) and (17). It is intended to show how the numbers are obtained from the transfer function as expressed in equation (21) to give the circuit of Figure 7.

In equation (21), a factor 2.2 is multiplied to both terms; so, one can design to get $Q_{fD}/2.2$ rather than Q_{fD}. One of the basic requirements in deriving an analog circuit is to keep the output of each amplifier less than $\pm$ 100 volts; but, at the same time not too small. Considering the magnitudes of the input and the Q'_{fD} from the theoretical values, $Q_{fD}/22$ is chosen as the machine output to give full dynamic ranges of operation. In order to cancel a factor of 22 in checking the unit pressure step response, the input is chosen to be -22 volts, and this requires:

$$P_8 = \frac{-22}{-100} = 0.22$$

The output of P_8 is then -22 volts. This -22 is then fed into amplifier 4 of which the output becomes:

$$\text{output of No. 4} = (-22)\left(-\frac{0.5}{1}\right) = +11 \text{ volts}$$

The positive 11 volt is applied to amplifiers No. 6 and 5. The input to amplifier No. 6 is to take care of the first term in equation (21).

$$\text{Output of No. 6} = (11)\left(-\frac{1}{1}\right) = -11 \text{ volts}$$

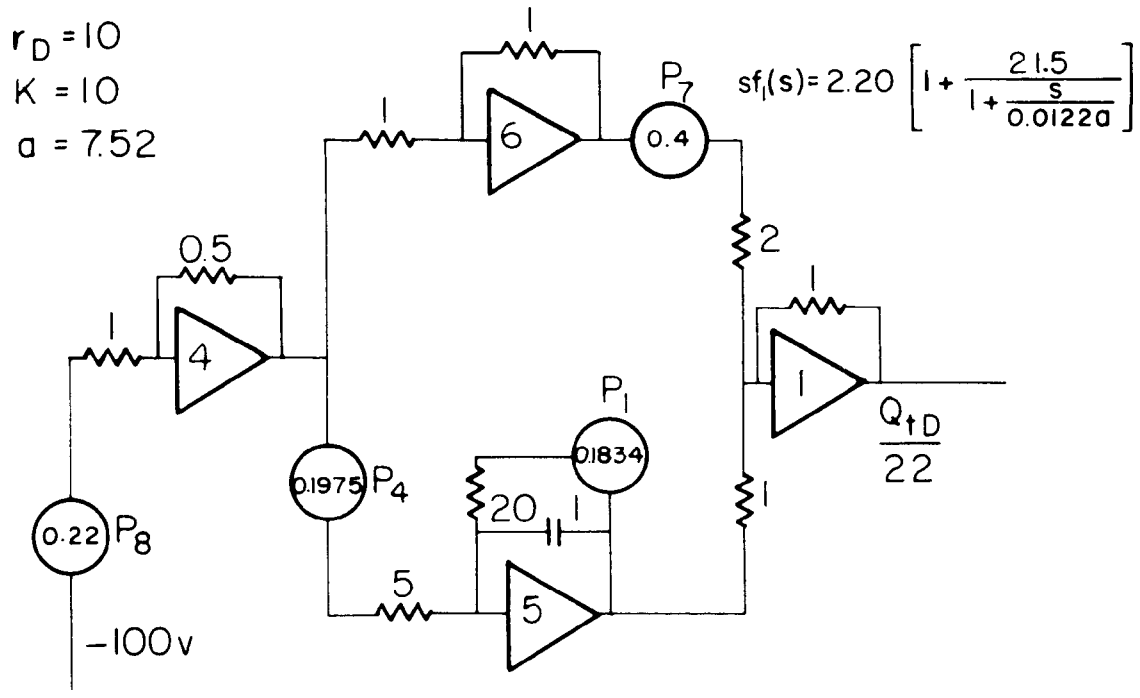


Fig. 7— LM10 circuit diagram for $r_D = 10$ to get cumulative flux function.

This -11 volt must somehow be reduced to give 2.2 toward the output of No. 1.

$$2.2 = (-11)(P_7)(-\tfrac{1}{2})$$

$$\text{or} \qquad P_7 = 0.40$$

The next step is to consider the second term. As shown in the simulation of equation (17):

$$R_f C_e = \frac{1}{0.0122a} \qquad \& \qquad \frac{R_f}{R_i} = 21.5 \quad (\text{Fig. 4})$$

$$\text{or} \qquad R_f = \frac{K}{(0.0122a)(C_e K)}$$

Choosing $C_e K = 1.0$ mf, and substituting $K = 10$ and $a = 7.52$,

$$R_f = 109 \text{ megohm.}$$

If we use 20 megohm input resistor to amplifier No. 5,

$$P_1 = 20/109 = 0.1834$$

$$\frac{R_f}{R_i} = 21.5 \quad \text{or} \quad R_i = 109/21.5 = 5.07 \text{ megohm.}$$

Since the output of No. 4 is 11 volts, this must be considered to give a factor of 2.2. If 5 megohm input to No. 5 is chosen,

$$\frac{2.2}{5.07} = (11)(P_4)(\tfrac{-1}{5})(-1) \quad \text{or} \quad P_4 = 0.1975$$

The outputs of No. 6 and 5 are summed up as required by equation (21), and the circuit to simulate the equation (21) is shown in Figure 7.

When specified pressure variation is fed in by generating with P_8, the output $(Q_{in}/22)$ is the cumulative water flux function for the given input.

Perhaps the example calculation shown here for the circuit in Figure 7 may be the simplest of all the circuits presented in this thesis, but the principles are just the same, except few special cases for which standard analog computer textbooks must be referred to.[22] [23]

APPENDIX II

Electronic Differential Analyzer Circuits Referred in the Thesis

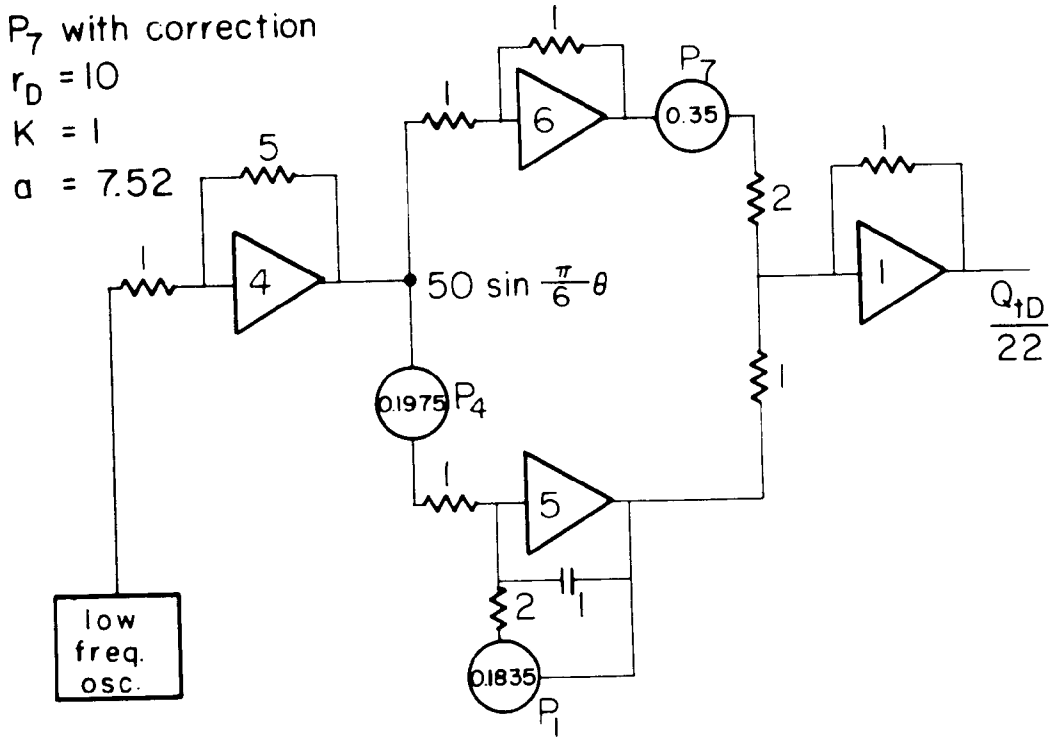


Fig.46 – LM10 circuit diagram for r_D = 10 to get cumulative flux function with annual sinusoidal pressure variation

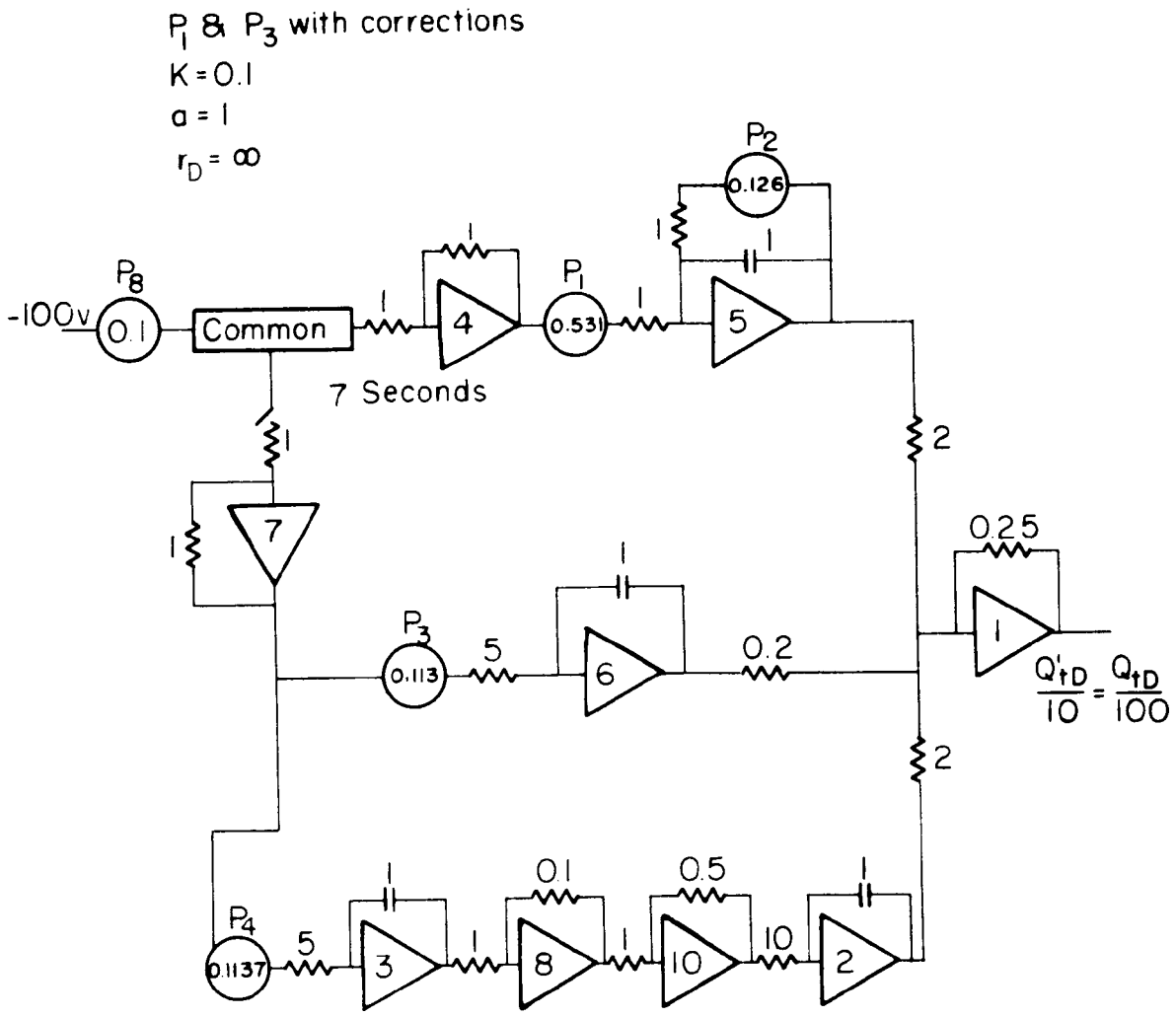


Fig.47- LM10 Circuit diagram for $r_D = \infty$ to get cumulative flux function

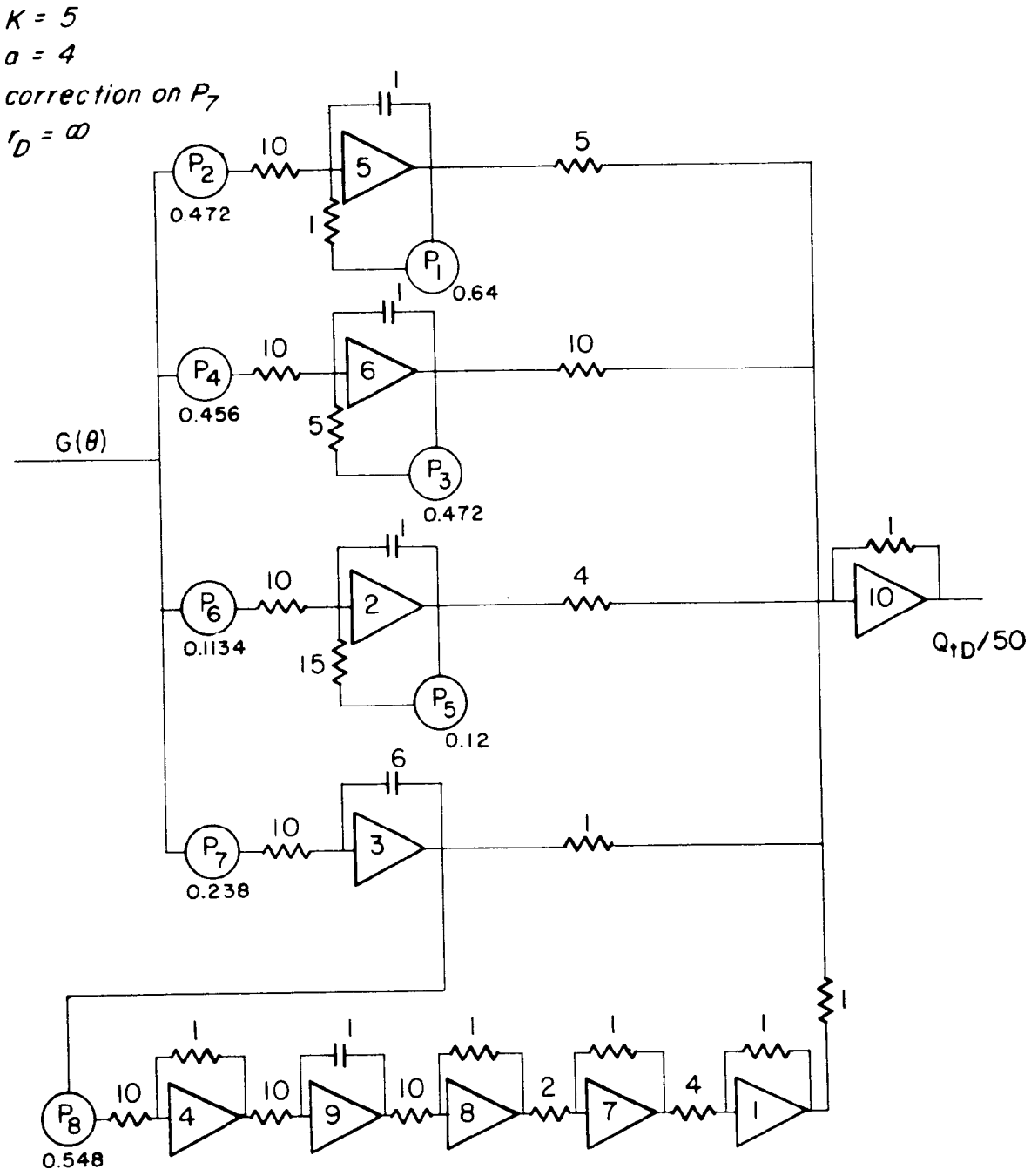


Fig. 48 - LM10 circuit diagram to get cumulative flux function for infinite aquifer

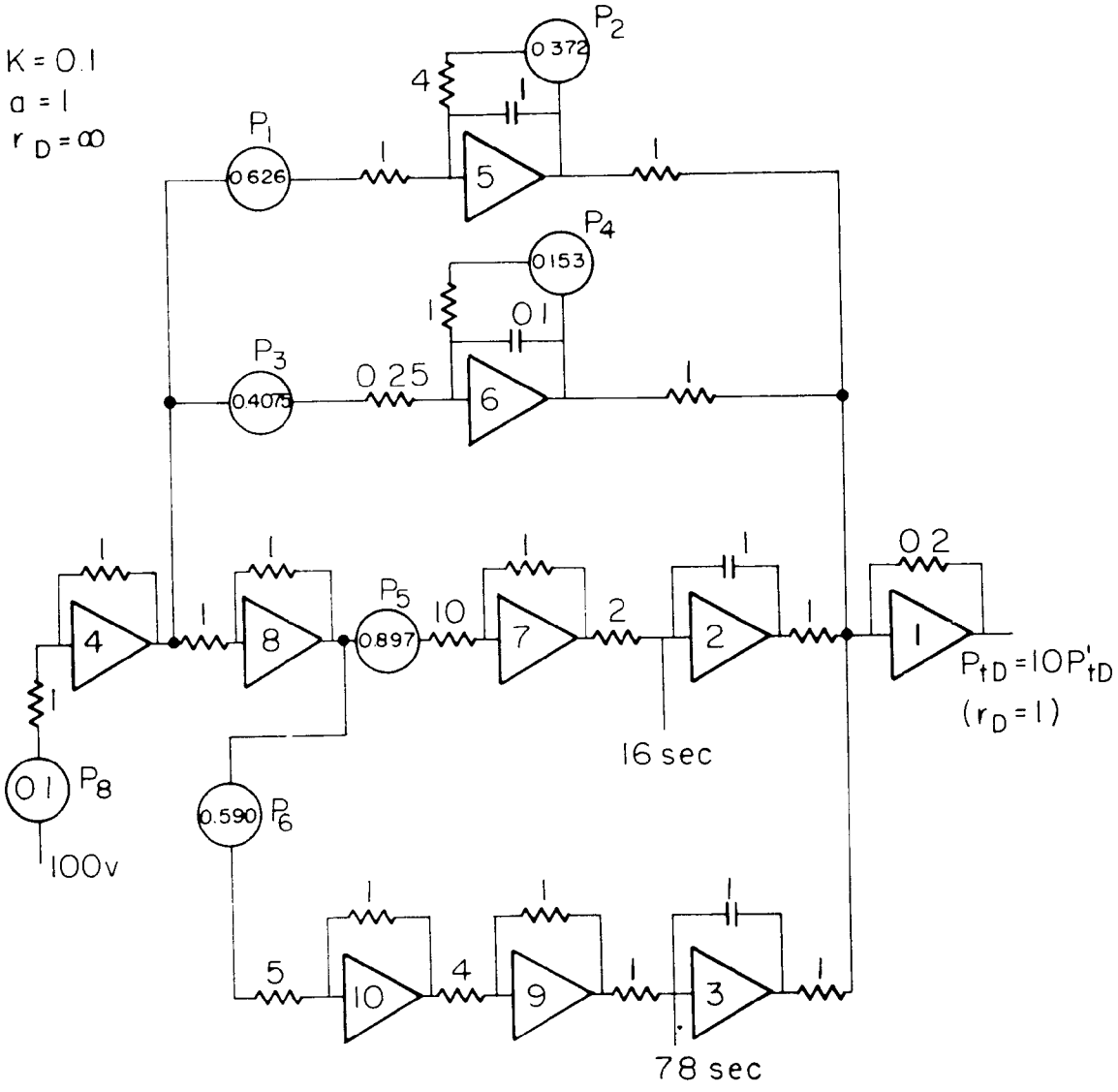


Fig 49 - LM10 circuit diagram for $r_D = \infty$ to get pressure change function $(r_D = 1)$

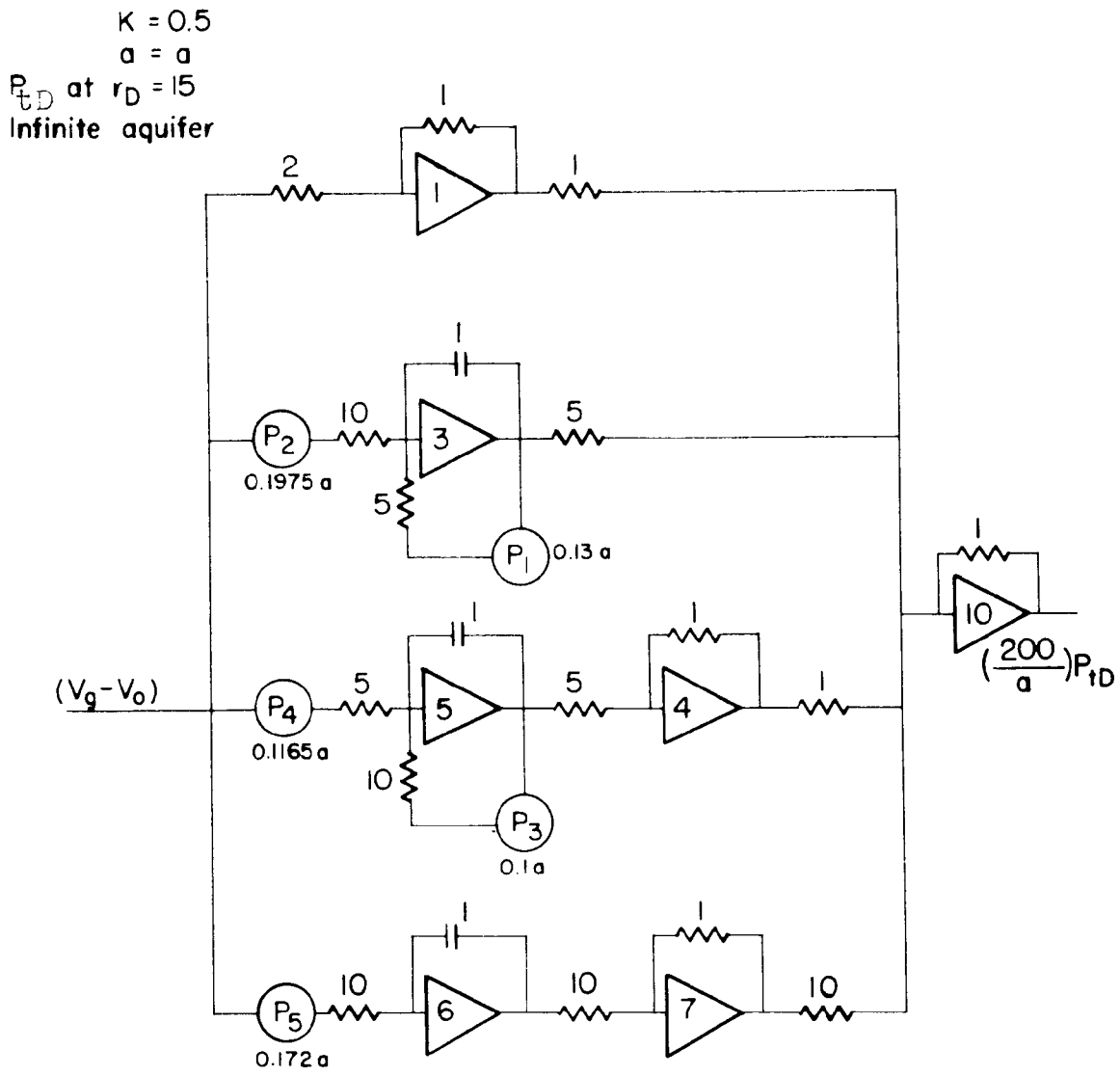


Fig. 50. LM10 circuit diagram to get pressure change function at r_D = 15

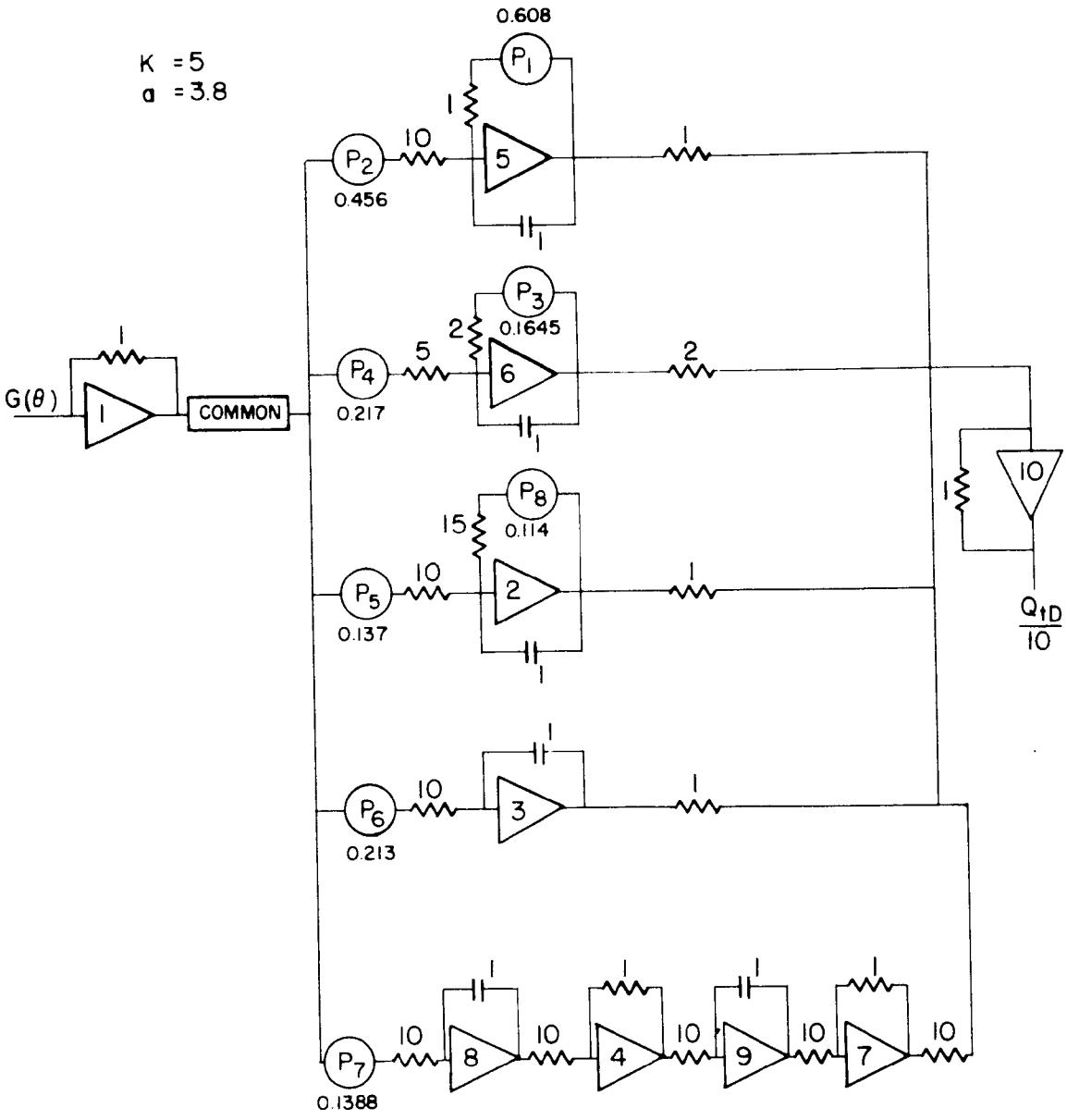


Fig. 51. LM10 circuit diagram to get cumulative flux function ($r_D = \infty$)

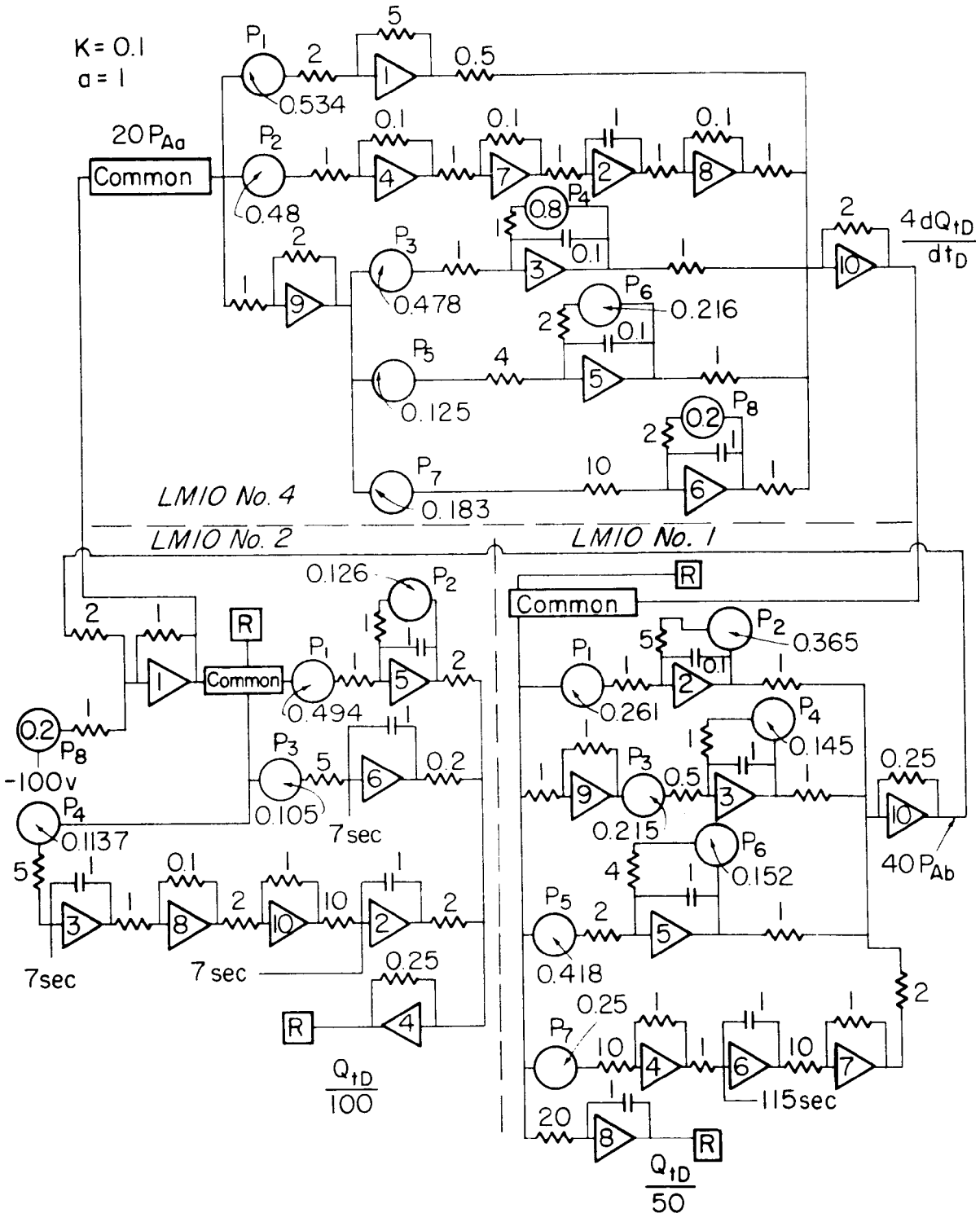


Fig. 52- LM10 circuit diagram to get cumulative flux function with a fault in the aquifer at $2d/r_g = 2.46$

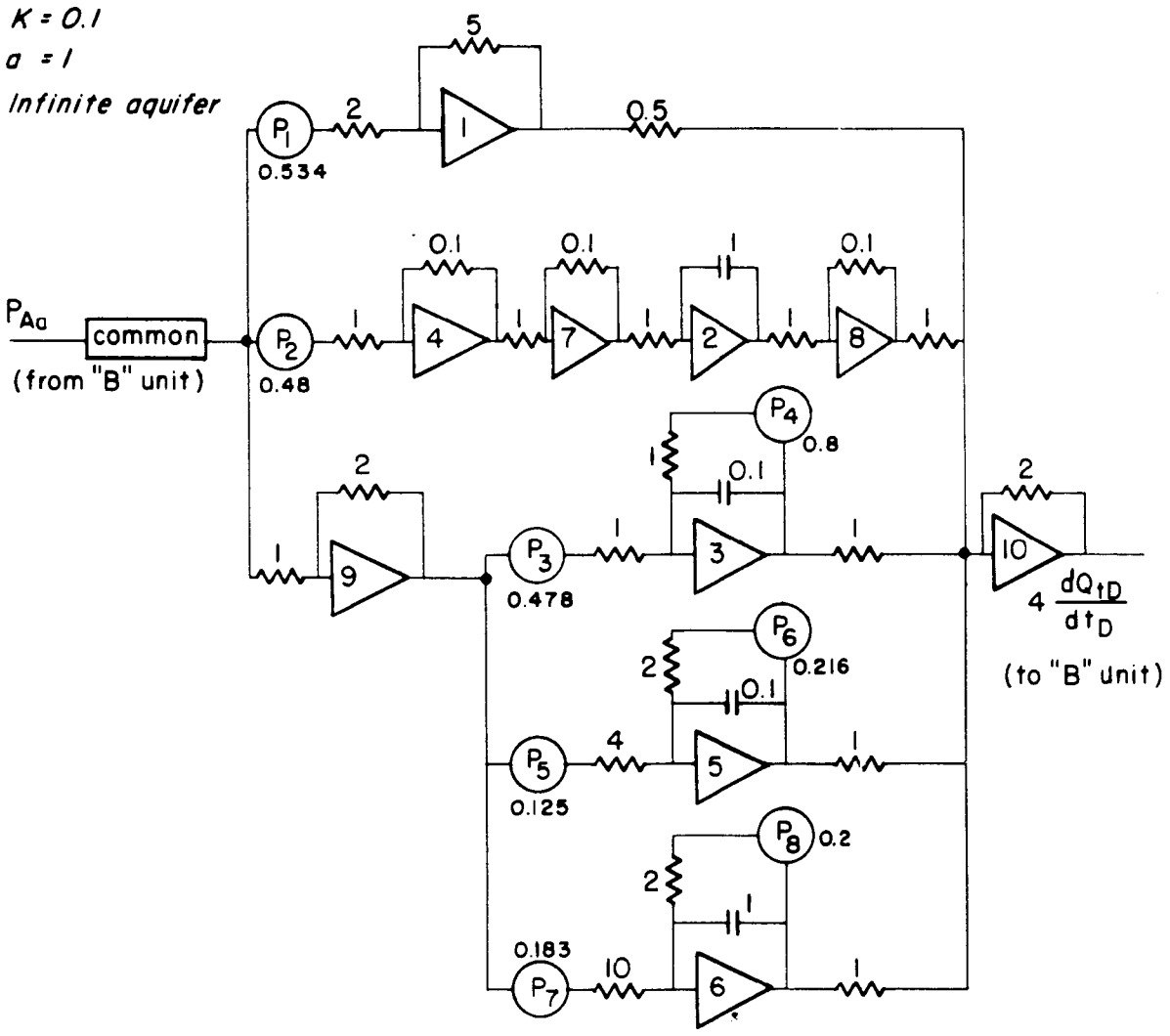


Fig. 53- LM10 circuit diagram of unit A to get flux function

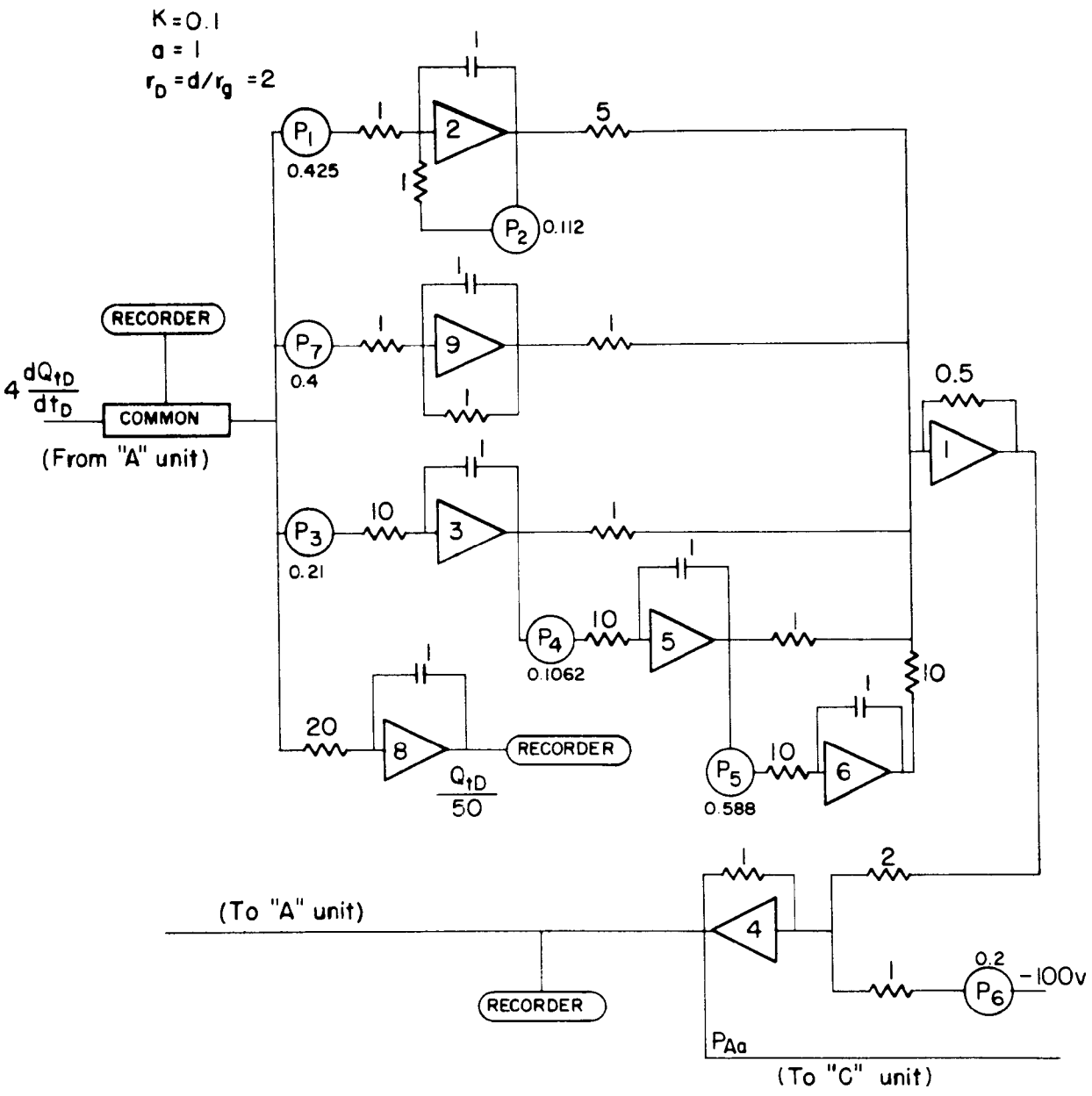


Fig. 54. LM10 circuit diagram of unit B for $r_D = 2$ to get pressure change function

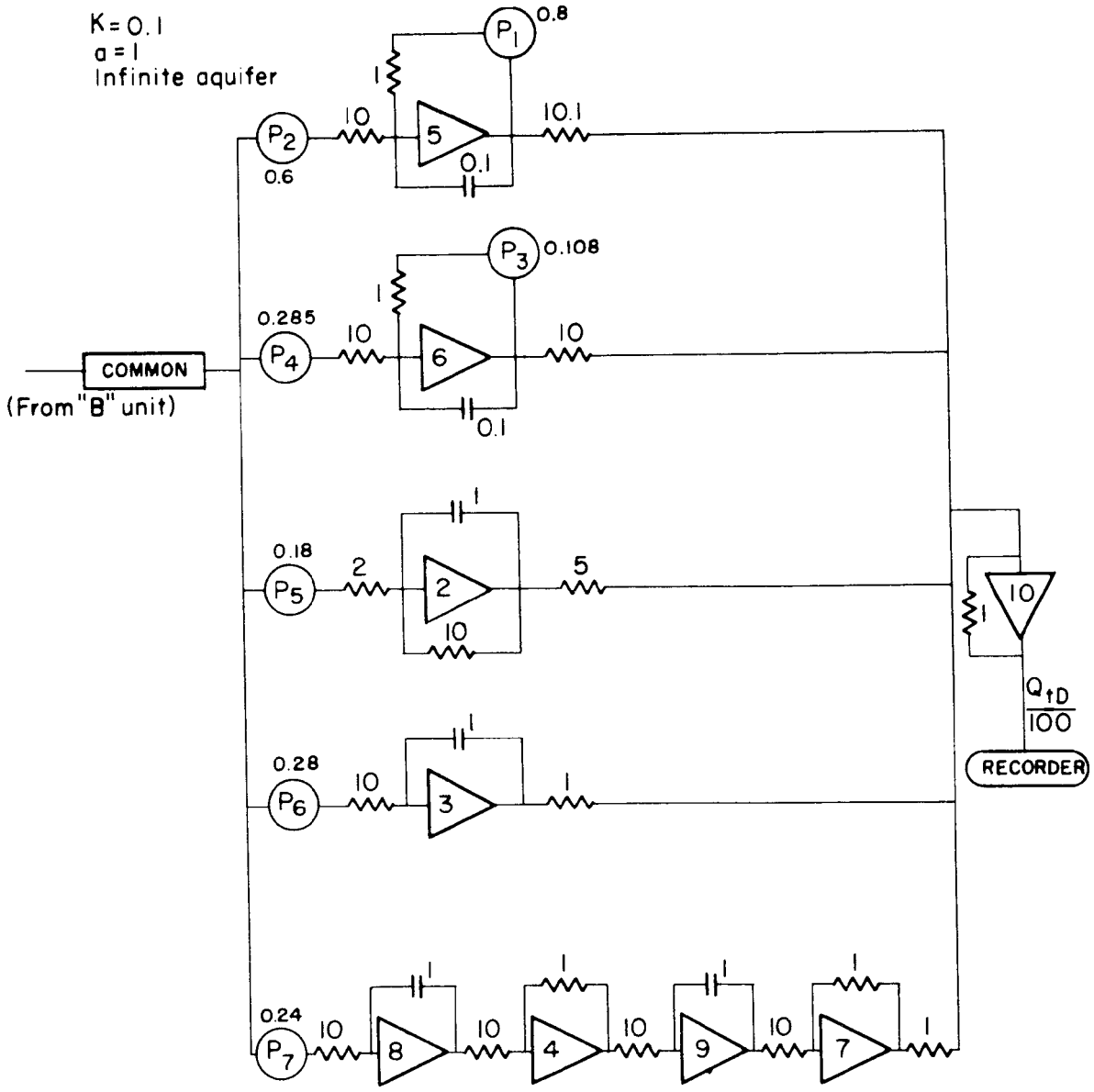


Fig. 55-LM10 circuit diagram to get cumulative flux function ($r_D = \infty$).

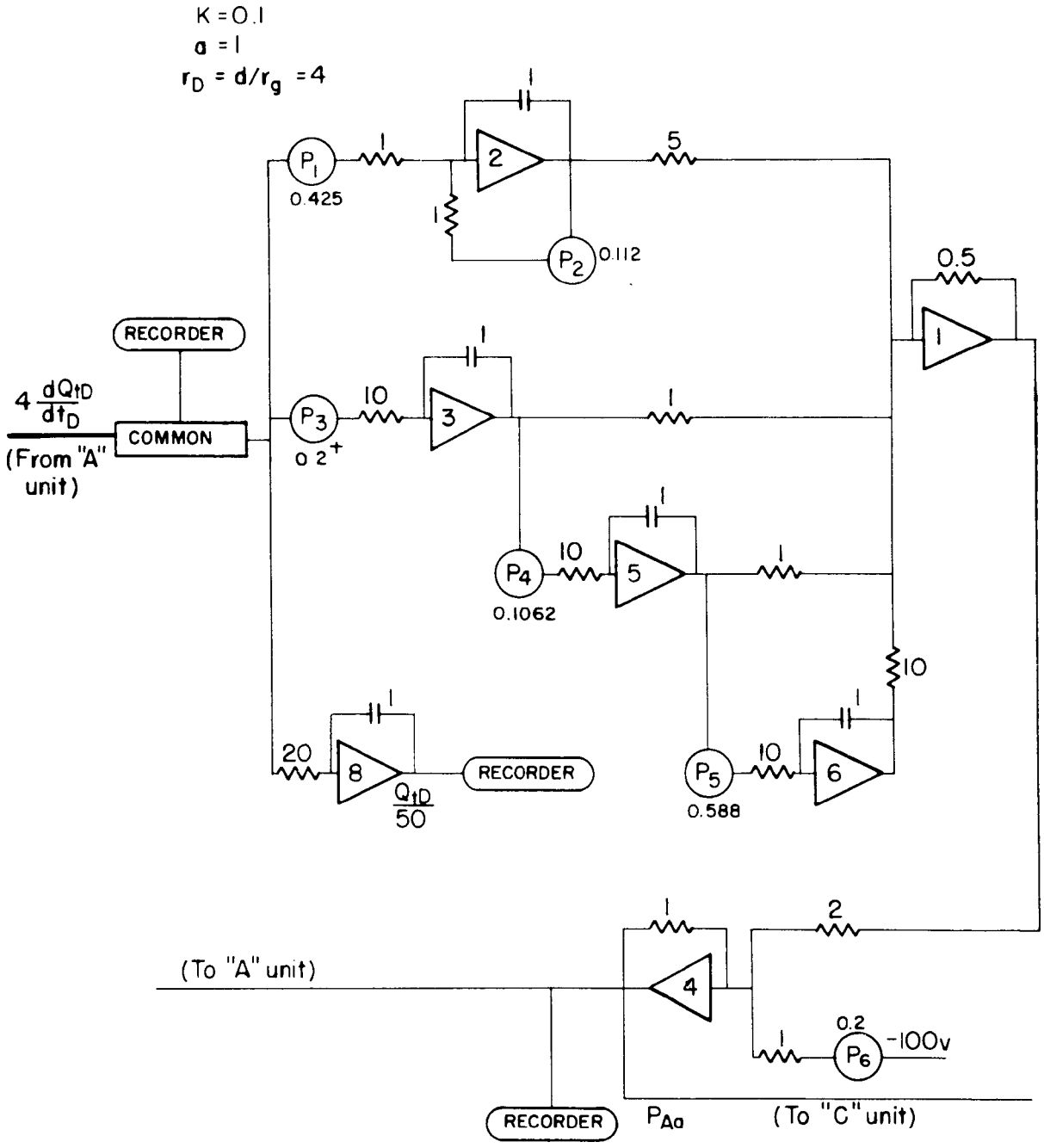


Fig. 56. LMIO circuit diagram of unit B for $r_D = 4$ to get pressure change function

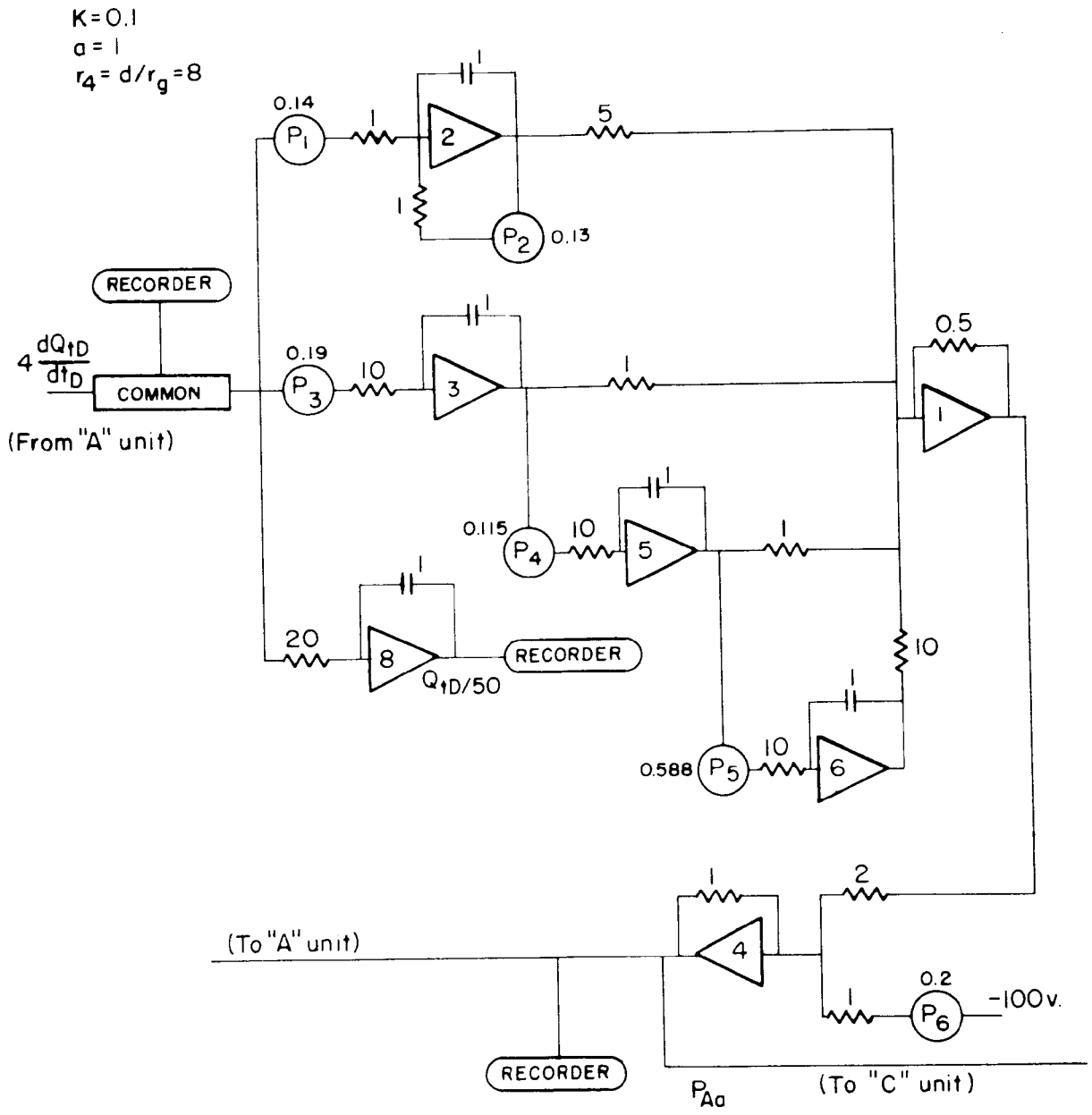


Fig. 57 – LM10 circuit diagram of unit B for $r_D=8$ to get pressure change function.

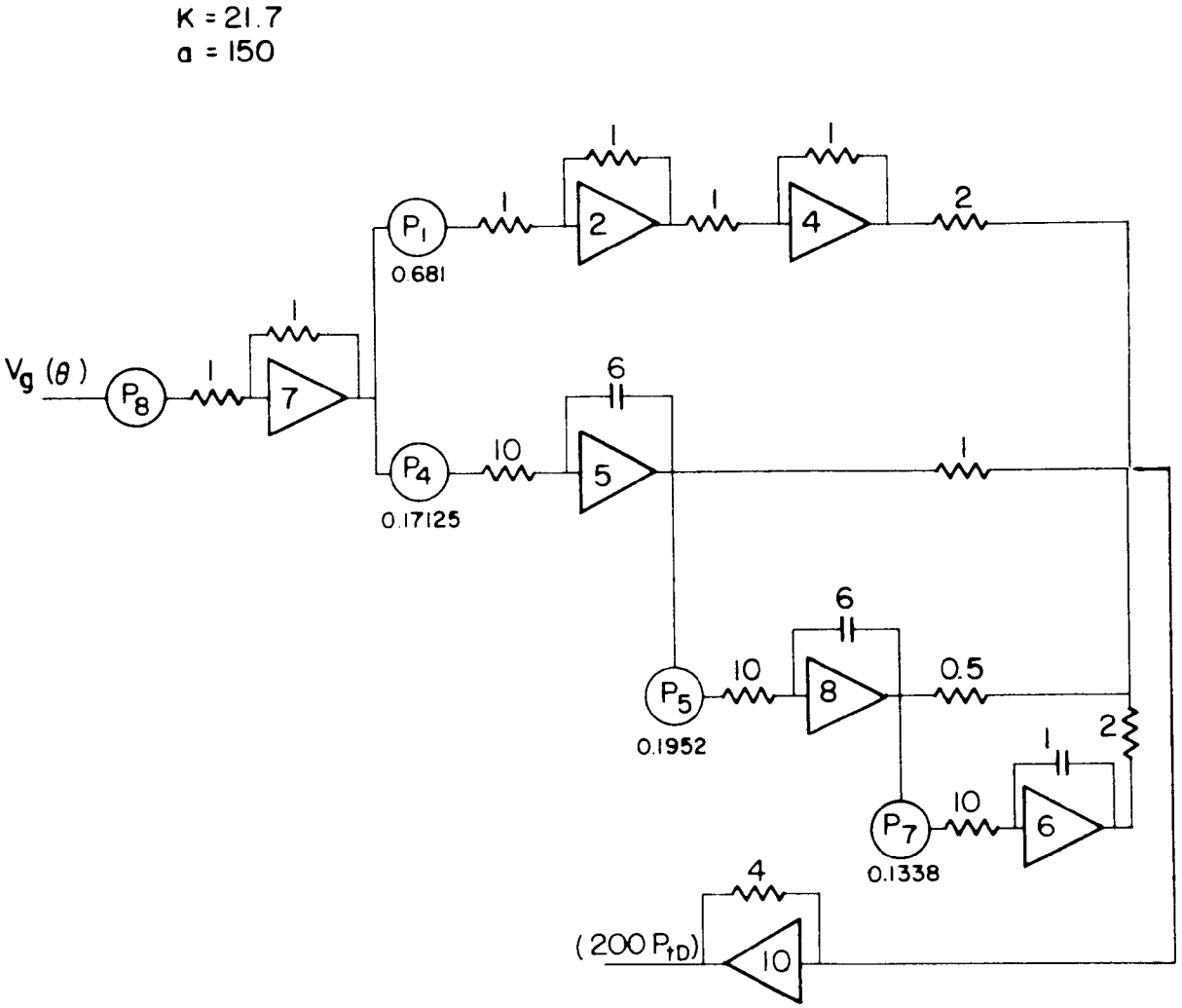
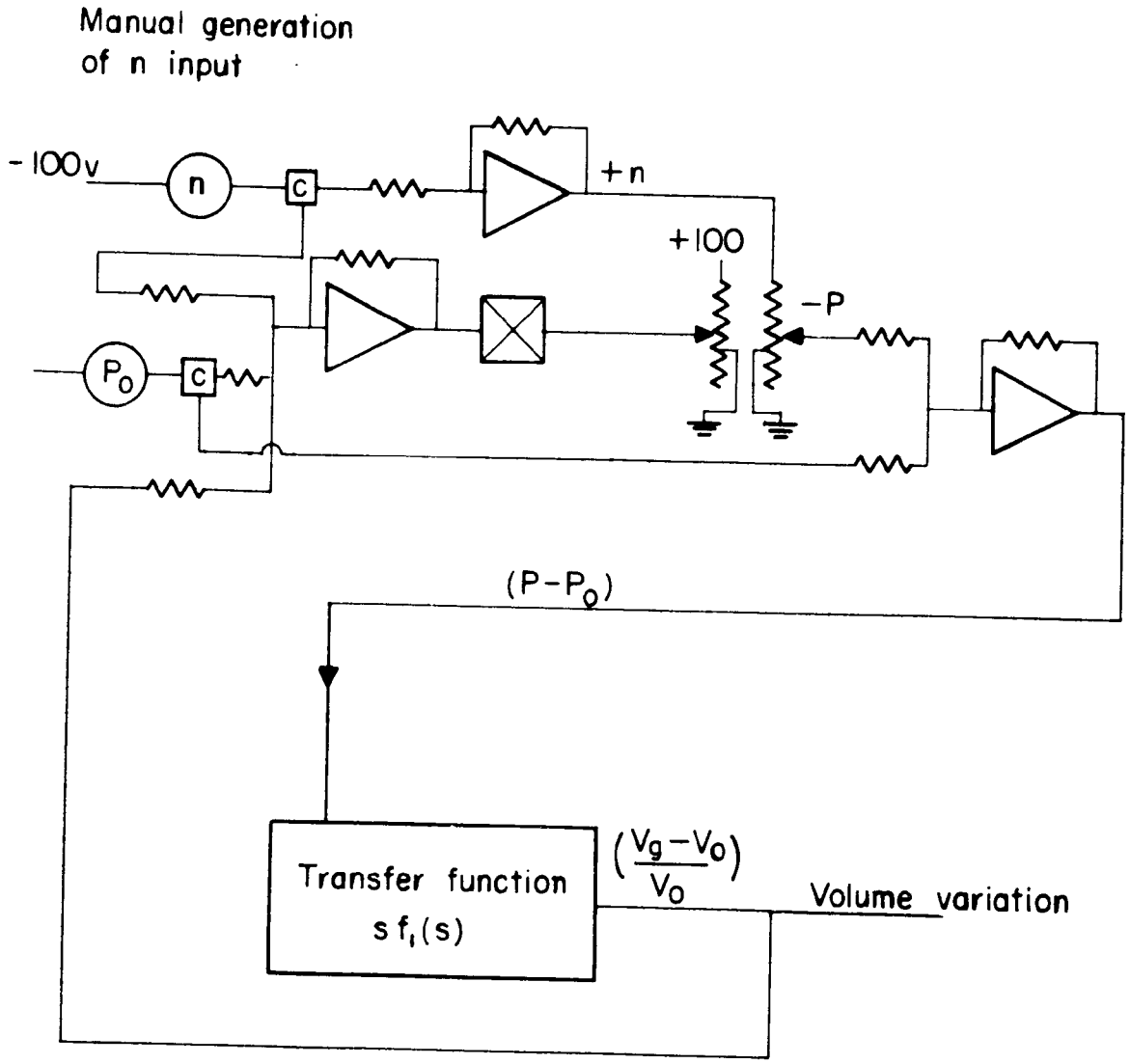
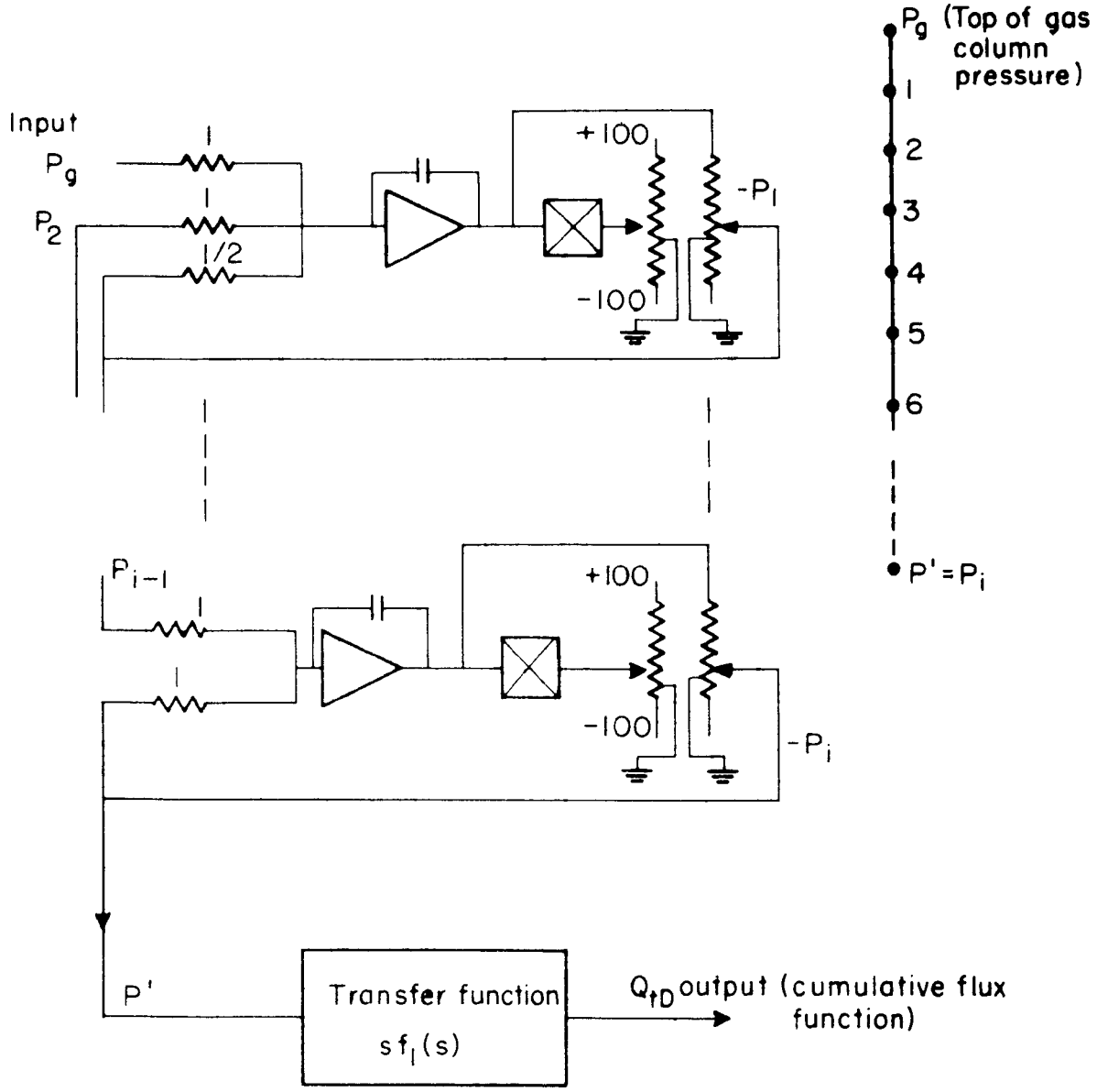


Fig. 58. LM 10 circuit diagram to get pressure change function using volume as input for growing disk model of finite aquifer thickness.



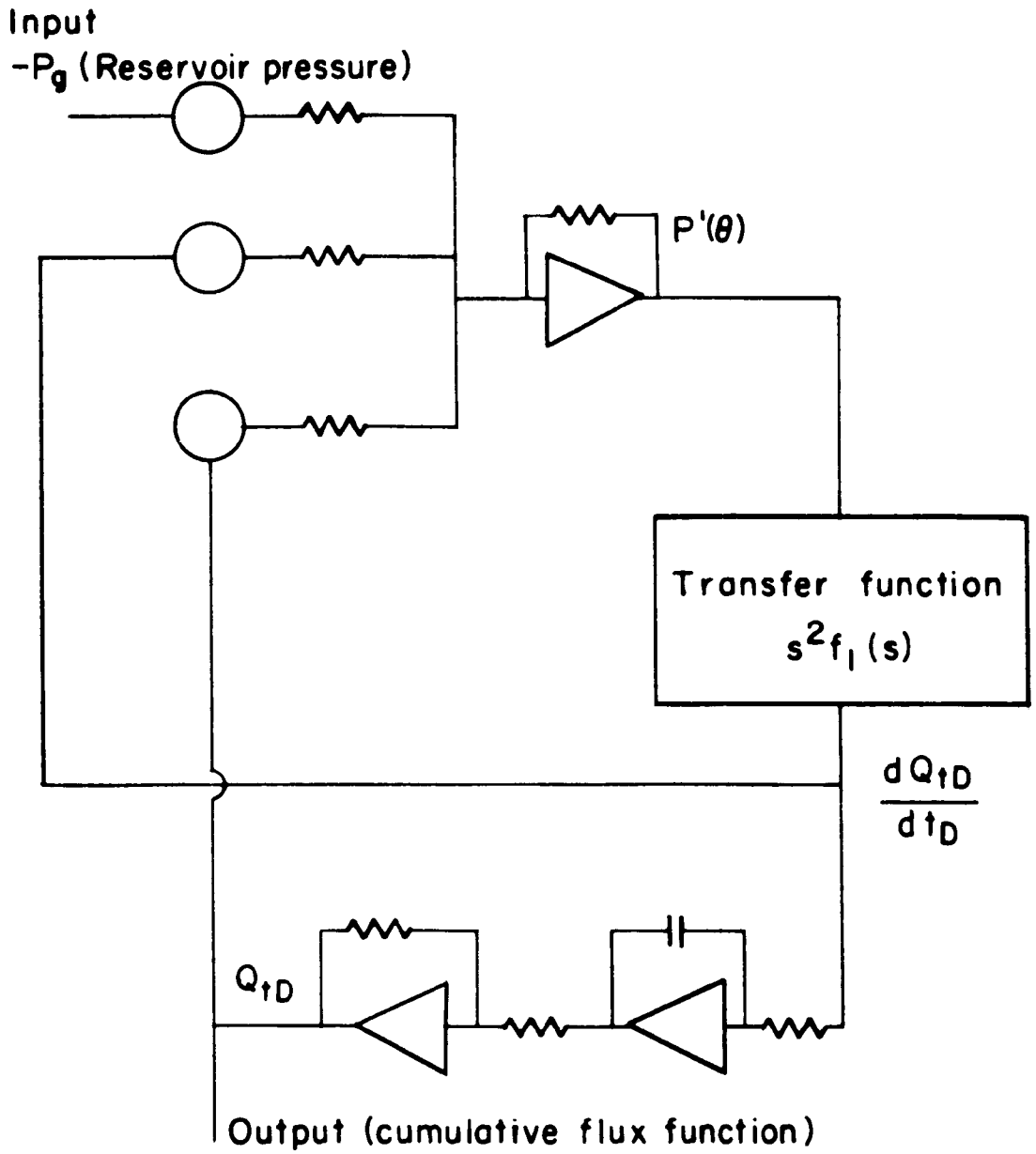
$f_1(s)$: Laplace transform of cumulative flux function for constant terminal pressure case

Fig. 59. Gas reservoir pore volume variation from gas content as input signal.



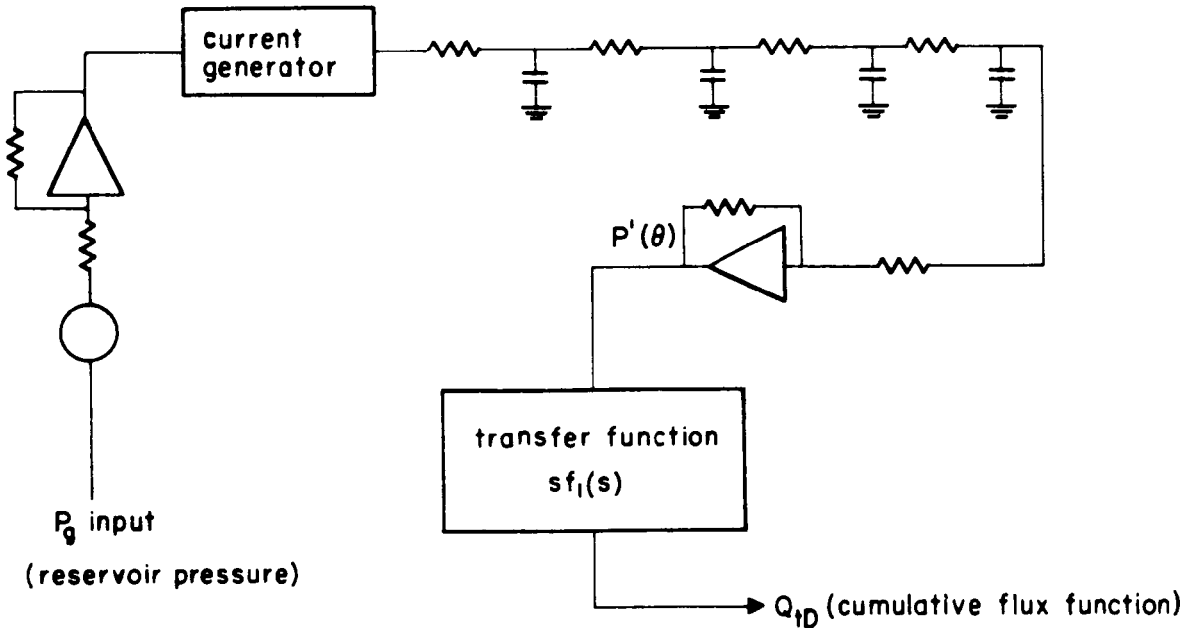
$f_1(s)$: Laplace transform of cumulative flux function for constant terminal pressure case

Fig. 60 - Circuit diagram for the effect of linear gas flow resistance on water flux.



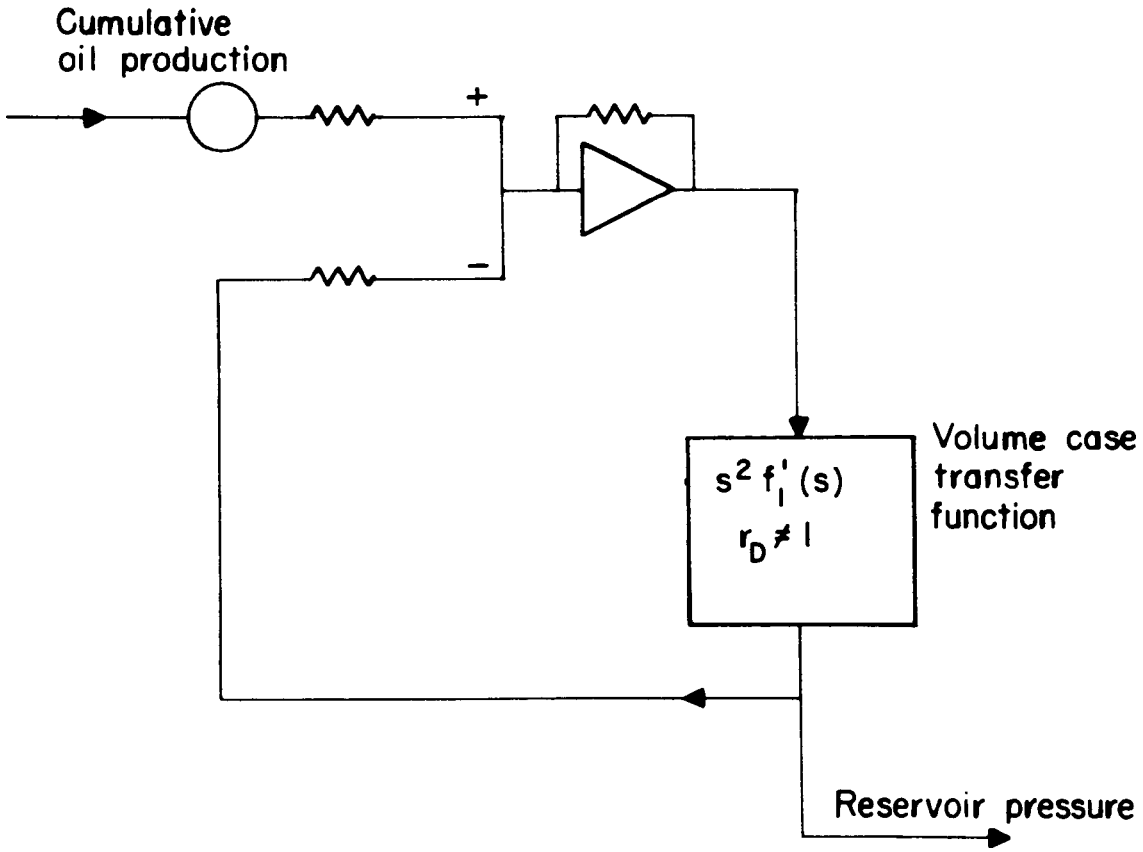
$f_1(s)$: Laplace transform of cumulative flux function for constant terminal pressure case.

Fig. 61 - General circuit to get cumulative flux with time-varying twilight zone resistance.



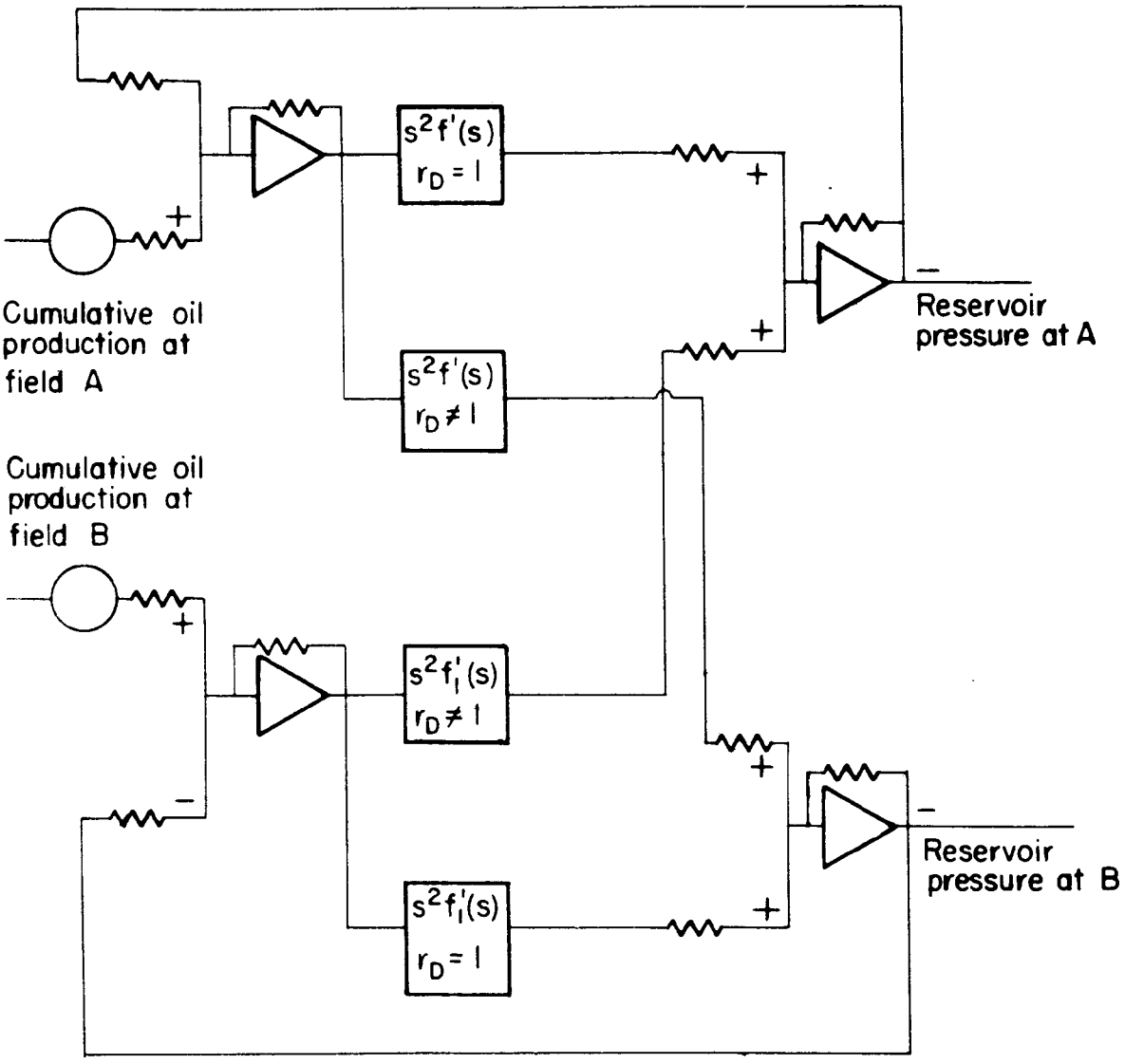
$f_1(s)$ = Laplace transformation of cumulative flux function for constant terminal pressure case

Fig. 62. Simulation of gas storage aquifer with thick low-permeability twilight zone.



$f_1'(s)$: Laplace transform of the pressure change function for constant terminal rate case solution

Fig. 63. Undersaturated oil field pressure decline from oil production data.



$f_1'(s)$: Laplace transform of the pressure change function for constant terminal rate case solution.

Fig. 64. Interference between undersaturated oil fields.

APPENDIX III

The Electronic Differential Analyzer Suitable for Reservoir Engineering Study

The electronic differential analyzer suitable for reservoir engineering study is somewhat exceptional because of the nature of the problem which requires a study of 1 - 20 years. So, it requires some special attention to select the type of electronic differential analyzer. For the work reported, LM 10 Sterling Model analyzers are used; but this should not mean that an LM 10 Sterling Model is the best or the only type that can be used.

a. The Peculiarity of the Reservoir Engineering Problems. The computation speed of an electronic differential analyzer is not usually a questionable matter because it can be made as fast as, or as slow as, one wishes to, so long as the scaling problem permits one to do so and the input can be generated correspondingly. For the time-varying boundary problems, the speed of the input generation is definitely the limitation of the speed of the computation. For the work reported here the input function is generated manually except for the sinusoidal input. There is no doubt that the manual generation of the reservoir pressure or the pore-volume variation with a potentiometer is the cheapest way of generating the desired function, because the variation of the input function is highly irregular. By experience, it is found that the machine time constant K must be 5 or 10 for practical problems when the data are given every month. K equals 5 means in the reservoir problems that 5 seconds of machine running time are equivalent to one month of reservoir time. So, in general, K equals 5 or 10 because of the input generation speed limitation.

Another peculiarity of the problem is the large span of the coefficients. With these two points in mind, the rest of the discussion becomes somewhat obvious.

b. Input Resistors: The input resistors to the amplifiers should be of flexible combination. Frequently, the large resistors are used. An example of the input resistor combination may be: 0.25; 0.5; 1; 1; 1, 1; 2; 4; 5; 10; 10; 20 megohm. Because of the small coefficients and exponents, the large resistors must be included.

c. Capacitors: Due to the large machine-time constant and the large span of the exponents, equipment with one size of capacitors is likely to present some difficulties. The equipment should have 0.1, 1, 5 mfd.

d. Amplifiers: The number of amplifiers in the equipment is thought of as a measure of the equipment size. It is difficult to generalize, but for an aquifer simulation which does one operation (e.g. Pressure case or Volume case), the number of amplifiers required usually runs 5 - 10, of which 50 percent are used as integrators. Therefore, an equipment with 20 - 30 amplifiers should be large enough to handle normal reservoir engineering problems.

e. Potentiometers: The number of potentiometers required is just about the same as that of amplifiers.

f. Others: Other than the computer itself, one will have to have recorders and servo multipliers (for non-linear problems), for which no comment can be given as to the selection of the equipment.

The above description of the suitable equipment is based on the author's experience and the difficulties encountered during the thesis work.

REFERENCES

1. Katz, D. L., Vary, J.A., and Elenbaas, J.R., "Design of Gas Storage Fields" AIME, Petroleum Trans., 216, 44, 1959.

2. Coats, K.H., Prediction of Gas Storage Reservoir Behavior Ph.D. Thesis, University of Michigan, April, 1959.

3. Muskat, M., The Flow of Homogeneous Fluids Through Porous Media, J.W. Edwards, Inc., Ann Arbor, 1946.

4. Van Everdingen, A.F., and Hurst, W. "The Application of the Laplace Transformation to Flow Problems in Reservoirs" AIME, Petroleum Trans., 186, 305, 1949.

5. Yoo, H.D., Katz, D.L., White, R.R., and Tek, M.R., "Methods for Predicting the Volume Variations of Gas or Oil Reservoirs Associated with Active Water Drive" Petro. Engr., Sept., 1959.

6. Katz, D.L., Tek, M.R., and Coats, K.H. "The Effect of Unsteady State Aquifer Motion on the Size of an Adjacent Gas Storage Reservoir" AIME, Petroleum Trans., 216, 18, 1959.

7. Bruce, W.A. "Electronic Computer's Magic Talents Speed Improved Production Technology" Oil and Gas J., June 3, 1957.

8. Karplus, W.J., Analog Simulation, McGraw Hill Book Co., New York, 1958.

9. McDowell, J.M., "Performance of Water Drive Reservoirs, Including Pressure Maintenance as Determined by the Reservoir Analyzer" AIME, Petroleum Trans. 204, 73, 1955.

10. Patterson, O.L., Dutton, G., and Ellis, H.E., "The Determination of the Water-Injection Program for the Delhi Field by Means of Automatic Multi-pool Analyzer", AIME, Petroleum Trans., 207, 73, 1956.

11. Rumble, R.C., Spain, H.H., and Stamm, III, H.E., "A Reservoir Analyzer Study of the Woodbine Basin", AIME Petroleum Trans., 192, 331, 1951.

12. Chatas, A.T., "A Practical Treatment of Nonsteady-State Flow Problems in Reservoir Systems", Petro. Engr., May, 1953.

13. Katz, D. L., et al, Handbook of Natural Gas Engineering, McGraw Hill Book Co., New York, 1959.

14. Mortada, Mohamed, "A Practical Method for Treating Oil Field Interference in Water-drive Reservoirs", AIME, Petroleum Trans., 204, 217, 1955.

15. Carslaw, H.S., and Jaeger, J.C., Conduction of Heat in Solids, Oxford at the Clarendon Press, 1947.

16. Churchill, R.V., Modern Operational Mathematics in Engineering, McGraw Hill, New York, 1944.

17. Otis, D.R., "Solving the Melting Problem Using the Electric Analogy to Heat Conduction" Heat Transfer and Fluid Mechanics Institute, Stanford University Press, 1956.

18. Bailey, H.R. and Larkin, B.K., "Heat Conduction in Underground Combustion", AIME, Petroleum Trans., 216, 123, 1959.

19. Ramey, H.J., "Transient Heat Conduction During Radial Movement of a Cylindrical Heat Source - Applications to the Thermal Recovery Process," AIME, Petroleum Trans., 216, 115, 1959.

20. Gardner, M.F. and Barnes, J.L., Transient in Linear Systems, Volume 1, John Wiley and Sons, Inc., 1948.

21. Josephs, H.J. and Radley, W.G., Heaviside's Electric Circuit Theory, Chemical Publishing Co., New York, 1946.

22. Johnson, C.L., Analog Computer Techniques, McGraw Hill Book Co., New York, 1956.

23. Korn, G.A. and Korn, T.M., Electronic Analog Computers, McGraw Hill Book Co., New York, 1956.

24. Bruce, G.H., Peaceman, D.W., Rachford, Jr., H.H., and Rice, J.D., "Calculations of Unsteady-State Gas Flow Through Porous Media" AIME, Petroleum Trans., 198, 79, 1953.

25. Hutchinson, T.S. and Sikora, V.J., "A Generalized Water-Drive Analysis", AIME, Petroleum Trans., 216, 169, 1959.

26. Hurst, W., "The Simplication of the Material Balance Formulas by the Laplace Transformation" AIME, Petroleum Trans., 213, 292, 1958.

27. Brown, G.G., et al Unit Operations, John Wiley and Sons, Inc., New York, 1955.